

**BEST COPY AVAILABLE.**

**VARIABLE PRINT  
QUALITY**

FACTORS INFLUENCING THE SWITCHING OF  
SUPERSONIC GAS JETS

Thesis presented for the Degree of  
Doctor of Philosophy of the  
University of Strathclyde.

by

R.V. Thompson, M.Eng., Dip.A.M., B.Sc.

April, 1967.

ABSTRACT.

The phenomenon of boundary layer separation is used to advantage in the operation of a high pressure, bistable, fluid switch. It has been shown that jets of air expanded through a non-adapted, convergent-divergent, two-dimensional duct at pressure ratios in excess of critical, can be encouraged to change their flow vector by the transverse introduction of further air at atmospheric pressure via strategically positioned control ports.

The position of separation and reattachment of the main jet have been determined experimentally by the measurement of pressure along the flow boundaries and verified by the Schlieren process.

A new theory has been evolved fully describing the conditions appertaining to the flow situation immediately upstream of the point of separation of a supersonic turbulent boundary layer under the duress of an adverse pressure gradient.

The derivation is also applicable to supersonic, laminar boundary layers.

It is considered that the concept applied to the switching of supersonic jets is original, as is the theoretical approach to boundary layer separation and therefore provide an extension of knowledge in this field.

## NOMENCLATURE

$A, A_t$	Cross-sectional and throat areas of duct
$c_1$	Velocity of sound
$C, C_p$	Constant and pressure coefficient
$D$	Wall offset or setback
$e$	Density
$G$	Coefficient defined in text
$h$	Enthalpy
$k,$	Ratio of specific heats unless otherwise stated
$L$	Duct wall length measured from throat
$M$	Mach number
$\dot{M}$	Momentum
$n$	Velocity profile power law index
$P$	Pressure
$r$	Ratio of boundary layer thickness
$R$	Reynold's number
$t_n$	Throat width
$T$	Temperature
$u, v$	$x$ and $y$ components of boundary layer velocity
$U$	Main stream velocity

w	Temperature law power index
$\alpha$	Total divergent wall angle
$\beta$	Turbulent coefficient unless otherwise defined
$\delta, \theta$	Boundary layer thickness, see Appendix 3
$\eta$	The ratio $y/\delta$
$\mu$	Absolute viscosity
$\nu$	Kinematic viscosity
<b>A</b>	Velocity profile shape factor
<b>C</b>	Nozzle expansion ratio
$f_1, F( )$ ,	
$\phi( )$	Functions.

Unless otherwise indicated suffix definitions are as follows;

o	refers to stagnation point or supply conditions
a	ambient
s	separation point
1, $\infty$	main stream
t	throat.

I N D E X

Page No.

ABSTRACT

NOMENCLATURE

CHAPTER 1	HISTORICAL DEVELOPMENT	1.
CHAPTER 2	THEORETICAL REVIEW	30.
CHAPTER 3	THEORETICAL APPROACH TO SEPARATION	63.
CHAPTER 4	EXPERIMENTAL INVESTIGATION	87.
CHAPTER 5	ANALYSIS OF RESULTS	129.
CHAPTER 6	SUMMARY AND CONCLUSIONS	147.
CHAPTER 7	REFERENCES	152.
CHAPTER 8	APPENDICES	166.

ACKNOWLEDGEMENTS

# C O N T E N T S

Page No.

ABSTRACT

NOMENCLATURE

CHAPTER 1 - HISTORICAL DEVELOPMENT

1.

1.1	Introduction	2.
1.2	Initial Investigations	3.
1.2.1	Mode of operation of conventional switch	4.
1.2.2	Vortex location	8.
1.2.3	Supersonic operation	10.
1.3	The Experiments of Dunaway and Ayre	12.
1.3.1	Experimental development	13.
1.3.2	Conclusions	14.
1.3.3	General comments	15.
1.4	Research by Holmes and Foxwell	19.
1.4.1	General development	19.
1.4.2	Summary of results	20.
1.5	The work of others	24.
1.6	Concluding Comment.	27.



<u>CHAPTER 2 - THEORETICAL REVIEW</u>		<b>30</b>
2.1	Introduction	<b>31</b>
2.2	Approximate Theoretical Methods	<b>32</b>
2.2.1	The method of Gruschwitz	<b>32</b>
2.2.2	Other approximate methods	<b>38</b>
2.3	Empirical Methods	<b>42</b>
2.3.1	Gadd's analysis for interaction causing separation	<b>42.</b>
2.3.2	The method of Stratford	<b>47.</b>
2.3.3	Arens and Spiegler	<b>53</b>
2.3.4	Mager	<b>58</b>
2.4	Concluding Comment.	<b>61.</b>
<u>CHAPTER 3 - THEORETICAL APPROACH TO SEPARATION</u>		<b>63.</b>
3.1	Introduction	<b>64</b>
3.2	The Concept of Boundary Layer	
	Feedback	<b>64</b>
3.2.1	Free Separation	<b>65</b>
3.2.2	Shock induced separation	<b>67.</b>
3.3	Theoretical Evaluation of the	<b>68</b>
	Conditions at Separation	
3.3.1/		

CHAPTER 3

3.3.1	Assumptions	68
3.3.2	Selection of the velocity profiles	72
3.3.3	General power law profile solution	74
3.3.4	Numerical example	79
3.3.5	The effect of reattachment	82
3.3.6	Example with reattachment	83
3.3.7	Brief note on Laminar Boundary Layers	85
3.4	Final Comment.	86.

CHAPTER 4 - EXPERIMENTAL INVESTIGATION 87

4.1	Introduction	88
4.2	Visual Methods	89
4.2.1	Schlieren apparatus	89
4.2.2	The test duct	92
4.3	Boundary Layer Pressure Measurement	95
4.3.1	The variable geometry duct	96
4.3.2	Pressure tapping	98
4.3.3	Variable port	100
4.3.4	Temperature measurement	103
4.3.5	The air supply system	103

CHAPTER 4

4.4	Test Procedure	106
4.5	Experimental Results	107
4.5.1	Schlieren results	107
4.5.2	Measurement of pressure distribution	115.
4.5.3	The effect of control port aspect ratio on switching	119

CHAPTER 5 - ANALYSIS OF RESULTS

		129
5.1	The General Situation	130
5.2	The Position of Separation	132
5.3	Reverse Flow Pressure	134
5.4	The Position of Reattachment	135
5.5	Minimum Pressure Situation	136
5.5.1	Comparison with theory	137
5.6	The Design Approach	140
5.6.1	Control port position	140
5.6.2	Control port width	142.
5.6.3	Effect of divergent angle on operation	143
5.6.4	Wall length	143
5.6.5	Splitter position	143
5.6.6	The effect of offset.	145

<u>CHAPTER 6 - SUMMARY AND CONCLUSIONS.</u>	147
<u>CHAPTER 7 - REFERENCES.</u>	152
<u>CHAPTER 8 - APPENDICES.</u>	166
Appendix 1.       The Method of Pohlhausen applied to Laminar Incompressible Boundary layers.	167
Appendix 2.       Theoretical prediction of the point of separation in a convergent divergent duct assuming incompressible flow.	175
Appendix 3.       Some definitions.	178
Appendix 4.       Experimental results.	180
Appendix 5.       The Results of Dunaway and Ayre.	226.

CHAPTER I

HISTORICAL DEVELOPMENT

## 1. HISTORICAL DEVELOPMENT

### 1.1 Introduction

The initial intention of this research programme was to develop an alternative form of missile wing surface control system to those already in existence. The system was unusual in that it was to be completely pneumatic, self supporting and, more important, was to form an integral part of the actual wing assembly.

To transform the idea into a working proposition it was necessary to develop a device capable of switching a hot gas travelling at supersonic velocities from one exit port to another. Envisaged, in principle, was a pneumatic, high pressure, bistable switch operating on the Coanda<sup>(1)</sup> effect.

A review of the extensive literature available on the subject of fluid logic devices indicated that little work had been directed toward the development of high pressure, compressible flow systems. A research programme was therefore initiated to investigate the possibility of useful development in this area. The prime result of the applied effort was the successful development of a device capable of switching supersonic

jets in a bistable mode of operation by systematically venting and closing the control ports to the atmosphere.

Before continuing with the historical development it is necessary to recognise that because of the somewhat restricted nature of relevant reports, etc., at the commencement of this research programme, the author had no indication that such a device of similar concept but different configuration had been developed in the United States. To the author's knowledge the work detailed herein has not been duplicated elsewhere and consequently is submitted as original.

1.2 Initial Investigations

The position of a vortex formed in a conventional subsonic bistable switch can be predicted with some accuracy due to the inability of the laminar boundary layer to support any sizeable adverse pressure gradient. It has been shown<sup>(2)</sup> (Appendix, 2, p. ) that separation will take place a short distance beyond the throat of a convergent-divergent duct. With suitable offset it may be considered to separate at the throat for most flow regimes up to the sonic condition.

Conventional fluidic bistable switches, therefore, incorporate control ports which are usually situated at the throat of the convergent-divergent duct and generally operate quite successfully in the following manner.

1.2.1 Mode of operation of a conventional switch.

With power applied to the inlet port, Figure 1.1, the output flow is either entirely from the right or from the left outlet port.

Assuming that flow is issuing from the left outlet, the main jet is reattached to the extreme left hand wall at a point located somewhere downstream. A low-pressure vortex is formed between the reattachment point and the main inlet position as shown in Figure 1.1. A pressure gradient therefore exists across the jet stream. In the conventional fluid switch, the jet is forced to move from the wall to which it is attached by the introduction of a transverse fluid jet injected through the adjacent control port. If the control flow is introduced to the low-pressure region at a faster rate than the main stream can remove it, the pressure will increase and the attachment point will move further



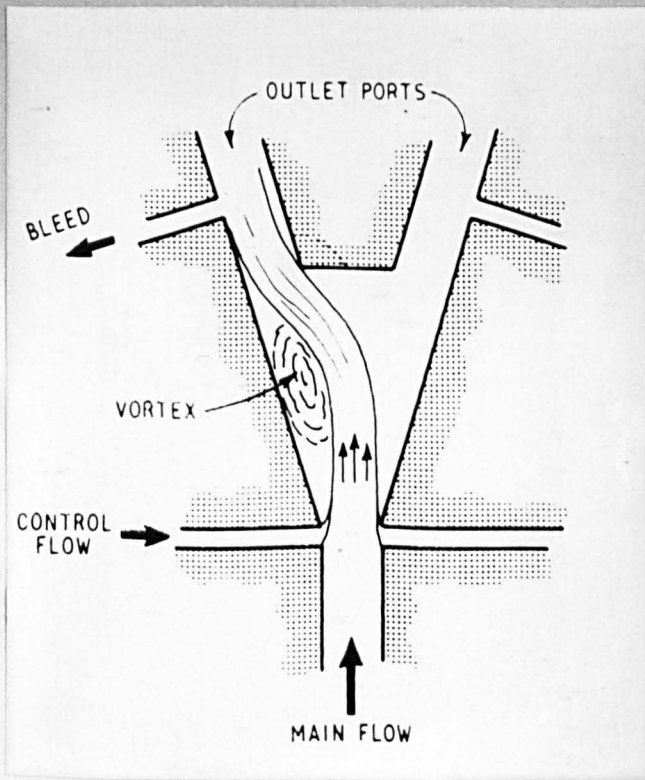
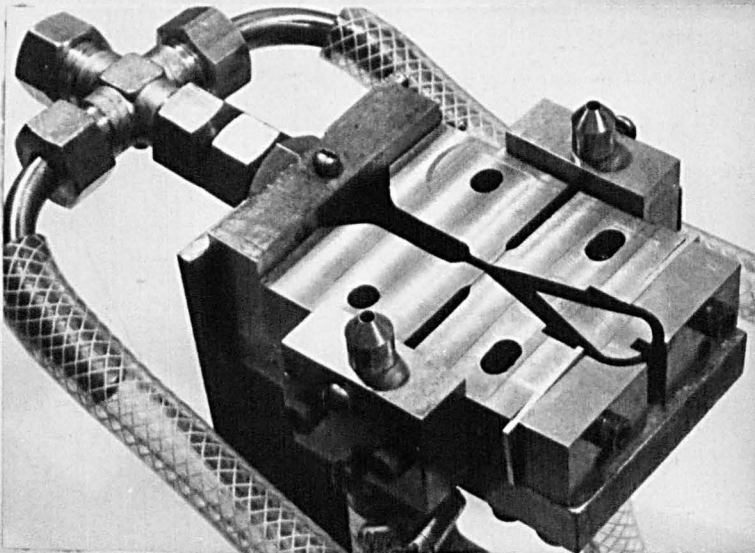


FIGURE 1.1

THE CONVENTIONAL FLUID SWITCH.

FIGURE 1.2

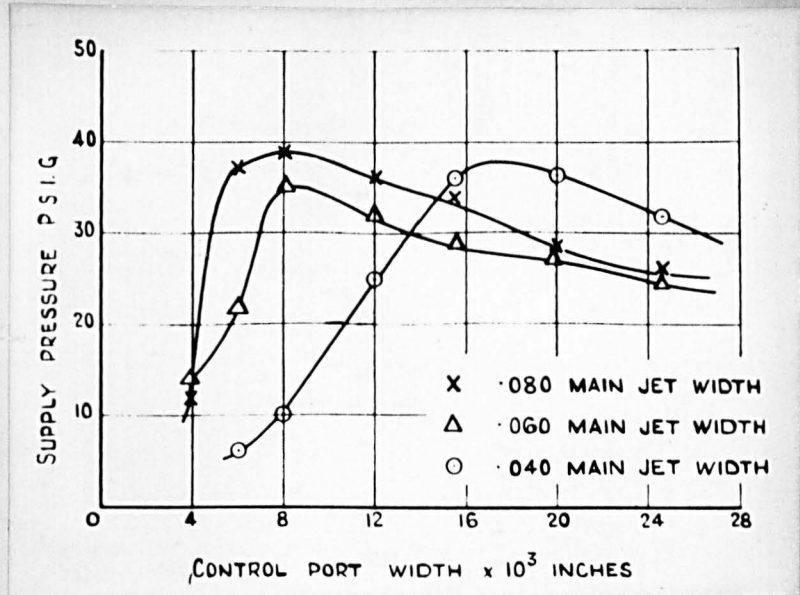
THE FIRST  
EXPERIMENTAL SWITCH.



downstream. When the bleed position is reached or interference occurs between main jet flow and the splitter, the jet switches to the other wall where, providing flow is maintained, the jet forms a vortex. The process is reversible.

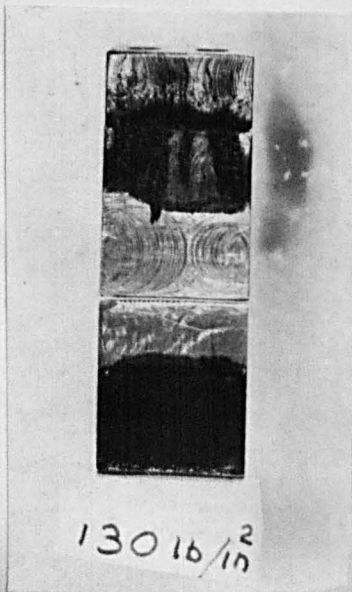
Experiments with a switch, Figure 1.2, having variable control ports situated adjacent to the main inlet port showed that switching was obtainable by opening the adjacent control port to the atmosphere as well as by the application of control pressure. There was, however, for each configuration, a limiting main jet supply pressure at which switching was possible by this means. Figure 1.3 shows, however, that increase of control port area did not improve the situation to any marked degree. It was assumed, therefore, that the vortex moved downstream with increase in supply pressure, thereby preventing the control flow from entering the low pressure region. This effect was contrary to common opinion<sup>(3,4,5)</sup> at that time and therefore required test evaluation.

FIGURE 1.3



MAXIMUM SUPPLY PRESSURE AT WHICH  
SWITCHING MAY BE AFFECTED USING  
ATMOSPHERIC AIR AS THE CONTROL MEDIUM.

FIGURE 1.4



SHOWING ENGINEERS BLUE  
REMAINING ON BOTH WALLS  
AFTER TESTING.

### 1.2.2 Vortex location.

Location of the vortex for any given supply pressure was determined by a simple paint technique. A mixture of Engineers' Blue and linseed oil was applied to the relevant amplifier walls and air of a predetermined pressure passed through the device. The relatively low reverse flow in the vortex left darker patches of the mixture than that of the main flow. With a suitable mixture, it was found that 'Blue' remained in the position of the vortex only (Figure 1.4).

Verification of the vortex position was obtained by pressure measurements using a hypodermic needle as the probe. Figures 1.5 and 1.6 show the respective characteristics obtained in this way. From these early results it can be seen that the position along the wall of the centre of pressure of the vortex is very nearly proportional to supply pressure throughout the test range - all other factors remaining constant. This led to a modified concept of operation.

FIGURE 1.5

EFFECT OF SUPPLY PRESSURE ON BUBBLE DISPLACEMENT

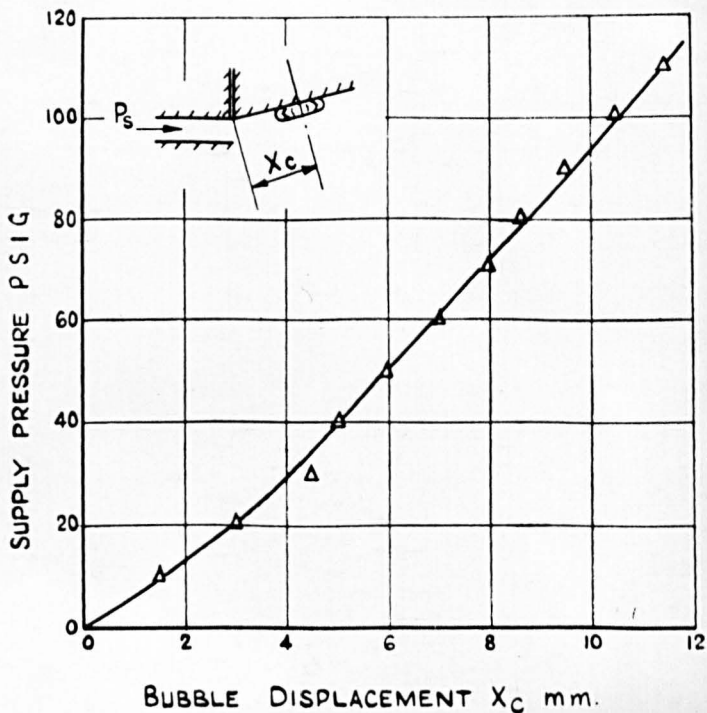
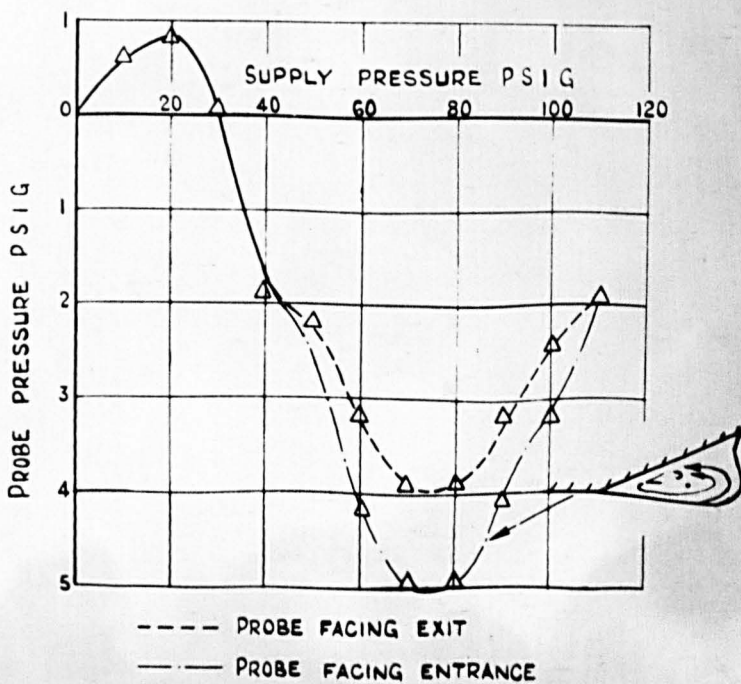


FIGURE 1.6

THE COMBINED EFFECT.



### 1.2.3 Supersonic operation.

As previously stated the subsonic fluid switch deflects the main jet stream by momentum interaction and flow entrainment etc., and, at the higher supply pressures, usually requires control pressure.

With the supersonic switch the preliminary results determined above suggested that, if the control ports were situated along the walls at a position coinciding with the vortex position corresponding to the mean of the operating supply pressure range, actuation could be accomplished by atmospheric venting alone. Simultaneous closure and venting of the far and near control ports would destroy the operating vortex causing the jet to accelerate transversely from the wall to which it was attached to form a vortex on the wall opposite. Verification was obtained by modifying the switch configuration to that shown in Figure 1.7.

The control ports were positioned approximately 1 cm. from the inlet port, which corresponded to the vortex position at a supply pressure of 100 lb/in<sup>2</sup>g. (from Figure 1.5). The control ports widths were

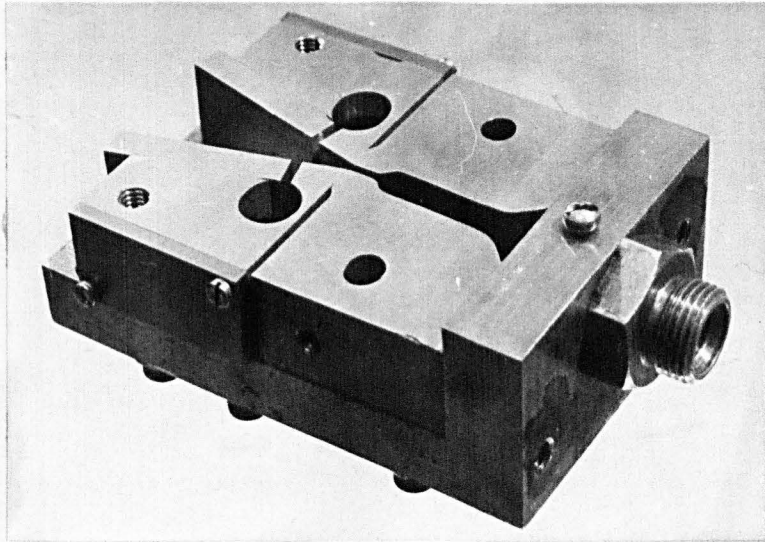


FIGURE 1.7     THE FINALISED DESIGN OF EXPERIMENTAL SWITCH.

adjustable and vented to the atmosphere.

Tests<sup>(6)</sup> on the device showed that switching was possible in the supply range 70 - 130 lb/in<sup>2</sup>g. for this setting, simply by the application of fingers to the control vents. Some small extension in the working range could be obtained by increasing the control port widths.

Having proved feasibility, it was decided to obtain information regarding the development of the vortex and the effect of the operating parameters on performance by more rigorous test techniques, i.e. boundary layer pressure measurements and visual interpretation by optical methods. The apparatus and test procedure evolved is outlined in a later section (Section 4, p. ).

### 1.3 The experiments of Dunaway and Ayre.

It was at this point in the research programme that the efforts of DUNAWAY and AYRE<sup>(7)</sup> became available. Their report describes "an effort toward the development of a hot gas jet reaction valve utilising boundary layer technique to control a high pressure, high temperature gas stream".



The programme objective was to apply known fluid amplifier techniques to a hot gas reaction control system for a particular missile. Three-dimensional control was anticipated, valves being placed in the pitch, yaw and roll axes. Resulting from their programme was a bistable "hot gas valve" tested with supply pressures up to 1300 psi, temperatures up to 2350°F and at maximum flow rates of 1 lb/sec cold air. The finalised control medium was air at atmospheric pressure and temperature.

#### 1.3.1 Experimental development.

The approach favoured by Dunaway and Ayre was apparently one of pure experiment rather than systematic analysis. Initial experiments were conducted at supply pressures up to 200 psi, switching being maintained throughout the range by considerable modification of the recovery section of the unit. Beyond this limiting condition supersonic nozzles of various expansion ratios were tried with adjustable type receiver sections, each experiment involving the variation of set back, wall length, control port size and wall angle in an attempt to encourage operation. During these experiments it was discovered that, for

particular configurations, switching could be obtained by using atmospheric air as the control medium.

In anticipation of control power economies all further experiments concentrated on this method of operation.

A variety of differently shaped nozzles, of various aspect ratios, were designed and tested. The final choice being circular shaped nozzles because of their relative thrust efficiency and ease of manufacture, with respect to two-dimensional nozzles.

Some attempt was made to recover pressure in the receiver units but with little success. The valve could not be made to switch into a back pressure of more than a few psi. Because of the intended application - missile stability control - the problem of reduced ambient pressure was briefly investigated with little conclusion.

Some 65 hot gas runs were attempted to the time of publication.

1.3.2 Conclusions.

From their experimental results (see Appendix P. ), the authors concluded that a higher supply

pressure could be switched by increasing;

(a) nozzle area ratio (test range 8.6 - 13.3)

(b) length of receiver section

and (c) area of exit manifold relative to  
exit area of receiver section.

(c) was found to reduce valve efficiency at  
the lower supply pressures.

The effect of increasing control port area was  
said to result in a wider switching range.

The authors considered, in view of their  
results, that a staged valve approach would provide a  
more predictable and acceptable solution to their  
immediate problems.

### 1.3.3 General comments.

In view of the work presented herein the  
following comments may be made.

Successful operation of the switch shown  
diagrammatically in Figure 1.8 would only be evident  
when the vortex position coincided with the respective  
control port. At low pressures the jet would either

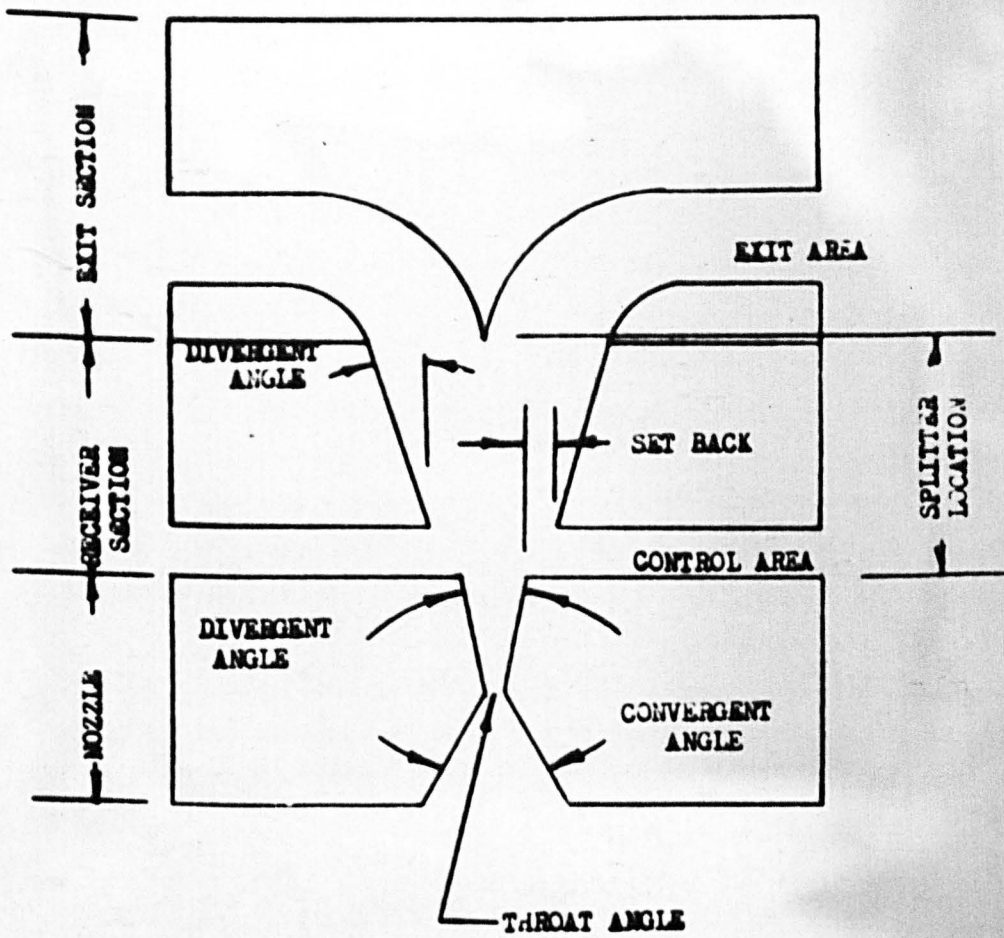


FIGURE 1.8 DIAGRAMMATIC SWITCH OF  
DUNAWAY AND AYRE

reattach prior to the control port position or, in the case of offset, not attach at all. Consequently the introduction of air to the control port, in this situation, would have no effect on the thrust direction. At excessive supply pressures, for the configuration shown, the jet would have sufficient energy to expand into the offset region axisymmetrically and not separate until some point further downstream. Once again, venting to the atmosphere would be inadequate or ineffectual. Figures 1.9 and 1.10 illustrate the points made - shock wave formation, etc., omitted.

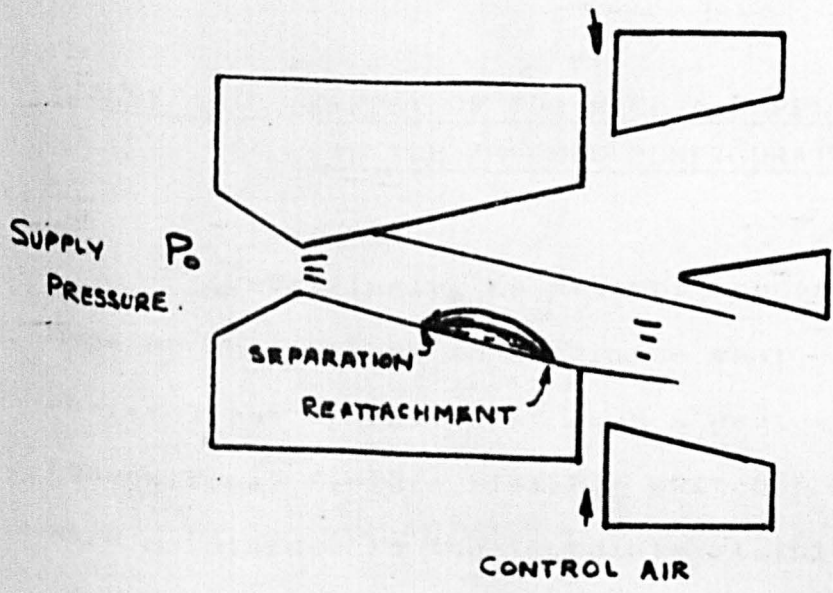


FIGURE 1.9. EFFECT OF TOO LOW A SUPPLY PRESSURE  $P_0$

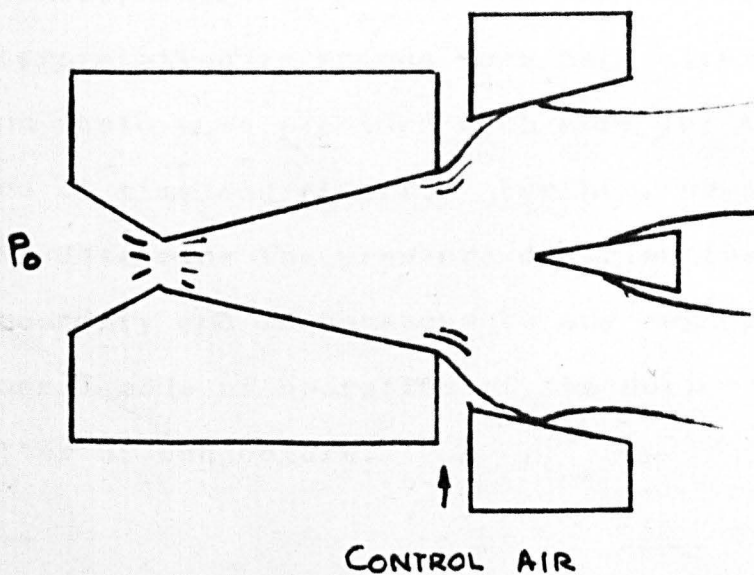


FIGURE 1.10 EFFECT OF TOO HIGH A SUPPLY PRESSURE  $P_0$   
FOR THE ASSUMED CONFIGURATION.

Surprisingly, no attempt appears to have been made by the authors to determine what caused or assisted the operation of such a device and, as with conventional fluidic bistable switches, the control ports were maintained in the immediate vicinity of the exit of the main flow nozzle - the nozzle being convergent-divergent to achieve supersonic velocities. Considering that the nozzles were made of stainless steel and

the receivers of formed copper, the difficulties encountered by the researchers must have been considerable. It is contended, therefore, that the use of some visual interpretation technique such as Schlieren or Shadowgraph would have provided much more for the given expenditure of time and effort. Further, no attempt was made to determine the pressure distribution along the flow boundary and in consequence any suggestion as to the general mode of operation of the device must have been a matter of conjecture.

#### 1.4 Research by Holmes and Foxwell.

Comparison of the report of HOLMES and FOXWELL<sup>(8)</sup> with that of Dunaway and Ayre shows similarities and considering that the work was attempted at the Harry Diamond Laboratories (H.D.L.) under the auspices of the U.S. Army Materiel Command, it must be concluded that it is a continuation of their initial efforts.

##### 1.4.1 General development.

The experimental work reported by Holmes and Foxwell is almost identical to that of Dunaway and Ayre; the theoretical arguments, however, are more progressive.

Mention is made of boundary layer and separation phenomena. It is suggested that the position of the point of separation may be predicted by using an approach attributable to GADD<sup>(15)</sup> (see Section 2, p. ) although no attempt is indicated. Separation was said to occur at a particular ratio of static exit pressure to separation pressure.

The original design is shown in Figure 1.11. Five conical nozzle insets with expansion ratios of 5, 10, 15, 20 and 25 were tested in the basic configuration. As can be seen offset was favoured for all pressure ratios. The frictional effect of duct length (1 to 15 diameters) was an additional variable used to obtain switching at a given supply pressure. Transducers were utilised to determine the lateral thrust during switching at expansion ratios of 20 to 25, the results of which are indicated in Figure 1.12.

#### 1.4.2 Summary of results.

Figure 1.13 shows the effect of output ducting and expansion ratio on switching plotted against supply pressure,  $P_0$ .



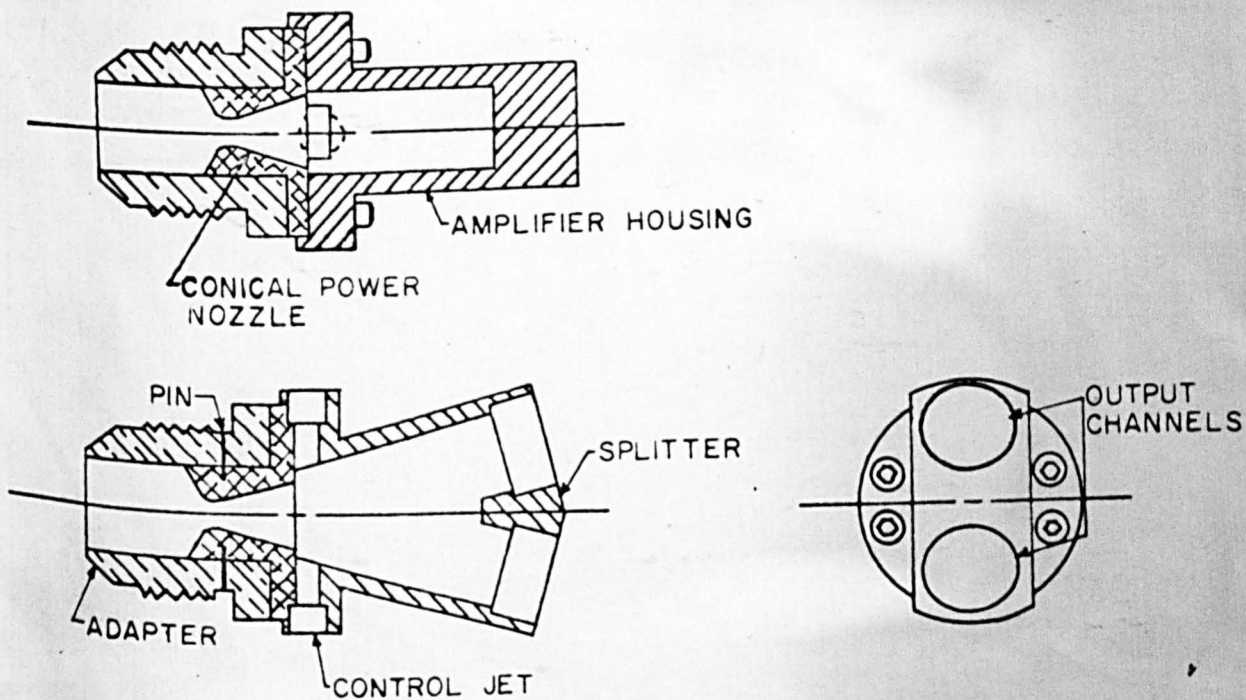


FIGURE 1.11 THE DESIGN OF HOLMES AND FOXWELL.

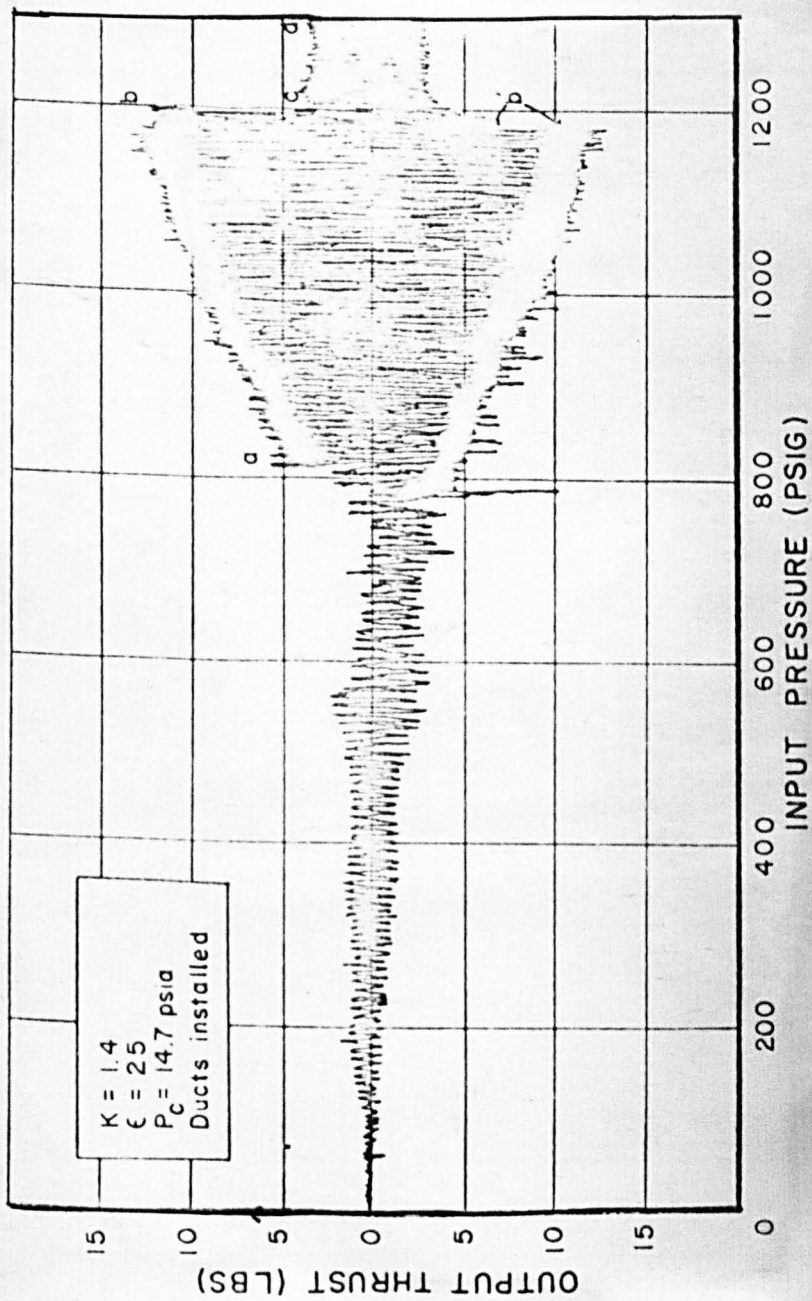


FIGURE 1.12 THRUST CHARACTERISTICS OF HOLMES AND FOXWELL.

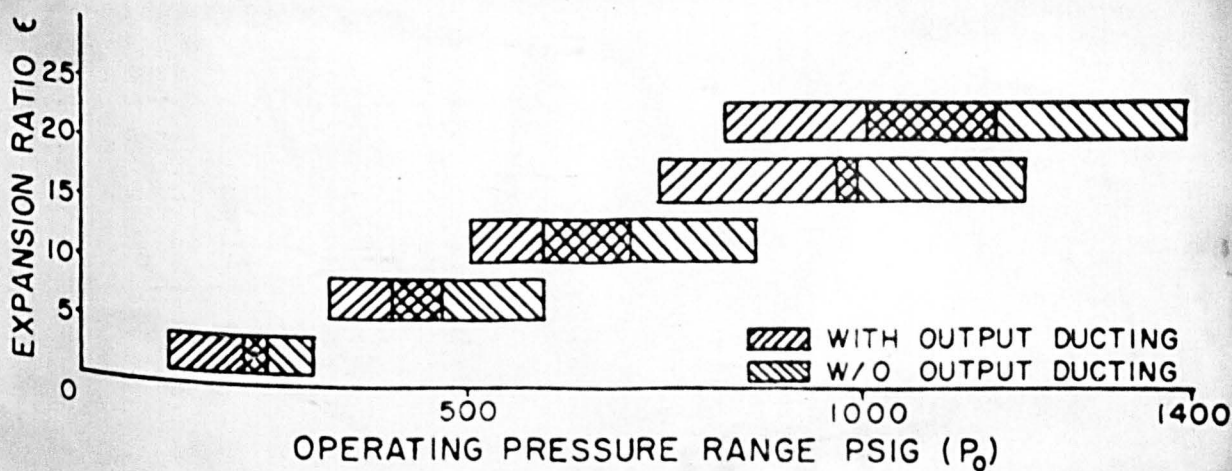


FIGURE 1.13 CHANGE IN OPERATING PRESSURE RANGE DUE TO NOZZLE EXPANSION RATIO AND OUTPUT DUCTING.

Obviously the smaller the expansion ratio the further downstream separation occurs and the lower the effective operating pressure range.

Surprisingly, although a critical pressure ratio was suggested to occur at separation no attempt at measurement was made. Further, the effect of the position of the reverse flow region was not considered of consequence.

The basic improvement on the work of Dunaway and Ayre rests purely in the decision to vary only two

basic parameters; expansion ratio and duct length and also in the measurement of thrust. Attention must also be drawn to the fact that interest was being shown in a theoretical approach; at that time still somewhat illusive. In both research programmes the basic concept of operation was not indicated.

1.5. The work of others.

The only other author of general publications appertaining to supersonic bistable switches known to this researcher are those of CAMPAGNUOLO<sup>(9)</sup> the most recent of which was presented at the Second Cranfield Fluidics Conference, 1967, and co-authored by Holmes.

The basic device was that developed by Holmes and Foxwell discussed previously. Campagnuolo's main contribution is in application. A pneumatic signal is generated from a gyroscope incorporated in a missile control system. The signal modifies by a process of pulse width modulation, the output thrust of a multistage fluidic bistable system, the final stage of which is the power switch previously discussed. Figure 1.14 illustrates the system.

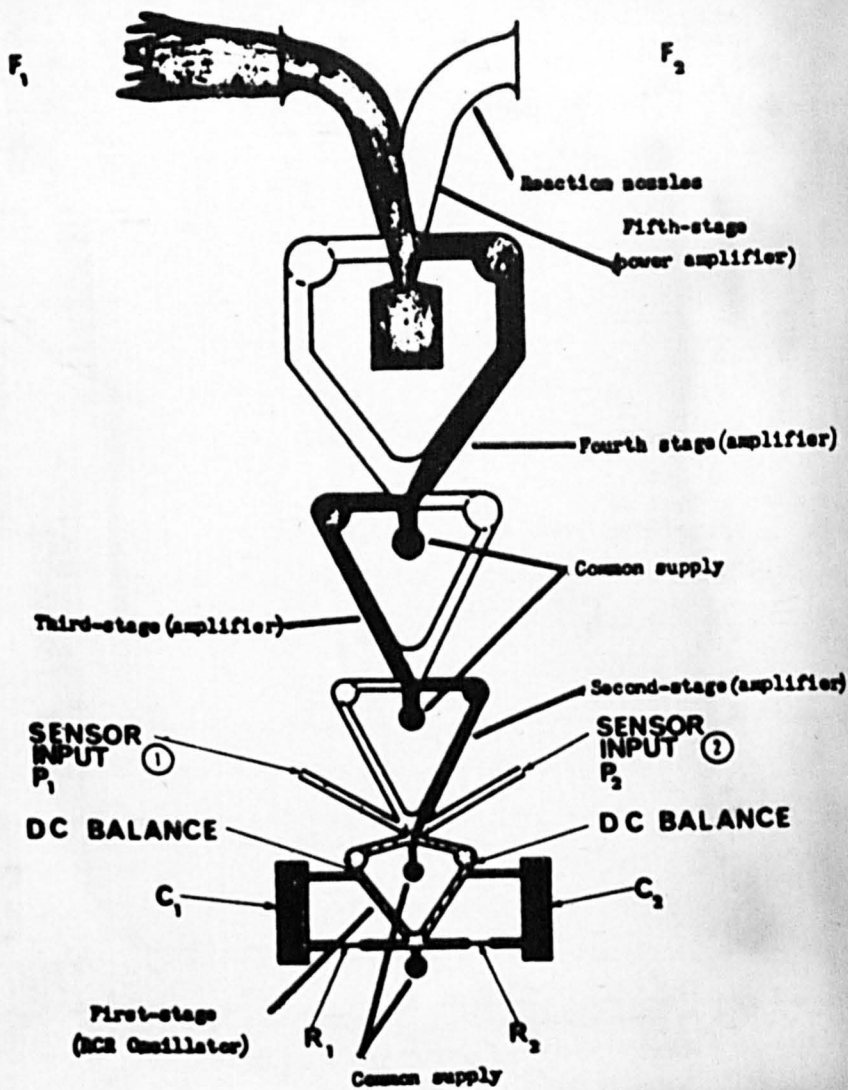


FIGURE 1.14 MULTISTAGE SYSTEM

In the composite design maximum frequency of operation reported was 140 c/s. at a jet pressure of 70 psig. in the oscillator although details are given graphically of output thrust versus power jet pressure in the range 200 - 800 psig. at a subsystem feed pressure of 40 psig.

Maximum output thrust was reported as 80 lb providing an overall power gain of  $10^6$ .

Atmospheric control of the subsystem is suggested together with the advantages thereof. The design is compact and reported operation most satisfactory.

Two other developments are known to the author those of SVENSKA FLYGMOTOR AB<sup>(10)</sup> of Sweden and the BRITISH AIRCRAFT CORPORATION (B.A.C.), Filton, Great Britain<sup>(11)</sup>.

The former have made an approach for the exchange of information and have forwarded details of their current research programme. Basically they have taken the work of Holmes and Foxwell as a starting point and have repeated a fair proportion of the test programme. Because of lack of theoretical knowledge

the company has run into some difficulties regarding operation through an extended range.

British Aircraft Corporation have run into similar difficulties when attempting to use power bistable switches to vector the output thrust of a missile main motor - see Figure 1.15. The problem evolved from the fact that operation was required in a range of parameters not covered by the members of Harry Diamond Laboratories, the lack of operating knowledge causing some difficulties.

One other known report is the paragraph contributed on the subject by WARREN<sup>(12)</sup>. He shows a Schlieren photograph and states quite simply that such a device can operate at pressures in excess of 1000 psig.; no other details being given. Presumably, by virtue of his H.D.L. experience, Warren is referring to the efforts of the researchers discussed above.

#### 1.6 Concluding comment.

From the work of others already discussed it would appear that the majority of researchers in this

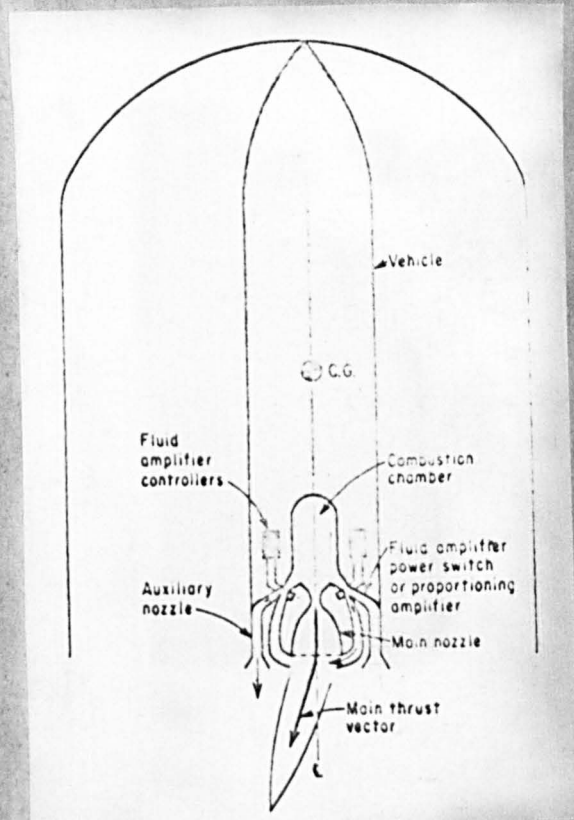


FIG. 1. 15. SCHEMATIC OF PROPOSED MISSILE THRUST VECTOR CONTROL SYSTEM.



field have derived their programme from the initial investigations of Dunaway and Ayre and in consequence progress has been somewhat slow. However, visits from members of the ROYAL AIRCRAFT ESTABLISHMENT<sup>(13)</sup> and communications from FEHRMANN<sup>(14)</sup> of "East Germany" and R. ROSIC, <sup>(15)</sup> of the Thompson Organisation of the United States indicate that interest and knowledge in the subject is becoming more diversified. It is concluded, therefore, that, together with the work presented herein and the expected results of a further parallel research programme in which the author is presently engaged, some acceleration of current progress can be expected.

CHAPTER II

THEORETICAL REVIEW

2. THEORETICAL REVIEW.

2.1 Introduction.

Many attempts have been made to rationalise and solve the positional problem of boundary layer separation under the duress of an adverse pressure gradient. Generally the approach is highly mathematical commencing with the generalised Navier Stokes equations, progressing by a series of transformations, substitutions and limiting boundary conditions to a group of differential equations requiring simultaneous solution. Because of the nature of the finalised equations simplified flow conditions are generally considered, e.g. main stream velocity commencing at some finite extreme value assumed to decrease as a linear function of displacement etc. Because of such assumptions most of the preferred solutions are only applicable to subsonic compressible flow as the retardation of supersonic flow presents discontinuities in the flow situation thereby not lending itself to direct mathematical analysis.

Semi-empirical methods are more acceptable to the practising engineer and by virtue of their derivations, may be applied to more general situations.

Details of the better known mathematical and semi-empirical methods are presented in an abbreviated form below permitting comparison with the new method detailed in the following section.

## 2.2 Approximate theoretical methods.

Such methods are, as yet, only applicable to laminar boundary layers.

The problem of the compressible laminar boundary layer with zero pressure gradient becomes extremely difficult unless suitable approximations are made concerning the value of Prandtl Number and the variation of viscosity with temperature. It is to be expected, therefore, that the additional problem of pressure gradient imposes severe restrictions on any rigid attempt at mathematical determination of the conditions applying to the point of separation.

### 2.2.1 The method of GRUSCHWITZ.<sup>(1)</sup>

The most favoured approach to the problems involved in the solution of the compressible boundary layer is some individual extension of the approximate

incompressible derivations.

The method outlined below is used most frequently because of its comparatively simple numerical calculation and because its applicability to practical problems is not rigidly restricted to any particular Prandtl number. It has been selected, also, because certain conclusions may be drawn from its solution, particularly as it leans on the approximate method of POHLHAUSEN<sup>(2)</sup> and HOLSTEIN-BOHLEN<sup>(3)</sup>.

Gruschwitz introduced a new boundary layer thickness

$$\eta = \frac{1}{\delta_1} \int_0^y \frac{\rho}{\rho_1} dy \quad (2.1)$$

where

$$\delta_1(x) = \int_0^{\delta(x)} \frac{\rho}{\rho_1} dy \quad (2.2)$$

As with the approximate incompressible method the velocity distribution is represented by a fourth degree polynomial

$$\text{i.e.} \quad \frac{u}{U} = C_1 \eta + C_2 \eta^2 + C_3 \eta^3 + C_4 \eta^4 \quad (2.3)$$

and obtain similar coefficients in  $\Lambda$  (see Appendix 1)

where  $\Lambda$  is modified to include the density ratio

$$\text{i.e. } \Lambda = \frac{e_1}{e_w} \cdot \frac{d_1^2}{\sqrt{1}} \cdot \frac{dU}{dx} \quad (2.4)$$

And, instead of obtaining an expression of  $e/e_1$  in terms of  $\eta$  he decided upon a quintic in  $\eta$  for the product

$$(1 - u/U) \cdot \frac{e_1}{e} \quad (2.5)$$

The six coefficients satisfied five boundary conditions and therefore he deduced the sixth from the energy integral equation, the constant coefficient

$$b_0 = \frac{e_1}{e_w} = \frac{T_w}{T_1} \quad \text{being SELECTED ;}$$

thereby giving

$$\Lambda = b_0 \cdot \frac{\int_1^2}{\sqrt{1}} \cdot \frac{dU}{dx} \quad (2.6)$$

As with the Pohlhausen method various convenient substitutions are made as well as expressing momentum and energy dissipation explicitly in terms of the shape factor  $\Lambda$ .

Ultimately the following two equations are evolved from the momentum equation (A.31), Appendix (3) p. , and the energy equation (A.33), Appendix (3) p. .

$$\theta \frac{U}{\sqrt{1}} \frac{d\theta}{dx} = F(k) - \frac{k}{b_0} \left[ 2 - M^2 F_2(k) \right] \quad (2.7)$$

$$b_0 = \left( 1 + \frac{\gamma-1}{2} M^2 \right) \frac{1 + M^2 F_3(k)}{1 + M^2 F_4(k)} \quad (2.8)$$

$$\text{where } k = A \left( \frac{\theta}{\delta_1} \right)^2 = b_0 \cdot \frac{\theta^2}{\sqrt{1}} \cdot \frac{dU}{dx} \quad (2.9)$$

The functions  $F_1(k)$   $F_2(k)$   $F_3(k)$  and  $F_4(k)$  have been tabulated by E. Gruschwitz (1,4). The point of separation being determined as before with incompressible flow;

$$\text{i.e. by } A = -12 \quad k = -0.1567$$

The quantities  $U(x)$   $dU/dx$   $\sqrt{1}(x)$  as well as  $M = U/c_1$  and  $P$  are to be considered given

Consequently, expressions (2.7), (2.8) and (2.9) constitute a system of three differential equations for the three variables, momentum thickness  $\theta(x)$ , the wall temperature  $b_0 = T_w(x)/T_1(x)$  and the shape factor  $K$ .

The process of integration is by the method of isoclines as with the Pohlhausen solution see Appendix ( 1 ), p. ); initial values at the stagnation point are obtained and with  $k_0 = 0.0770$  the following equations result

$$\theta_0 = \sqrt{K_0 \nu_1 / \left(\frac{dU}{dx}\right)_0} \quad (2.10)$$

$$\left(\frac{d\theta}{dx}\right)_0 = -0.424 \theta_0 \left(\frac{d^2U}{dx^2}\right)_0 / \left(\frac{dU}{dx}\right)_0 \quad (2.11)$$

### 2.2.2 General comments on the applicability of the method.

The shape factor  $\Lambda$  is basically the ratio of pressure to viscous forces in the boundary layer modified, in the compressible case, by the temperature ratio  $T_w/T_1$ .

The method of solution, as suggested, commences with some finite value of the form factor  $k$  (i.e.  $k_0$ ) which immediately involves a positive value of  $\Lambda$ , indicating a particular shape to the velocity profile. Successive isocline solution produces a progressive reduction in the value of  $\Lambda$  which in turn modifies the assumed velocity profile. The actual process is one of progressive decrease in momentum in the boundary



layer involving an increase in the pressure to viscous force ratio until, at some discrete value, ( $\Lambda = -12$ ) separation occurs. Figure 2.1 shows the profile progression for the incompressible situation.

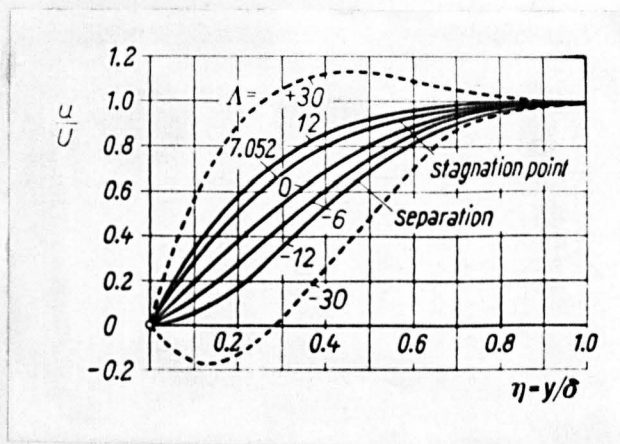


FIGURE 2.1 THE ONE PARAMETER FAMILY OF VELOCITY PROFILES.

It should be noted that  $M$  is a function of the initial main stream flow velocity  $U$  and that  $U(x)$  must be determined from the stagnation point. Therefore any erroneous assumptions involved in the derivation of the basic equations must be propagated from the stagnation point through the parameters

$\frac{d\bar{U}}{dx}$ ,  $v_1(x)$ ,  $T_w(x)/T_1(x)$ ,  $k$  and  $A$ , the latter modifying the assumed velocity profiles appreciably. As the shape of the profiles indicate the momentum energy available at any given time which may be opposed by an adverse pressure gradient sufficiently large to cause separation, the theoretical position of separation must vary as the coefficients of the power terms in the velocity distribution polynomial as too, will the accuracy.

A further limitation with the method is the difficulty involved in obtaining an expression for main stream flow in terms of displacement  $x$  with a particular wall profile. For example, a convergent-divergent duct in compressible flow requires the simultaneous solution of the isentropic equations.

Turbulent profiles cannot be entertained by the method of Gruschwitz but this is generally the case with derivations developed from the Navier Stokes equations.

### 2.2.2 Other approximate methods.

HOWARTH<sup>(5)</sup> introduced the stream function  $\psi$  to satisfy the continuity equation (see Appendix (3) p. ).

$$\text{i.e. } eu = e_1 \frac{\partial \phi}{\partial y} ; \quad ev = -e_1 \frac{\partial \phi}{\partial x} \quad (2.12)$$

and assumed a viscosity distribution of

$$u = \mu_1 T/T_1 \quad (2.13)$$

and attempted to reduce the momentum equation to an incompressible form by the use of assumed transformations, for viscosity and pressure ratios.

By utilising the thermal energy equation and progressing along the method of Pohlhausen he finally arrived at the shape parameter

$$\lambda = \frac{\delta'^2}{\sqrt{1}} \cdot \frac{dU}{x} b_0 \quad (2.14)$$

$$\text{where } b_0 = \left[ 1 - \frac{1}{2}(\gamma - 1) M_1^2 \right] \quad (2.15)$$

$$\delta' = \int_0^{\infty} \left( 1 - \frac{u}{U_1} \right) dY \quad (2.16)$$

$$\text{and } Y = \int_0^y \left( \frac{\sqrt{s}}{\gamma} \right)^{\frac{1}{2}} dy \quad (2.17)$$

It can be seen that the shape factor as derived by Howarth has certain similarities with that of Gruschwitz when the Prandtl number,  $P = 1$ . Surprisingly

there is a sign change involved in  $b_0$ .

Because of the similarity and the necessity to progress from the stagnation point the method is open to the criticisms applied to the method of Gruschwitz. The criticism appertaining to the derivation of  $U(x)$  seems particularly valid in this instance as Howarth was only prepared to forward a solution to velocity decreasing linearly with displacement  $x$ .

An alternative method of generalizing Pohlhausen's method has been suggested by YOUNG<sup>(6)</sup> and subsequently improved<sup>(7)</sup> to include flow with heat transfer at the wall. The method is valid for arbitrary  $P$  and  $w$ , where  $w$  is the temperature - viscosity relationship index.

STEWARTSON<sup>(8)</sup> and ILLINGWORTH<sup>(9)</sup> have improved Howarth's method by a more involved transformation in order to effect a complete transformation between a compressible and incompressible layer with differing mainstream velocity. Other transformations have been suggested by ROTT<sup>(10)</sup>, OSWATITSCH and WEIGHARDT<sup>(11)</sup>, ILLINGWORTH<sup>(13)</sup> and FRANK<sup>(13)</sup>, the most interesting of which is that of

Illingworth.

He attempted detailed calculations for flow with zero pressure gradient, using a number of possible forms of the functions  $F(\eta)$  and  $G(\eta)$ , (see Appendix (1), p. ). In particular he considered cases where the two functions were polynomials of the same order; quadratic, cubic and quartic and a further case in which  $F(\eta)$  was quintic and  $G(\eta)$  sextic. Of particular interest, however, was the consideration given to the trigonometric forms,

$$F(\eta) = \sin \frac{1}{2}\pi\eta ; \quad G(\eta) = (\sin \frac{\pi\eta}{2X})^2 \quad (2.18)$$

and his conclusions that the trigonometric and cubic forms appear to give the most accurate values in comparison with the accurate calculations of EMMONS and BRAINERD<sup>(14)</sup>.

When the problem is specifically that of the determination of the point of separation in laminar compressible flow it is considered that the above methods are rather prone to error due to the basic similarity in the method of approach. Further, when considering relatively complicated profiles the

arithmetical effort involved in solving for main stream velocity etc. become so great as to become prohibitive.

The following methods are therefore considered to have, in comparison, something better than an equal capability of predicting, with some accuracy, the point of separation, principally because they are semi-empirical and apply to the separation region alone.

### 2.3 Empirical methods.

#### 2.3.1 Gadd's analysis for interactions causing separations.

GADD<sup>(15)</sup> has studied the problems associated with the two dimensional interaction between the boundary layer on a flat plate and an incident oblique shock wave assumed to be of sufficient strength to cause separation. He considered two distinct cases - wholly laminar or wholly turbulent flows.

Because of the nature of the assumed problem, i.e. flat plate condition, his analysis is not rigidly applicable to the situation forming the subject matter of this thesis; however, he draws several conclusions which other investigators have applied to the convergent/divergent flow situation.

With regard to laminar flow it is assumed that in the region immediately upstream of interaction, where there is no pressure gradient, the velocity within the boundary layer is given by

$$\frac{u}{U} = \sin \frac{\pi y}{2\delta} \quad (2.19)$$

By lengthy argument he concludes that separation pressure ratio is independent of shock strength and is a function of Mach Number and  $R_x$  only.

Making the assumptions that  $w = P = 1$  and zero heat transfer, the isentropic equations may be used for the determination of the density and viscosity ratios. Substitution of the relevant expressions together with the assumed velocity ratio in the expression for displacement thickness obtains

$$\delta_z^* = \delta_z \left[ 1 - \frac{2 \tan^{-1} \left[ \left( \frac{\gamma-1}{2} \right)^{1/2} M_0 \right]}{\pi [(\gamma-1)/2]^{1/2} M_0} \right] \quad (2.20)$$

This is equated to the displacement thickness obtained by YOUNG<sup>(16)</sup> involving Reynolds number to give an expression for boundary layer thickness  $\delta_z$  in terms of  $M_0$  and  $x$  only, viz.

$$\delta_z = \frac{1.721 [1 + 0.693(\gamma-1) M_o^2] x}{\left[ 1 - \frac{0.636 \tan^{-1} \left[ \left( \frac{\gamma-1}{2} \right)^{1/2} M_o \right]}{[(\gamma-1)/2]^{1/2} M_o} \right] \sqrt{R_x}} \quad (2.21)$$

At this point Gadd proffers arguments in favour of dividing the boundary layer into two distinct portions - that which is viscosity dependent and that which is pressure dependent. The velocity distribution expression is divided likewise and conditions imposed on the two portions such that continuity is maintained at the assumed joining streamline.

Near the wall it is assumed, from the Navier Stokes equation that

$$dP/dx = \mu \left( \partial^2 u / \partial y^2 \right) \quad (2.22)$$

Also the relationship between pressure and deflection of the external streamlines is derived from supersonic flow theory for small angles and equated to the rate of change of displacement thickness commencing at a zero adverse pressure gradient condition.

By further argument the difference of the displacement thicknesses is assumed to vary parabolically



to the point of separation as too is the pressure difference. By successive substitution in the respective equations is derived an expression for pressure rise at separation, viz:

$$\frac{P_3 - P_0}{P_0} = \frac{0.780 \gamma M_0^2}{[(M_0^2 - 1) R_{x1}]^{1/4}} \left[ \frac{(1 + \frac{\gamma-1}{2} M_0^2) \left( 1 - \frac{0.636 \tan^{-1} \left[ \left( \frac{\gamma-1}{2} \right)^{1/2} M_0 \right]}{[(\gamma-1)/2]^{1/2} M_0} \right)}{1 + 0.693 (\gamma-1) M_0^2} \right]^{1/2} \quad (2.23)$$

Which, in comparison with practical results, gives fair agreement up to Mach numbers of 3. Beyond this value divergence is high.

Gadd suggests that a similar approach to turbulent boundary layers is not justifiable due to the nature of the problem and contents himself with the following empirical discussion of the problem.

It is assumed that the profile

$$u/U = (y/\delta)^{1/7}$$

appertains to the free boundary layer, i.e. that in the immediate vicinity of separation but not affected by it.

Sketching the profile he suggests that a knee occurs at a velocity ratio approximating to  $u/U = 0.6$ .

Suggesting, from experimental results, that the bulk of the pressure rise associated with separation takes place steeply it is postulated that the pressure gradient forces in this region are considerably greater than the friction forces except near the wall. Consequently changes occurring in the velocities of the outer boundary layer due to the pressure increase may be calculated by Bernoulli's relationship. It is concluded that separation occurs when the velocity corresponding to the ratio  $u/U = 0.6$ , is brought to rest by the pressure increase

i.e. 
$$\frac{P_0}{P} = \left[ 1 + \left( \frac{\gamma-1}{2} \right) M^2 \right]^{\gamma/\gamma-1} \quad (2.24)$$

and

$$\frac{P_0}{P_s} = \left[ 1 + \left( 1 - \frac{u^2}{U^2} \right) \left( \frac{\gamma-1}{2} \right) M^2 \right]^{\gamma/\gamma-1} \quad (2.25)$$

giving

$$\frac{P_s}{P} = \left[ \frac{1 + \frac{\gamma-1}{2} M_0^2}{1 + 0.64 \left( \frac{\gamma-1}{2} \right) M_0^2} \right] \quad (2.26)$$

Once again comparison with experimental results is fair up to a Mach number of 3.

Summing up, Gadd suggests that an analysis on the lines of that applied to the laminar boundary layer, taking a more adequate account of the fluid at the wall would be preferable.

This was not attempted, however, because of uncertainties as to the relation between the turbulent friction stress and the shape of the velocity profiles.

### 2.3.2 The method of Stratford.

STRATFORD<sup>(16)</sup> suggests a method, for the determination of the position of separation for the turbulent boundary layer, which results from an approximate solution of the equations of motion and involves a single empirical factor. The equations involved are integrated by a modified "inner and outer" solutions technique; the resulting expression being applicable directly to the separation position.

The contention that the turbulent boundary layer in a "pressure rise" may be divided into two distinct regions - an outer historical region with almost zero shear losses and an inner region with small inertia forces such that pressure gradient and

shear stress are balanced within a distorted, anchored profile - is identical to the method of GADD<sup>(15)</sup> as applied to the laminar boundary layer. Stratford, apparently, is not so uncertain as to the effect of turbulent shear stress on the assumed velocity profile.

The treatment applied by Stratford is summarised in Figures 2.2 and 2.3. At  $x = x_0$ , the profile is assumed to be unchanged except at  $y = 0$ . Just downstream of  $x_0$  there is a general lowering of the velocity in the outer layer (A) and an assumed change of shape in the inner layer (B) as indicated below.

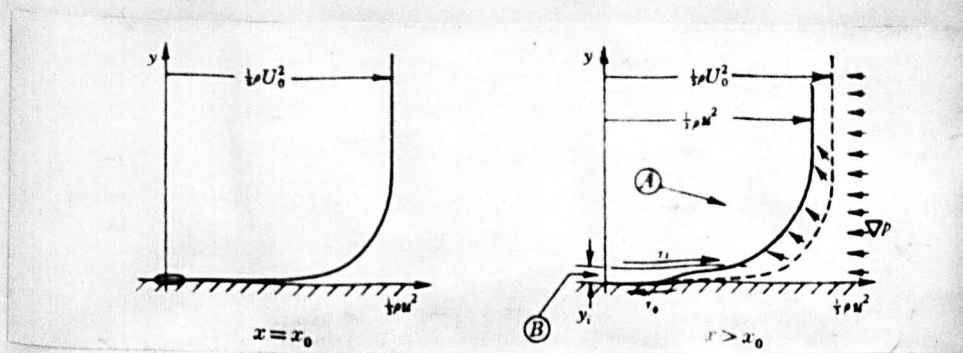


FIGURE 2.2 DEVELOPMENT OF A BOUNDARY LAYER IN  
A SUDDEN PRESSURE GRADIENT.

At the separation position (Figure 2.3) it is postulated by Stratford that the zero skin friction situation is reached when the backward force  $y_i \Delta p$  is balanced by the shear stress  $(T_i - T_0)$  where  $T_0 = 0$ .

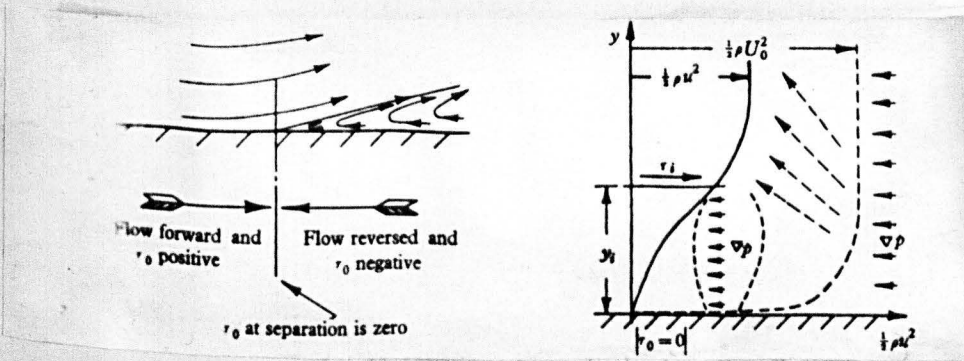


FIGURE 2.3 THE SEPARATION POSITION.

For the inner layer Stratford argues that the pressure forces must be balanced entirely by the shear force gradient, i.e.

$$\frac{\partial P}{\partial x} = \frac{\partial T}{\partial y} ; (y = 0) \quad (2.27)$$

Also, if the wall stress  $T_0$  is zero, dimensional similarity requires that;

$$u = \left( \frac{y}{e} \frac{\partial T}{\partial y} \right)^{1/3} \cdot F \left[ \frac{1}{e} \left( \frac{\partial T}{\partial y} \right) \frac{y^3}{v^2} \right] \quad (2.28)$$

when considering a region very near to the wall, i.e. satisfying  $y \left( \frac{\partial^2 T}{\partial y^2} \right)_0 \ll \left( \frac{\partial T}{\partial y} \right)_0$ .

In the fully turbulent part of the inner flow, the relative motion is independent of the viscosity and therefore Stratford contends

$$u = A \left( \frac{y}{e} \cdot \frac{\partial T}{\partial y} \right)^{1/2} + B \left( \frac{y}{e} \cdot \frac{\partial T}{\partial y} \right)^{1/3} \quad (2.29)$$

where  $A$  and  $B$  are constants.

By approximation, equation 2.29 gives

$$\frac{1}{2} eu^2 = \frac{1}{2} A^2 y \left( \frac{\partial T}{\partial y} \right)_0 = \frac{1}{2} Ay \frac{\partial P}{\partial x} \quad (2.30)$$

giving, in turn

$$u = y^{1/2} \left( \frac{A}{e} \frac{\partial P}{\partial x} \right)^{1/2} \quad (2.31)$$

which Stratford prefers to write in the form

$$\frac{1}{2} eu^2 = \left( \frac{2}{0.41 \beta^2} \right) \cdot \frac{\partial P}{\partial x} \cdot y \quad (2.32)$$

Where  $\beta$  is an empirical factor considered to be essential to the analysis of turbulent boundary layers by virtue of the necessary approximations involved.

For the outer flow region, Stratford's imposed conditions suggest that the dynamic head at any point in a turbulent boundary layer acted upon by an adverse pressure gradient is equal to the dynamic head of a free boundary layer minus the rise in static pressure, i.e.

$$\frac{1}{2} \rho u^2(x, \phi) = \frac{1}{2} \rho u_i'^2(x, \phi) - (p - p_0) \quad (2.33)$$

$$\text{for } \phi \geq \phi_i;$$

where  $\phi$  is a stream function given by

$$\phi = \int_0^y u \, dy \quad (2.34)$$

Note: The suffix  $i$  denotes the assumed streamline dividing inner and outer flow regions.

Suffix  $o$ , in this derivation, refers to the situation where a normally free boundary layer meets a sudden, small pressure rise, sufficiently large to cause an instantaneous change in the assumed profile.

Using the results of the work by GOLDSTEIN(17) and SCHLICHTING(18), Stratford gives the empirical solution for the velocity of the free boundary layer as

$$\frac{u^*}{U_0} = \left(\frac{y^*}{\delta^*}\right)^{1/n} \quad (2.35)$$

where 
$$\delta^* = \frac{(n+1)(n+2)}{n} \theta^* \quad (2.36)$$

$$\theta^* = 0.36 \cdot x \cdot R_x^{-1/5} \quad (2.37)$$

The joining situation between the inner and outer layers is said to occur where  $\delta, \partial u / \partial y|_{\text{inner}} = \delta, \partial u / \partial y|_{\text{outer}}$ . By differentiation, equating equations 2.35 and 2.36 and eliminating the quotient  $(y^*/\delta^*)$  by substitution from equations 2.35, 2.36 and 2.37 he obtains

$$(2C_p)^{1/4} (\eta-2) \left(x \frac{dC_p}{dx}\right)^{1/2} = 1.06 \beta (10^{-6} R_x)^{1/10} \quad (2.38)$$

FOR  $\left[C_p \leq \frac{\eta-2}{\eta+1}\right]$

where  $C_p = (p - p_0) / \frac{1}{2} \rho U_0^2$ ,  $R_x =$  local value of the Reynolds number based on distance  $x$  and peak velocity  $U_0$ . The limitation on  $C_p$  results formally from the join of the inner and outer layers reaching the edge of the boundary layer when using the



idealised velocity profiles. The same limitation applies to the empirical determination of  $\beta$ .

Comparison with experimental results<sup>(16)</sup> suggests that equation 2.38 should be satisfied for values of  $\beta$  between 0.66 and 0.73, in order to obtain values of the various parameters appertaining to the point of separation. The method is said to predict pressure rise to separation values from 0 to 10 per cent low but Stratford contends that it has the advantage of speed and rationality over other methods<sup>(17, 19, 20, 21, 22, 23, 24)</sup> involving the solution of the momentum and energy equations with the aid of various empirical functions.

TOWNSEND<sup>(25)</sup> states, however, that the theoretical results are "worse than expected" when compared with the experiments of SCHUBAUER & KLEBANOFF<sup>(26)</sup>.

### 2.3.3 Arens and Spiegler.

ARENS and SPIEGLER<sup>(27)</sup> apply a similar approach to that of Gadd, when considering turbulent boundary layer separation in a convergent divergent duct.

They commence their treatise with a description of the various forms of separation to be expected in a duct as described by SHAPIRO<sup>(28)</sup>. They continue with a discussion of practical results obtained by various researchers, FRAZER et al<sup>(29)</sup>, MCKENNEY<sup>(30)</sup> and FOSTER and COWLES<sup>(31)</sup> and conclude that separation occurs at the point where the nozzle wall pressure reaches a particular fraction of the ambient pressure, quoting the Summerfield criterion of  $P_s/P = 0.4$ . It is stated that, within the scatter of experimental data for the ratio of wall to ambient pressures at separation, there is no consistent significant difference between two dimensional and axisymmetric nozzles, nor can any trend be detected as a function of nozzle half angle for a range between  $7^\circ$  and  $30^\circ$ . Further assumptions are:

- (1) Reynolds number has no significant effect on the separation pressure ratio.
- (2) The effect of pressure gradient and boundary layer history may be neglected.
- (3) The pressure ratio required to separate a turbulent boundary layer is independent of the geometry of the interactions.

(4) Pressure rise must be sufficient to stagnate a characteristic velocity  $u_s$  in the boundary layer, as first suggested by Gadd.

(5) Stagnation temperature is constant.

Using the above assumptions they suggest a characteristic Mach number of

$$M_s^* = \frac{M_s (u_s^*/u_s)}{\left\{1 + [(\gamma-1)/2] M_s^2 [1 - (u_s^*/u_s)^2]\right\}^{1/2}} \quad (2.39)$$

For  $M_s^* < 1$ , stagnation is assumed to occur isentropically giving a pressure ratio requirement, as per Gadd, of

$$\frac{P_b}{P_s} = \left\{ \frac{1 + [(\gamma-1)/2] M_s^2}{1 + [(\gamma-1)/2] M_s^2 [1 - (u_s^*/u_s)^2]} \right\} \quad (2.40)$$

definitions being shown in Figure 2.4 below.

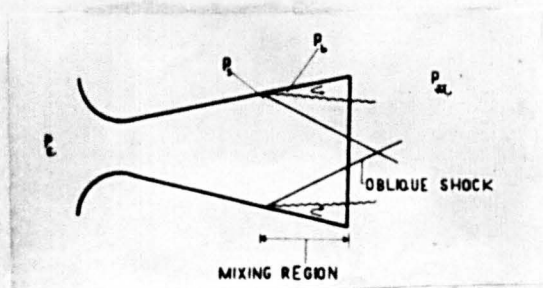


FIGURE 2.4

OVEREXPANDED NOZZLE WITH SEPARATED FLOW.

For  $M_s^* > 1$  isentropic stagnation is assumed to be preceded by normal shock compression and an expression produced accordingly.

Comparison of the ratio  $P_s/P_b$  as computed by the equations 2.39 and 2.40 above with results available at the time of publication (29, 32, 33, 34, 35, 36) are shown in Figure 2.5 below for  $U_s^*/U_s = 0.6$ .

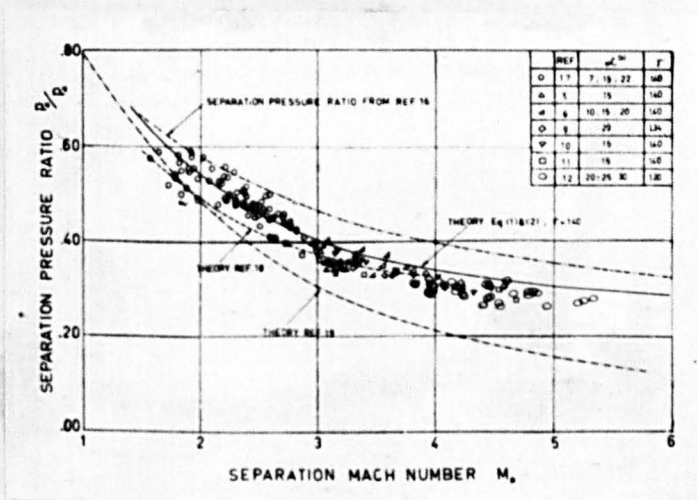


FIGURE 2.5 NOZZLE SEPARATION PRESSURE RATIO.

A further relationship is derived by eliminating  $M_s$  between the expression

$$M_s^2 = [2/(\gamma-1)] [(P_c/P_a)^{(\gamma-1)/\gamma} (P_a/P_s)^{(\gamma-1)/\gamma} - 1] \quad (2.41)$$

and 2.40 shown above giving, explicitly, the ratio of separation pressure to ambient pressure as a function of the nozzle pressure ratio. Which, for  $M_s \ll 1$  and assuming  $P_b = P_a$  becomes

$$\frac{P_s}{P_a} = \frac{P_c/P_a}{\left[ \frac{(P_c/P_a) - (u_s^*/u_s)^2}{1 - (u_s^*/u_s)^2} \right]^{\gamma/(\gamma-1)}} \quad (2.42)$$

an extremely simple equation to use if the value of  $u_s^*/u_s$  is approximated. Arens and Spiegler suggest 0.56 as a sensible value to agree with experimental results.

It is interesting to note that the final expression applies for  $M_s^* \ll 1$  which by substitution corresponds to an  $M_s$  of approximately 2. Therefore, if it assumed that back pressure only affects the velocity in the subsonic boundary layer

$$u_s^*/u_s \approx 1/M_s$$

which is the basic assumption appertaining to the new theory contained herein (Section 3, p. ).

## 2.3.4 Mager.

MAGER (38) commences with an approach to the effects of an oblique plane shock impinging on a turbulent boundary layer and suggests that the results may be applied to free separation occurring in divergent nozzles.

Referring to Figure 2.6 Mager makes the following assumption

$$M_s^2 = K M_i^2 \quad (2.43)$$

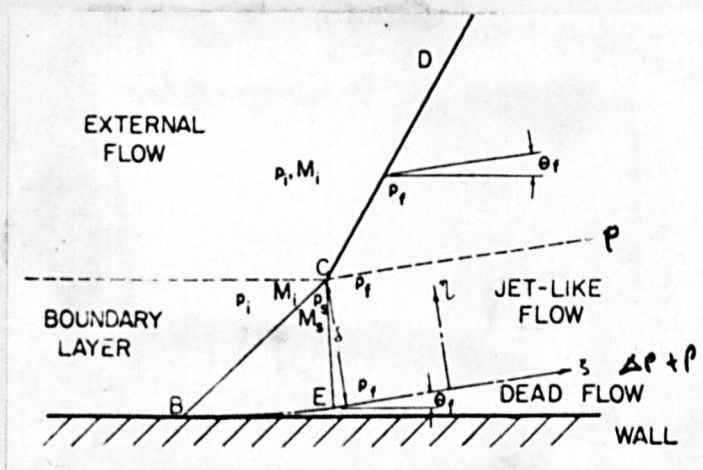


FIGURE 2.6 MODEL OF THE FREE SHOCK SEPARATED  
TURBULENT BOUNDARY LAYER.

which, together with the oblique shock approximation, gives the pressure ratio across the separation wave B - C, i.e.

$$p_s/p_i = 1 + \frac{\gamma M_i^2}{2} \frac{(1 - K)}{1 + [(\gamma - 1)/2] M_i^2} \quad (2.44)$$

Since the boundary layer cannot stand a very large pressure ratio without separation, the conditions across the wave B - C must be similar to those across a Mach wave - that is, the use of the oblique shock approximation is essential to the determination of the correct pressure ratio  $p_s/p_i$ .

The boundary layer is assumed to curve, after separation, under the action of a transverse pressure differential  $\Delta P$ . Assuming that the pressure in the transition region is dependent on  $\Delta P$  and some function of  $(\eta_b/\delta)$ , see Figure 2.6, utilising the momentum equation in the  $\eta_b$  direction and using an incompressible transformation suggested by DERODNIETZYN-STEWARTSON<sup>(39)</sup>, Mager, after much manipulation, obtains

$$\frac{p_f}{p_i} = 1 + 0.328 \frac{\gamma M_s^2 \theta_f}{1 + [(\gamma - 1)/2] M_s^2} \quad (2.45)$$

$\theta_f$  being defined in Figure 2.6.

As per Gadd, Mager uses the main stream shock wave approximation to give another expression relating  $\theta f$ ,  $M_s$  and  $p_f/p_i$

$$\text{i.e. } \theta f \doteq (\sqrt{M_1^2 - 1/\gamma} M_1^2) [(p_f/p_i) - 1] \quad (2.46)$$

giving the ultimate approximation

$$\frac{P_f}{P_i} \doteq (P_s/P_i) \{ 1 + G [ 1 - (P_s/P_i) ] \} \quad (2.47)$$

where 
$$G \equiv -0.328 \frac{K\sqrt{M_i^2 - 1}}{1 + (\gamma - 1/2)KM_i^2} \quad (2.48)$$

Comparison with the data proffered by SCHUH(40) indicated to Mager that  $K = 0.55$  would be a suitable value to assume for fair comparison of his theory with practice.

The theory is shown plotted in Figure 2.7 and is compared with the results of various investigators.



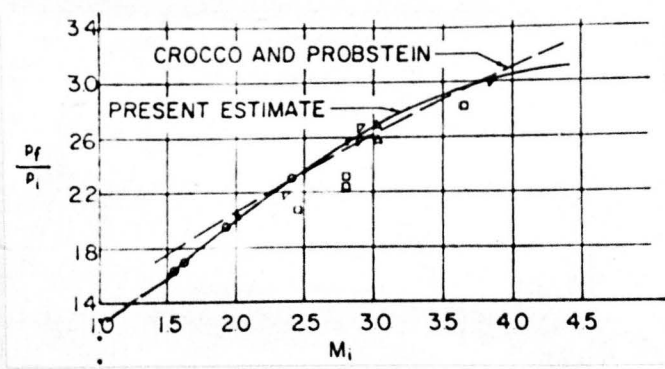


FIGURE 2.7 PRESSURE RATIO OF FREE SHOCK SEPARATED  
TURBULENT BOUNDARY LAYER . ( $\gamma = 1.4$ , Plane shock)

The theory, it is suggested, may be used for free shock separation simply by plotting  $P_a / P_i$  versus  $M_i$  on Figure 2.7, the point of intersection corresponding to the separation situation, i.e. it is assumed that  $P_a = P_f$  for free separation. Turbulent mixing processes are ignored.

2.4 Concluding comment.

Many other methods are available for the solution

of turbulent boundary layers, e.g. the methods of BURI, TRUCKENBRODT<sup>(41)</sup>, DOENHOFF and TETERVIN<sup>(19)</sup> and GARNER<sup>(42)</sup>, each attempting to derive particular shape factors applicable to the problems associated with separating boundary layers. Generally, though, they are not readily applicable to the problems occurring in overexpanded supersonic jets.

It is concluded, from the brief review put forward above, that the methods of Arens and Spiegler and Mager, neglecting their theoretical limitations, are probably the easiest to apply and give a fair indication of the conditions appertaining to separation of the boundary layer under the duress of an adverse pressure gradient. For theoretical plausibility, and perhaps better accuracy, the method derived in the following section would seem to be more applicable in this situation.

CHAPTER III

THEORETICAL APPROACH TO SEPARATION

3. THEORETICAL APPROACH TO SEPARATION.

3.1 Introduction.

Considered is a discrete point in the formation of the boundary layer; that of the beginning of the process of separation. Use of the theory shows that supersonic, laminar or turbulent, compressible boundary layers with imposed adverse pressure gradient may be treated with equanimity providing the immediate velocity profile is known or may be approximated. Fortunately, sufficient detail is given in the literature of experimental velocity profile determination such that use no longer becomes assumptive.

Before considering the mathematical argument, the suggested cause of separation must be accepted. This is as follows.

3.2 The concept of boundary layer feedback.

In what follows, free separation refers to that which may occur in supersonic flow through convergent-divergent ducts, i.e. not induced by manufactured discontinuities such as a shock generated

by a knife edge in the free stream or an abrupt step occurring in the wall adjacent to the boundary layer considered. The latter form of separation will be referred to as shock induced separation.

### 3.2.1 Free separation.

Theoretical consideration of a gas expanding through a duct requires knowledge of the conditions prevailing in two principle flow regions - main stream and boundary layer. The former, in a convergent and divergent duct, is usually assumed to be inviscid and isentropic with virtually zero transverse velocity gradient; the latter, viscous flow with a varying transverse velocity profile. If the velocity of the main stream is supersonic it seems reasonable to assume that the downstream conditions can have little or no effect on the flow characteristics unless somewhere in the total flow development there is a feedback path provided. The assumption with boundary layer theory is that at an adjacent wall the stream velocity is zero with a large transverse velocity gradient, until at some clearly defined thickness the velocity is approximately that of the main stream. Obviously,

somewhere between these two boundaries is situated a sonic stream line. The gas trapped between the sonic line and the duct wall is conscious of the prevailing downstream conditions and, more important, provides a feedback path for this information.

The high pressure experienced in the convergent portion of the duct is followed by rapid expansion and subsequent pressure drop, often to pressures as low as 2 lb/in<sup>2</sup> absolute when followed by reattachment. This pressure distribution, for most purposes, may be assumed constant across the total flow section. Therefore, a superimposed adverse or positive pressure gradient introduced to the boundary layer by ambient conditions acting downstream, will cause a slowing down of the subsonic flow stream causing, in turn, a general thickening of the boundary layer. If the adverse pressure gradient is of sufficient magnitude, the boundary layer separates from the duct wall causing a series of compression wavelets which combine to form an oblique shock. This has a distinct effect on the main stream flow because of the abrupt pressure rise which occurs across the shock wave. Of importance is the suggestion that the main stream oblique shock occurs as a consequence of, and immediately after, separation,

which is itself a function of the momentum and pressure gradient in the immediate vicinity. From the results of free separation contained herein, it is obvious that the resulting shock has little or no effect on the separation condition once affected - i.e. no iteration is necessary about the initial point of separation due to any subsequent pressure developments associated with the generated shock. The adverse pressure initially causing separation is greater than that which may occur due to any rise across the shock. Therefore, it is further postulated that the consideration of the shock wave in the determination of the point of separation is unjustifiable in the free separation situation.

3.2.2 Shock induced separation.

Following this argument to its logical conclusion it can be seen that the process may be extended to include shock and step induced separation also. For example, a generated shock impinging on a boundary layer will cause an abrupt pressure rise downstream of interaction which is, in turn, fed back through the subsonic boundary layer until the momentum/force compatibility situation is reached,

whereupon separation takes place ahead of the shock. Similar reasoning is applicable to the sudden step situation.

On the basis of the previous argument the following simple theory has been developed. It will be shown that it is not only applicable to laminar compressible flow but also to turbulent boundary layers with or without subsequent reattachment.

### 3.3 Theoretical evaluation of the conditions at separation.

The conditions appertaining to the situation of separation may be obtained by equating the momentum forces of the subsonic boundary layer to those associated with the immediate pressure gradient. The resulting expression provides a simple relationship between isentropic Mach number at the beginning of separation and the overall pressure ratio. A dependence on Reynolds number is indicated.

#### 3.3.1 Assumptions.

1. All the conditions are those appertaining at the minimum pressure situation immediately prior



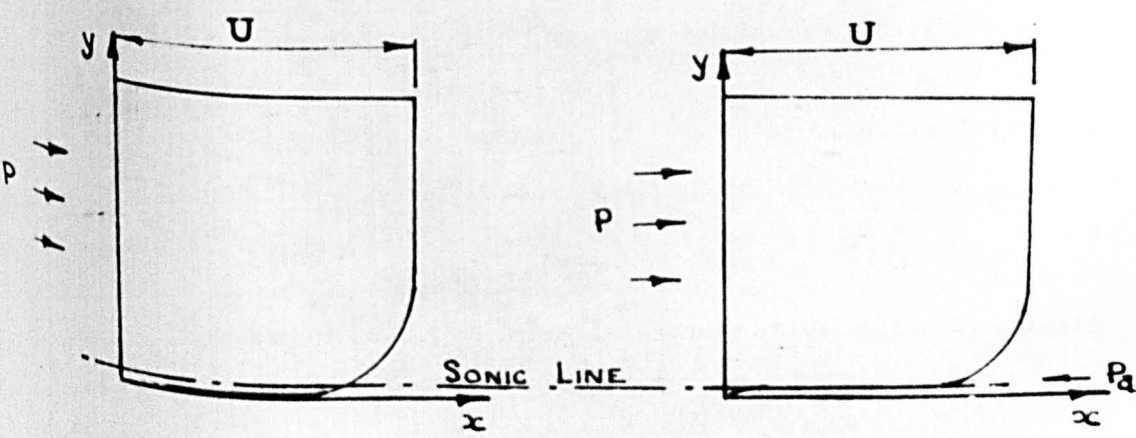
to the commencement of separation.

2. The velocity profile of a free boundary layer, i.e. that which is not subjected to an adverse pressure gradient, is known and may be related to the local Reynolds number.

3. Density may be assumed constant across the flow section considered.

4. Main stream conditions at the point considered may be determined by the one dimensional isentropic gas equations.

5. The adverse pressure gradient affects the subsonic layer only. Turbulent jet mixing may be neglected.



(a) Free boundary layer profile.

(b) Free boundary layer profile with superimposed pressure gradient.

FIGURE 3.1 THE ASSUMED SITUATION NEAR SEPARATION.

Figure 3.1 shows the assumed effect of an adverse pressure differential superimposed on a free boundary layer velocity profile at a position close to separation.

The momentum of the boundary layer below the sonic stream line per unit width of flow is

$$\bar{M}_s = \int_0^{\delta_s} \rho \cdot u^2 dy \quad (3.1)$$

where

$$\frac{u}{U} = \phi\left(\frac{y}{\delta}\right) \quad (3.2)$$

At the beginning of the process of separation it is assumed that the momentum of the fluid between the sonic line and the wall boundary is reduced to zero by the action of the fed back pressure.

The force capable of such action is given by

$$\int_0^{\delta_s} (P_a - P) dy \quad (3.3a)$$

Invoking the usual assumption with boundary layer theory,

$$\text{i.e.} \quad \frac{dP}{dy} = 0$$

(3.3a) becomes

$$(P_a - P) \delta_s \text{ per unit width of flow} \quad (3.3b)$$

Therefore, at the instant of separation

$$\bar{M}_s = \int_0^{\delta_s} U^2 \phi_2 \left( \frac{y}{\delta} \right) dy = (P_a - P) \delta_s \quad (3.4)$$

where  $\phi_2 \left( \frac{y}{\delta} \right) = \left[ \phi \left( \frac{y}{\delta} \right) \right]^2$   $\phi = f(\eta)$

$P$  is the local mainstream pressure corresponding to the local Mach number  $M$  - assuming a zero transverse pressure gradient.

By selecting a particular velocity profile, equation (3.4) may be satisfied by a method of trial and error to obtain the assumed point of separation. If the left-hand side (L.H.S.) is larger than the right-hand side (R.H.S.), the subsonic boundary layer has an excess of momentum and separation has not yet been reached, a larger Mach number must therefore be assumed. Obviously the converse obtains for  $R.H.S. > L.H.S.$

It will be shown later (section 3.3.3), however, that an explicit relationship equating overall pressure ratio to Mach number, may be obtained when assuming isentropic expansion to the point of separation, simplifying the arithmetical effort considerably.

### 3.2.3 Selection of the velocity profiles.

A dependable relationship for the variation of the mean velocity profile with Reynold's number, Mach number and pressure gradient for compressible turbulent boundary layers is, at present, unknown and in this context unnecessary. From the experimental evidence available<sup>(1, 2, 3, 4, 5, 6)</sup> it is known that the mean velocity profile in a compressible turbulent boundary layer under zero or favourable (negative) pressure gradients can be approximated by the similar power law profile

$$\frac{u}{U} = \left(\frac{y}{\delta}\right)^{1/n} \quad (3.5)$$

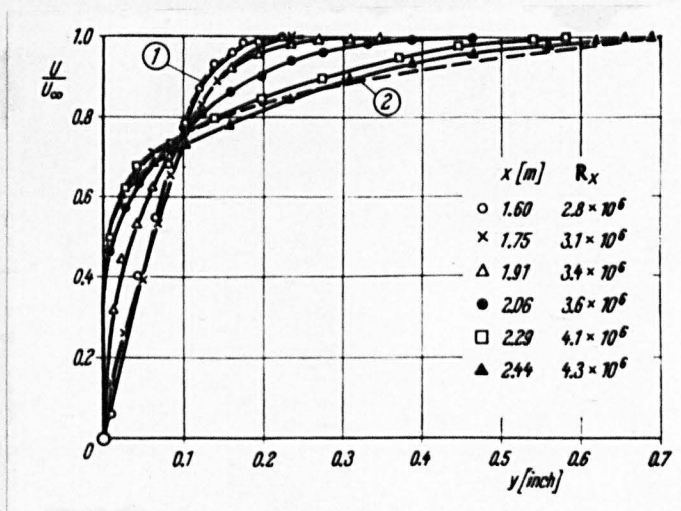
In his experiments with smooth pipes and flat plates, NIKURADSE<sup>(7, 8)</sup> has shown that expression (3.5) holds for the discrete range of Reynold's numbers  $Rx = 1.7 \times 10^6$  to  $18 \times 10^6$ . Indications are that the value of the profile parameter increases with increase in Reynold's number<sup>(1, 3, 6)</sup> and as an approximate guide TUCKER<sup>(2)</sup> suggests

$$n = 2.6 Rx^{1/14} \quad (3.6)$$

to be valid, where  $Rx$  is based on the effective

length of boundary layer growth. The expression was obtained empirically.

For an indication of the velocity profiles appertaining to the transition region the reader is referred to the results of Schubauer and Klebanoff; a selection of profiles being shown in Figure 3.2 for a turbulence intensity of 0.03%. Usually turbulence intensity is of the order of 0.5% in flow situations similar to those under consideration whereupon transition is likely to occur at  $R_x = 3.5 \times 10^5$  to  $10^6$ .



- (1) Laminar flow. Blasius profile. ( $\delta = 1.36$  in.)  
 (2) Turbulent  $n = 7$  power law. ( $U = 89$  ft/sec.)

FIGURE 3.2 VELOCITY PROFILES IN A BOUNDARY LAYER  
ON A FLAT PLATE IN THE TRANSITION REGION. (ref.9)

Therefore, it is concluded that for the range suggested by Nikuradse the power law (expression 3.6) will hold. For laminar profiles of relatively high Reynold's numbers the Blasius profile<sup>(10)</sup> is acceptable and at low values of  $R_x (< 10^5)$  the Prandtl profile may be assumed or the approximation  $n = 2$  used in this context. Similar results may be expected when using the sine approximation to the laminar profile.

### 3.5.3 General power law profile solution.

Assuming, initially, that the velocity profile in a boundary layer before an adverse pressure gradient is superimposed may be represented by the power law, i.e.

$$\frac{u}{U} = \left(\frac{y}{\delta}\right)^{1/n} \quad (3.5)$$

then

$$u^2 = U^2 \left(\frac{y}{\delta}\right)^{2/n}$$

From (3.1)

$$\bar{M}_s = \int_0^{\delta_s} e U^2 \left(\frac{y}{\delta}\right)^{2/n} dy$$

which, by virtue of assumption (3) integrates to:

$$\begin{aligned} \bar{M} &= \frac{e U^2}{\delta^{2/n}} \frac{n}{(n+2)} \left[ y^{(2/n)+1} \right]_0^{\delta_s} \\ &= \frac{n e U^2}{(n+2)} \left(\frac{\delta_s}{\delta}\right)^{\frac{2}{n}} \cdot \delta_s \end{aligned} \quad (3.7)$$

From equation (3.5), when  $u = u_s$

$$\frac{u_s}{U} = \left(\frac{\delta_s}{\delta}\right)^{1/n} = \frac{1}{M} \quad ? \quad T, /$$

which modifies (3.7) to

$$\bar{M}_s = \frac{n e U^2}{(n+2) M^2} \cdot \delta_s \quad (3.8)$$

This may be substituted in (3.5) to give

$$n e U^2 / (n + 2) M^2 = P_a - P \quad (3.9)$$

$e$ ,  $U$  and  $P$  are the local values of density, mainstream velocity and pressure which may be expressed in terms of their respective stagnation values and local Mach number by the one dimensional isentropic equation, i.e.

$$\frac{P_0}{P} = \left[ 1 + \frac{k-1}{2} M^2 \right]^{k/k-1} \quad (3.10)$$

$$\frac{e_0}{e} = \left[ 1 + \frac{k-1}{2} M^2 \right]^{1/k-1} \quad (3.11)$$

$$\frac{T_0}{T} = \left[ 1 + \frac{k-1}{2} M^2 \right] \quad (3.12)$$

$$U^2 = 2 k R (T_0 - T) / (k-1) \quad (3.13)$$

Letting  $\beta = 1 + (k-1) M^2/2$  for convenience; the velocity expression (3.13) becomes

$$U^2 = 2 kR (\beta - 1) T_0 / \beta (k - 1) \quad (3.14)$$

which, on substitution in (3.9) together with the respective expressions for  $e$  and  $P$  (3.11 and 3.10) gives

$$\frac{P_0}{\beta^{k/(k-1)}} + \frac{2kn T_0 e_0 R (1 - 1/\beta)}{(k-1)(n+2) \beta^{1/(k-1)} M^2} = P_a \quad (3.15)$$

Using the universal gas equation viz:

$$P_0 = e_0 R T_0$$

rearranging and substituting back for  $\beta$  gives

$$\left[ kn/(n+2) + 1 \right] P_0/P_a = \left[ 1 + M^2(k-1)/2 \right]^{k/(k-1)} \quad (3.16)$$

Resulting in the expression for local Mach number at the beginning of separation;

$$M^2 = 2 \left\{ \left[ kn/(n+2) + 1 \right] (P_0/P_a)^{(k-1)/k} - 1 \right\} / (k-1) \quad (3.17a)$$

when  $n = 7$   $k = 1.4$ , equation (3.7) simplifies to

$$\left[ 6.17 (P_0/P_a)^{0.286} - 5 \right]^{0.5} = M \quad (3.17b)$$



It will be noted that a 40% change in  $n$  results in a variation of the Mach number,  $M$ , of only 1%.

Figure 3.3 shows the variation of separation Mach number with pressure ratio for  $n = 7$ .

Determination of the Mach number at separation enables the area ratio to be computed from

$$\frac{A}{A_t} = \frac{1}{M} \left[ \frac{1 + \left[ \frac{(k-1)}{2} \right] M^2}{\left( \frac{k+1}{2} \right)} \right]^{(k+1)/2(k-1)} \quad (3.18a)$$

with  $k = 1.4$

$$A/A_t = \left[ (5 + M^2) / 6 \right]^3 / M \quad (3.18b)$$

It is interesting to note that separation will theoretically occur at a particular value of  $P/P_a$  for any given Reynold's number or choice of index  $n$ .

The point of separation may be derived from (see Figure 3.4)

$$(A/A_t - 1) \tan(\alpha/2) = a \quad (3.19)$$

$$\text{and } x_t = a \cos \alpha \quad (3.20)$$

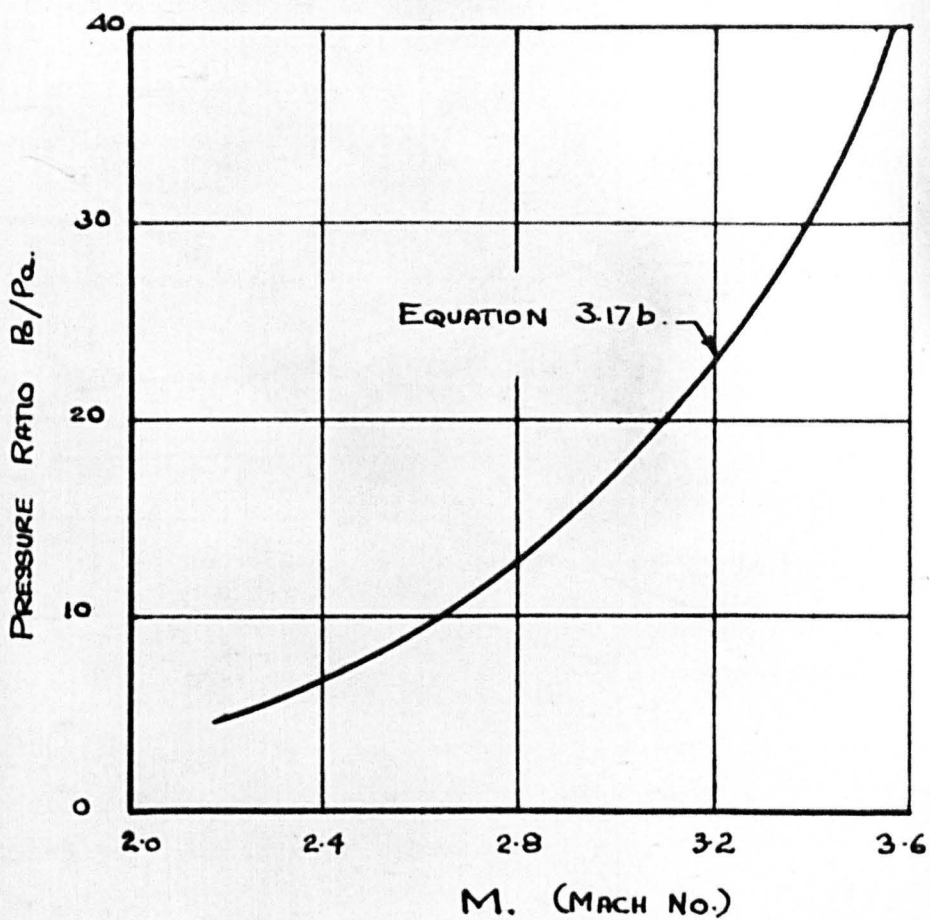


FIG 3.3 THEORETICAL MACH No. AT THE MINIMUM PRESSURE SITUATION PRIOR TO SEPARATION V/S OVERALL PRESSURE RATIO.

Where  $x_t$  is the distance from the throat to the point of separation.

### 3.3.4 Numerical example.

Consider the duct shown below (Figure 3.4)

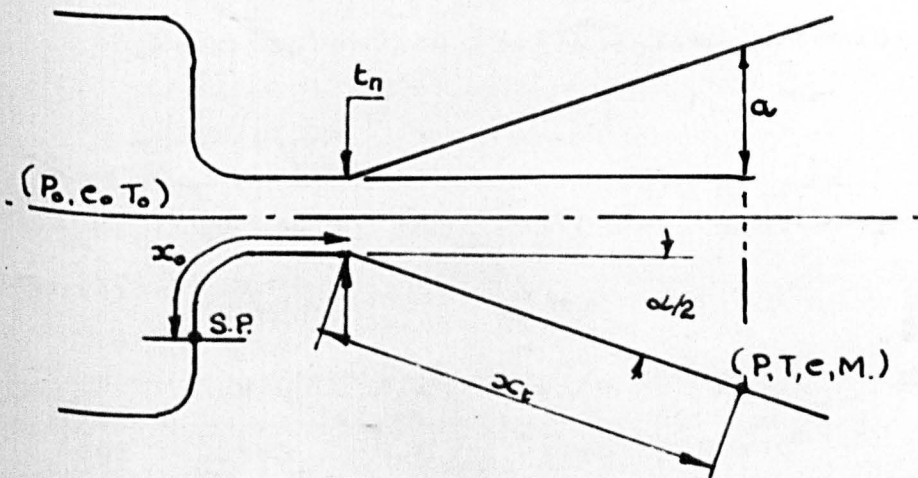


FIGURE 3.4 THE EXPERIMENTAL DUCT.

$x$  is measured from the assumed stagnation point (S.P.) and for the configuration shown is given by

$$x = x_0 + x_t \quad (3.21)$$

where, in this case,  $x_0 = 0.752$  inches.

Requirement:

To derive the theoretical position of the beginning of separation for the conditions

$$P_o = 215 \text{ lb/in}^2 \text{ Abs. } T_o = 480^\circ\text{K}$$

$$t_n = 0.20 \quad \alpha = 40^\circ$$

$P_a$  is assumed to be  $14.7 \text{ lb/in}^2 \text{ Abs.}$

From expression (3.17b), i.e. assuming  $n = 7$ ,

$$M = 2.885$$

giving, from use of the isentropic equations, separation conditions

P	M	A/At	$e_o/e$	$U^2$	$P_o/P_a$
6.98	2.885	3.8	11.6	$3.59 \times 10^6$	30.8

corresponding to

$$a = 0.28 \text{ inches} \quad x_t = 0.82 \text{ inches}$$

i.e.  $x_t/t_n = 4.1$

Using the value of viscosity  $\mu_o$  at temperature  $T_o$  obtained from Figure 3.5 in combination

with the viscosity approximation of SUTHERLAND's (11) formula, i.e.

$$\frac{\mu_0}{\mu} = \frac{T_0}{T}^{0.76} \quad (3.22)$$

The Reynold's number  $R_x$  calculates to  $5.3 \times 10^6$  suggesting that the computed values may be accepted at  $n = 7$ .

Comparable experimental results are

$$b = 0.85 \quad P = 6.8 \quad x_t/t_n = 4.25$$

showing a positional variation of approximately 2 - 3%.

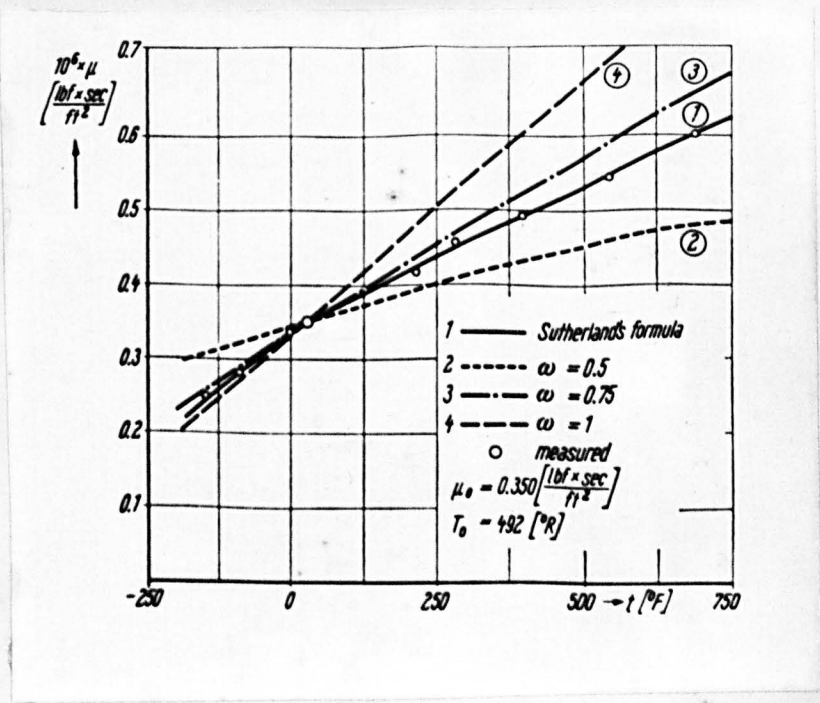


FIG. 3. 5. VARIATION OF VISCOSITY WITH TEMP.

### 3.3.5 The effect of reattachment.

Immediately after separation the main flow stream experiences conditions similar to those of a free jet exhausting near an inclined wall.

The boundary of the separated flow mixes with the surrounding air of ambient pressure promoting large velocity gradients with subsequent localised pressure drop between the jet boundary and the duct wall resulting from the turbulent jet mixing process.

The pressure gradient across the shock, together with main stream momentum and localised entrainment, modifies the flow direction from that of separated flow to one of progressive reorientation toward the wall, culminating in reattachment at a point somewhere downstream.

At reattachment, the flow/momentum relationship stabilises in the enclosed reverse flow region, the average pressure of which is somewhat below ambient but above  $P$  and the average static pressure in the jet. As suggested earlier, for any assumed velocity profile separation begins at a particular pressure ratio ( $P/P_a$ ) consequently, the point of separation

iterates downstream until momentum/force balance is once again achieved. Providing the value of the average pressure in the vortex is known or may be approximated the above theory holds.

Surprisingly, even allowing for the errors involved due to asymmetric separation experienced in a duct designed for overexpansion with subsequent reattachment, comparison with experiment show differences of similar order to the free separation situation.

### 3.3.6 Example with reattachment.

Assuming a duct of similar dimensions to that shown in paragraph 3.3.4, but including reattachment, the respective initial conditions become

$$P_o = 215 \text{ psia.}; \quad T_o = 480^\circ\text{K.}; \quad t_n = 0.200 \text{ inches}$$

$$\alpha = 40^\circ; \quad P_a = 5.2 \text{ psia. (measured).}$$

The theoretical values at separation are, therefore,

P	M	A/At	$e_o/e$	$U^2$	$P_o/P$
2.46	3.6	7.5	24.4	$4.16 \times 10^6$	87.5

and should be compared with the values determined for the free separation condition (paragraph 3.3.4).

From equations (3.19) and (3.20)

$$a = 0.65 \text{ inches} \quad x_t = 1.9 \text{ inches}$$

giving  $x_t/t_n = 0.95$

Actual measured values being

$$P_a = 5.2; \quad P_s = 2.6; \quad x_t/t_n = 0.925$$

Therefore, even allowing for the errors involved due to the asymmetric separation experienced in a duct designed for overexpansion with reattachment (see Figure 3.6 below), the results are surprisingly close.



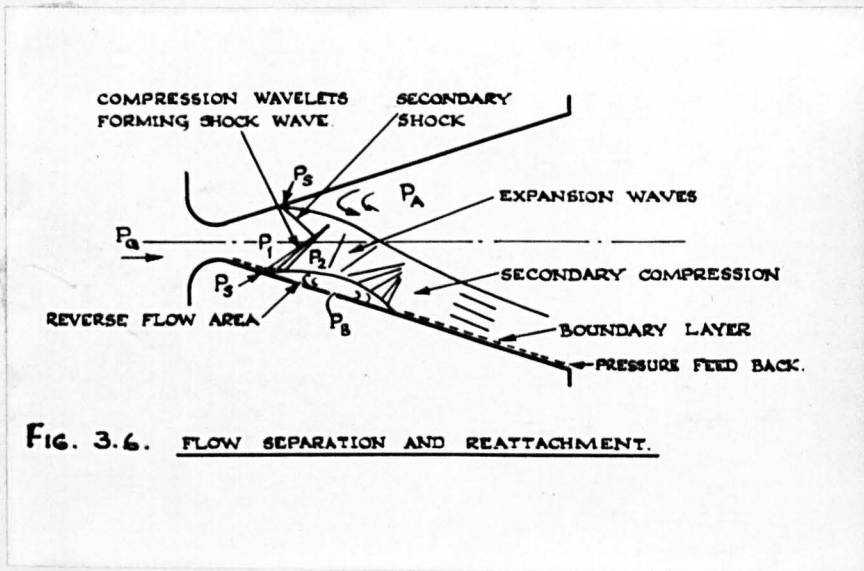


**FIG. 3.6. FLOW SEPARATION AND REATTACHMENT.**

### 3.3.7 Brief note on laminar boundary layers.

It is suggested that for boundary layers of relatively low Reynold's number, i.e.  $R_x < 10^5$  the sine approximation should be used. An alternative is to put  $n = 2$  on the power law series.

The expressions relating to the sine approximation are:

$$u/U = \sin \left( \frac{\pi y}{2\delta} \right) \quad (3.2.3)$$

$$U^2 e \left[ 1 - \frac{r}{\pi} \sin \left( \frac{\pi}{r} \right) \right] / 2 = (P_a - P) \quad (3.2.4)$$

where

$$1/r = \delta_s / \delta = \frac{2}{\pi} \sin^{-1} \left( \frac{1}{M} \right) \quad (3.2.5)$$

Use of the above expressions with fully developed turbulent flow show positional errors ( $x/t_n$ ) of the order of 10% - suggesting that the method may be applied with confidence.

### 3.3.8 Final comment.

Several attempts were made to solve, theoretically, the problem of reattachment but with small success. As with BOURQUE and NEWMAN<sup>(12)</sup>, and SAWYER<sup>(17)</sup> any such approach required the substitution of empirical coefficients which tended to invalidate the theoretical argument.

Their submission, it was considered, would add little to the subject and in the circumstances, offer no real advantages over a purely empirical approach. They have, therefore, been excluded.

CHAPTER IV

EXPERIMENTAL INVESTIGATION

#### 4. EXPERIMENTAL INVESTIGATION

##### 4.1 Introduction.

As detailed in an earlier chapter (1), successful operation of a supersonic bistable switch was thought to depend on axisymmetric separation followed by subsequent asymmetric autonomous reattachment. Results available in the literature generally appertained to convergent-divergent ducts with either shock or step induced separation or free separation without subsequent reattachment. In addition, most of the work was attempted on relatively large scale apparatus. Therefore, to promote a further understanding of the underlying principles involved a comprehensive research programme was instigated. Two basic processes were involved - Schlieren for visual interpretation and pressure tappings for analytical purposes.

##### 4.2 Visual methods.

Excluding holography, three optical methods are generally available for the analysis of a flow field; interferometry, shadowgraph and Schlieren. Of these, interferometry was considered to be an unnecessary

complication for the relatively straightforward experimental requirement. Shadowgraph methods proved useful but for clear representation Schlieren was found to be more acceptable. Comparison of results obtained from the latter two methods are shown in Figure 4.1.

#### 4.2.1 Schlieren apparatus.

The Schlieren apparatus used was conventional and consisted of a mercury vapour lamp source, condensing lens and slit, two 8 inch diameter spherical mirrors of 6 ft. focal length, a variable position knife edge, focussing lens and a reflex camera. The knife edge, focussing lens and camera were supported on an optical bench.

The only problem encountered during the experimental work was found to be in the correct positioning of the various components with respect to each other. This was overcome with familiarity and experience.

Figure 4.2 shows the positional arrangement of the apparatus.

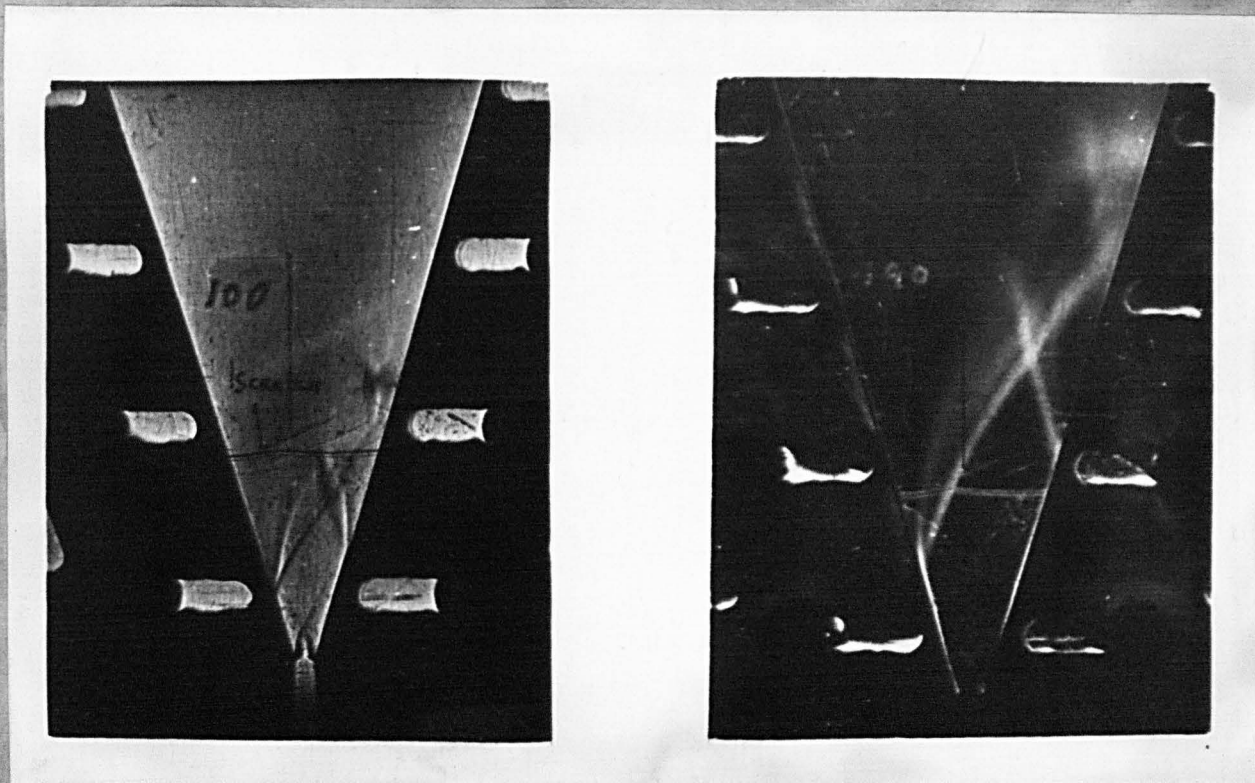
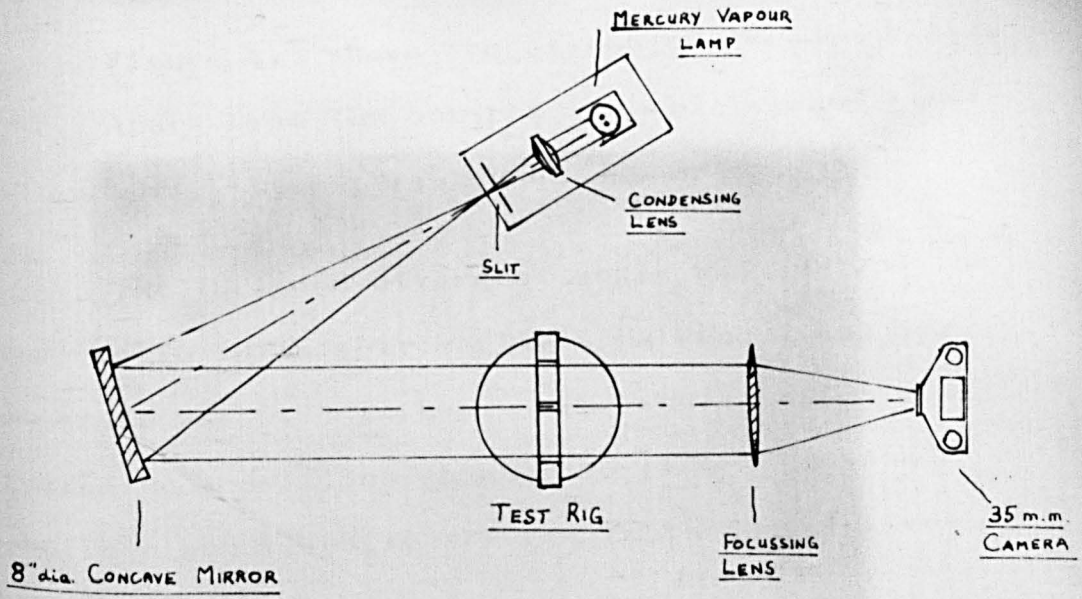


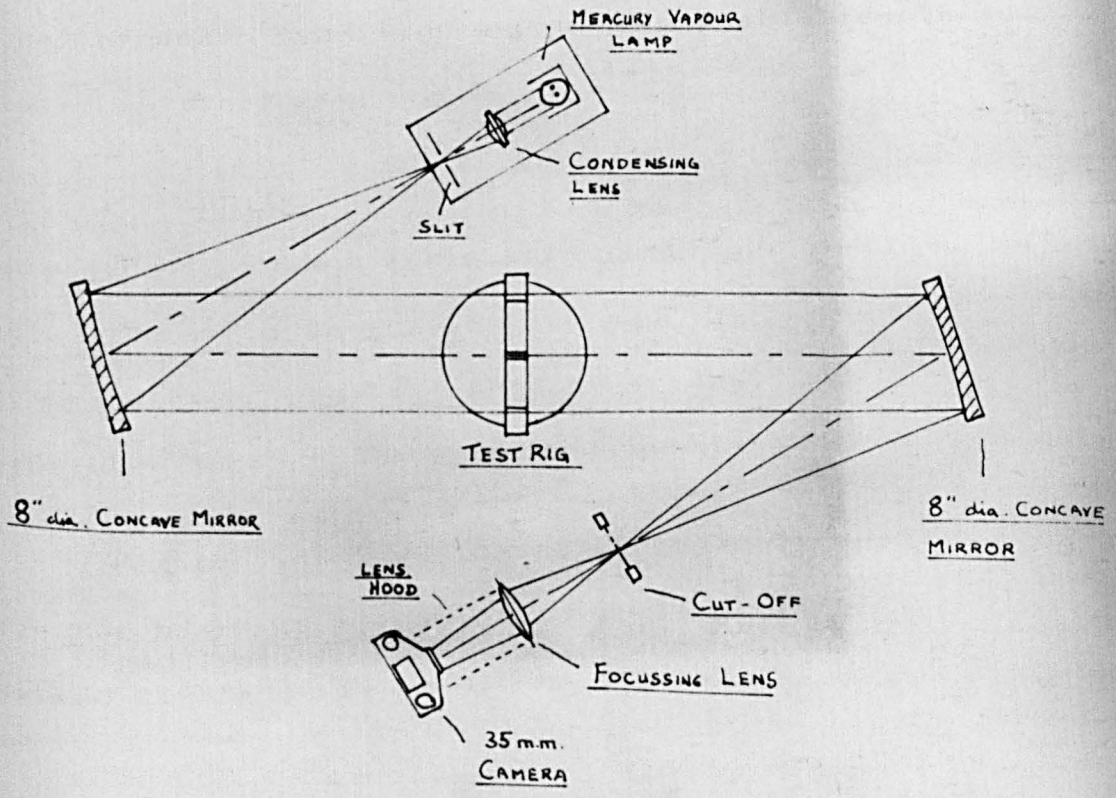
FIGURE 4.1

Shadowgraph

Schlieren



SHADOWGRAPH APPARATUS



FLg 4:2 SCHLIEREN APPARATUS

#### 4.2.2 The test duct.

Figure 4.3 shows the assembled two-dimensional duct. Apart from the perspex side plates and steel base support, the material used was brass.

The included divergent angle was  $30^\circ$  and the aspect ratio infinitely variable between 2 and 40. Duct width was 0.75 inches. The whole assembly was situated on a settling chamber to reduce unwanted turbulence and velocity effects in the supply stream.

It will be noted that the inlet nozzle was convergent to permit the acceleration of the supply air to the sonic condition and of reasonable length to minimise intrinsic turbulence.

Proving tests showed severe leakage in the supply area. Rubber seals were therefore inserted into machined recesses in this region and the perspex side plates supported by metal held by screws. No appreciable leakage occurred subsequently.

Figure 4.4 shows the total assembly with deflector board in situation to prevent damage to the overhead lighting system of the laboratory.



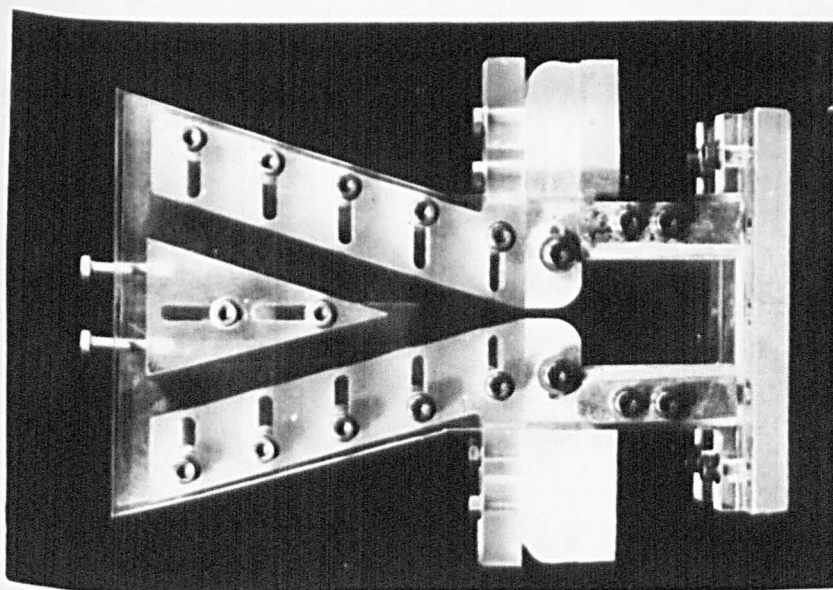
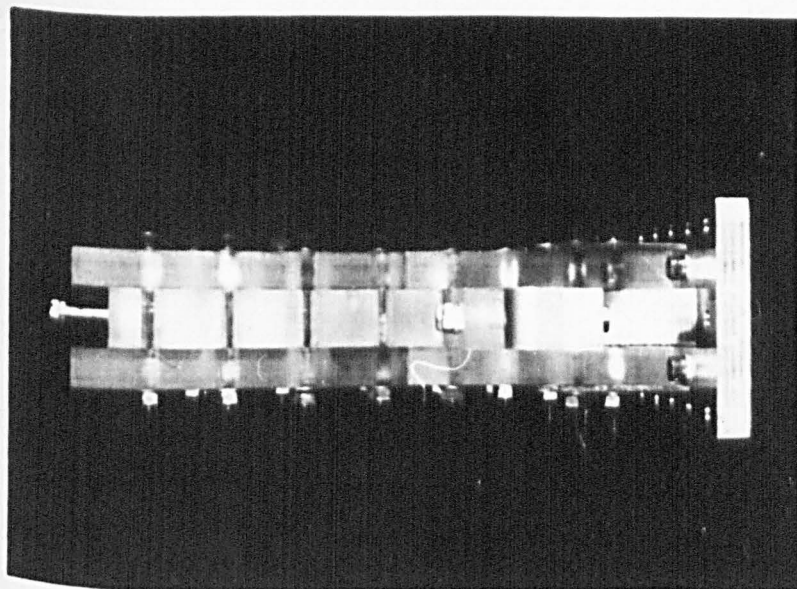


FIG. 4.3. THE ASSEMBLED DUCT.

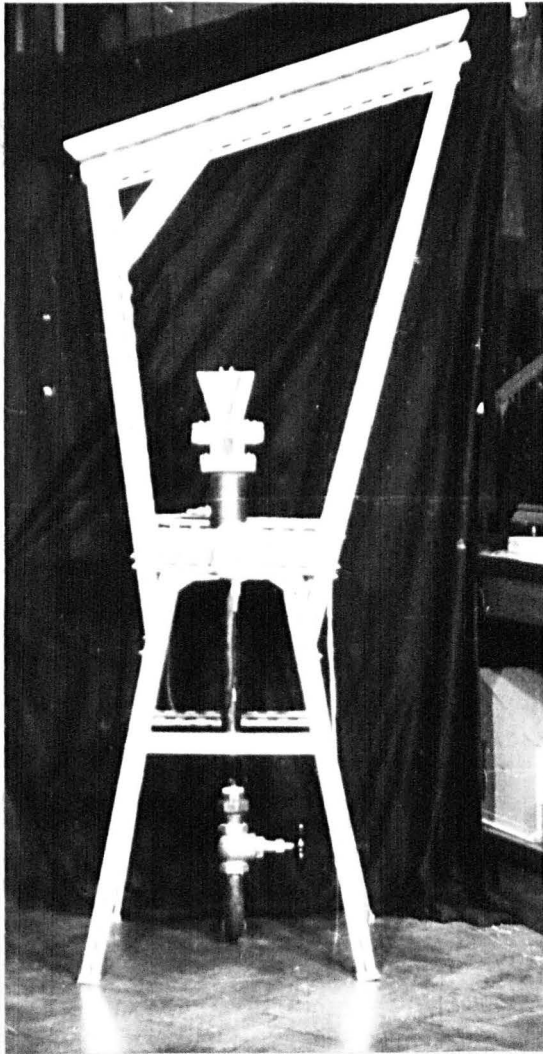


Fig.4.4. The Total Assembly.

#### 4.2.3 Test procedure.

Photographs were taken of the flow situation in the divergent portion of the duct, supply pressures ranging from 40 psig. to 200 psig. in increments of 10 psi. for a range of aspect ratios. For these tests, offset or setback was zero and the splitter removed. The photographs were subsequently measured to give the positions of separation, reattachment and the dimensions of the reverse flow region.

Further qualitative tests were attempted to determine the effect of setback and splitter distance on flow configuration and stability. They were taken mainly out of interest and not for the purpose of detailed assessment.

#### 4.3 Boundary layer pressure measurement.

The concept of pressure measurement in the boundary layer is simple, i.e. drill a series of small holes in the wall of a duct and connect them to some form of pressure transducer. Implementation, however, was found to be a little more difficult, particularly when considering the design of a relatively small duct

with variable geometry configuration capability.

#### 4.3.1 The variable geometry duct.

Figure 4.5 shows the basic configuration of the duct under consideration. As with the previous design, the aspect ratio was variable between 2 and 40; in this case, however, the inclusive wall angle was also variable between  $20^{\circ}$  and  $110^{\circ}$ . The fundamental material was brass. An additional feature was the incorporation of a variable width slot machined into one of the oblique walls to permit switching of the main jet by the ingress of air from the atmosphere. During pressure measuring experiments the control port was kept closed.

Pressure measurement was by 25 pressure gauges connected by screw connections to a support board, via polythene and brass tubes to a series of small diameter holes drilled in one wall of the duct. The gauges were progressively connected to each successive 24 tappings during testing thereby obtaining a complete pressure distribution characteristic. The first gauge was left in position for checking purposes. By far the most difficult problem encountered was the

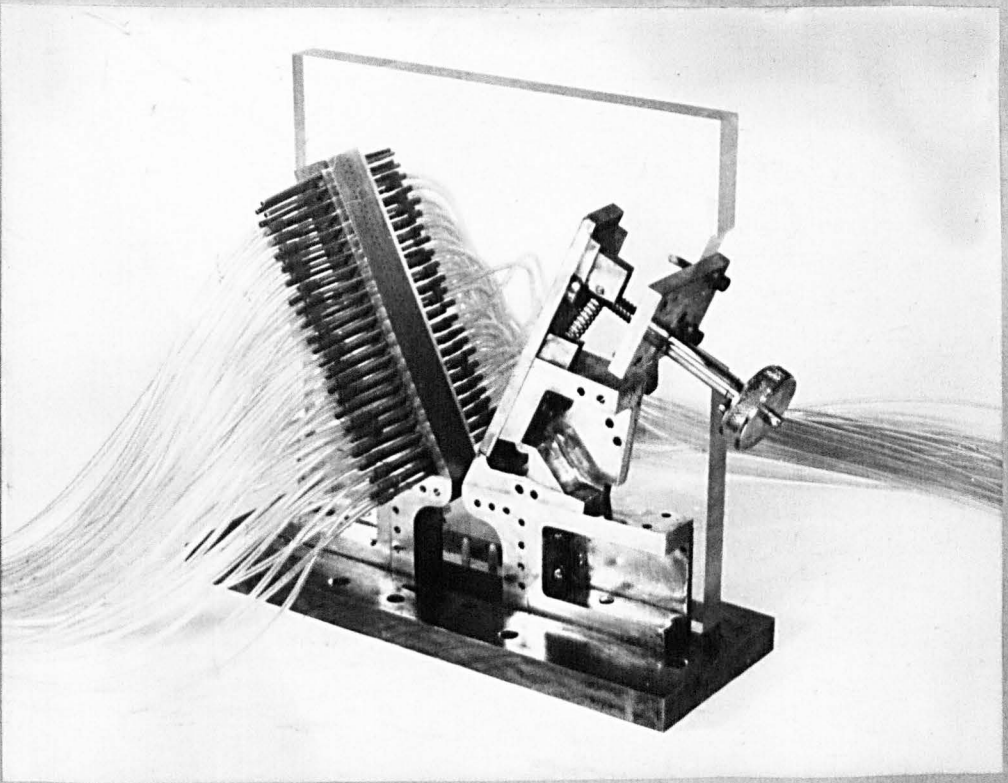


Fig. 4.5. The Variable Geometry Duct.

machining of the small bores in the wall such that pressure measurements could be taken with the minimum of difficulty.

#### 4.3.2 Pressure tapping.

Figure 4.6 shows the first attempt at the problem. Three rows of .013 inch diameter holes were bored perpendicular to the divergent face of the duct at .050" intervals (see Figure 4.7) and cross drilled by vertical bores of .080 inches diameter. Brass tubing was driven into the .080 inch diameter holes and sealed with solder. Polythene tubes ran from these tubes to the screw connectors, which in turn were connected by flexible tubes to the pressure gauges.

The .080 inch holes were zig-zagged as shown to allow sufficient room for the shrinking on of the polythene tubing. The tubes, prior to connection to the pressure gauges, were passed through the appropriate slot in the perspex wall.

When assembled the aspect ratio could be altered without too much difficulty by moving the opposite wall the required distance. A change in wall angle, however, required a new top plate.

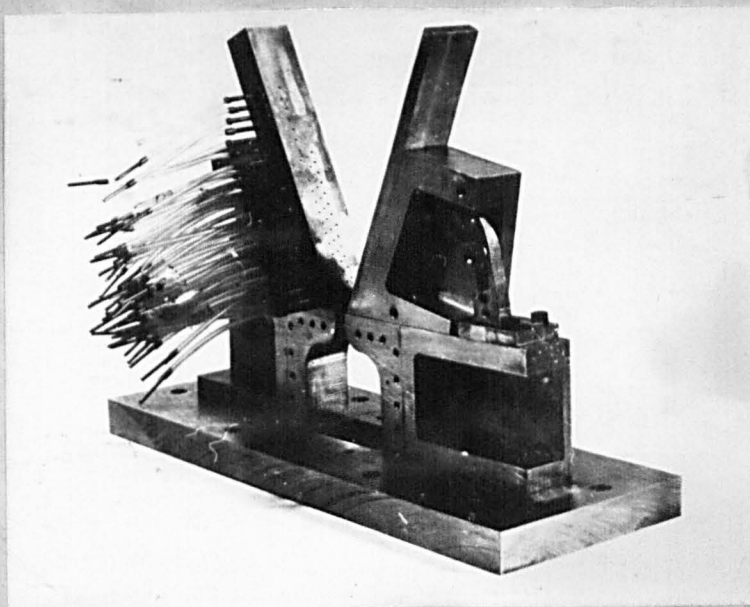


Fig. 4.6 The First Attempt At Pressure Measurement.

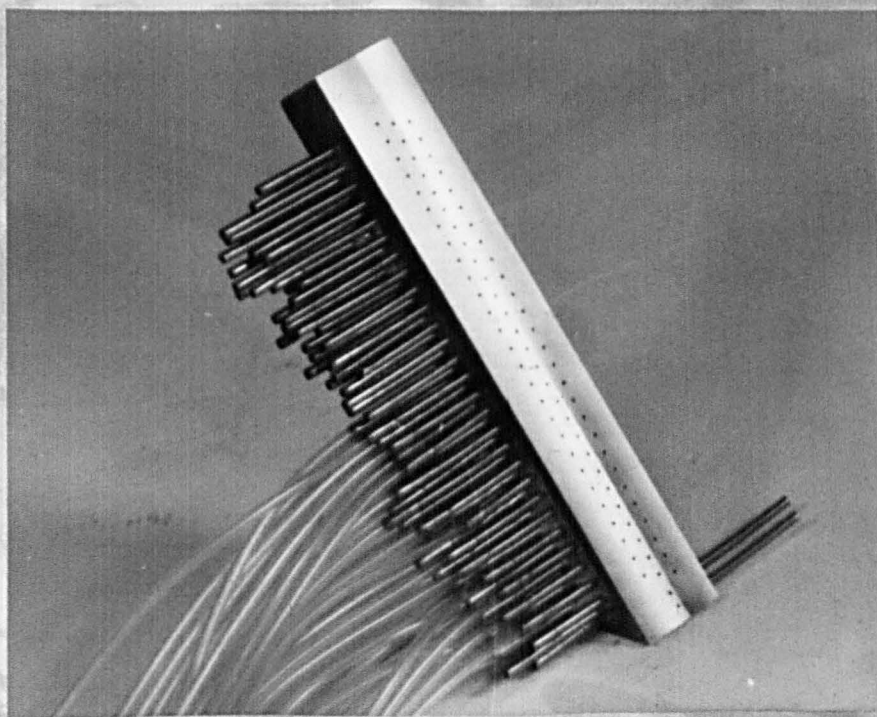


Fig. 4.7. The Test Wall.

Results with this configuration were considered unacceptable because they showed transverse pressure gradient effects. Figure 4.8 shows the "see-saw" tendency of the plotted curves. This was attributed to the necessity of drilling the .013 inch diameter holes in three rows to permit unidirectional access.

A new wall was manufactured with all the holes bored in two rows straddling the centre line of the wall. Because of access these holes were tapped alternately from both top and bottom of the wall and sealed with hot wax. Therefore, change of divergent angle necessitated the re-manufacture of both perspex walls. Results were found to be most acceptable and form the basis of Chapter 5.

#### 4.3.3 Variable port.

To obtain some idea of the effect of control port area on switching operation it was necessary to be able to increase or decrease the area during actual testing. Figure 4.9 shows the small spring loaded cam device designed for this purpose. Two springs are in evidence, one to maintain contact between the moving plate and the cam, the other to hold the plate against the wall when in the process of being moved.



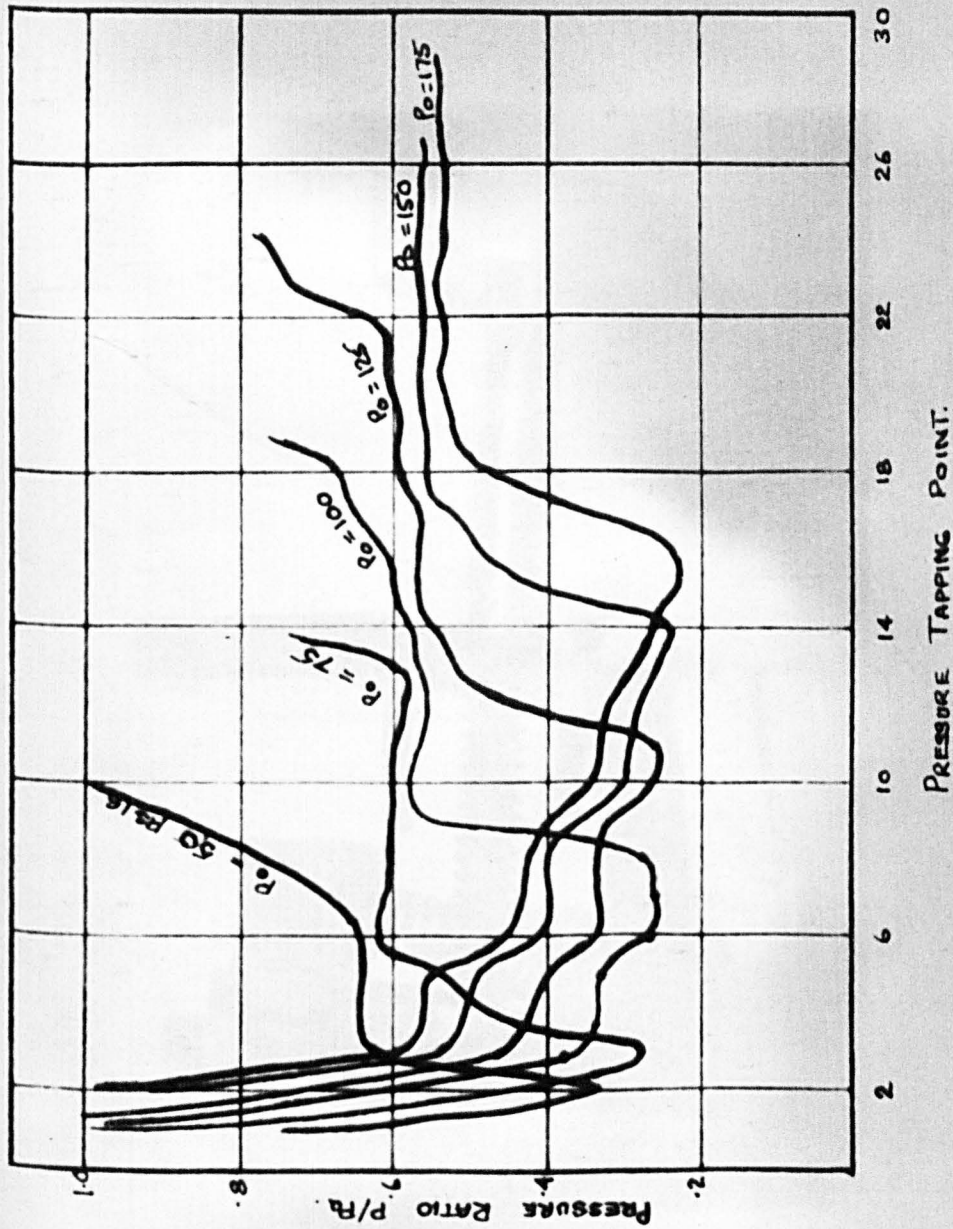


FIG. 4.8 RESULTS OBTAINED WITH THE FIRST TEST DUCT.

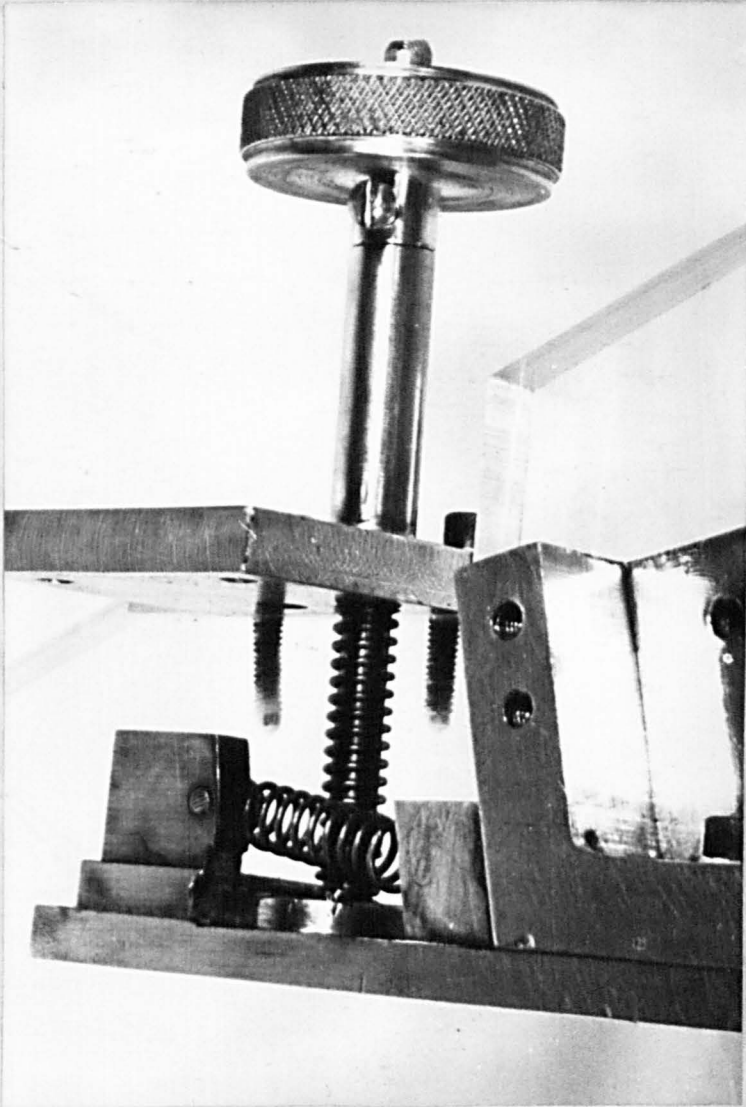


Fig. 4.9. Variable Port Cam Device.

#### 4.3.4 Temperature measurement.

To facilitate a comprehensive theoretical approach some indication of stagnation temperature was required. Therefore thermocouples were inserted in small recesses in the perspex plates and connected via a cold junction (i.e. ice in a thermos flask) to a potentiometer box. Temperature was obtained by reference to a chart in the normal way.

Figure 4.10 shows the assembled apparatus.

#### 4.3.5 The air supply system.

The air used in the test programme was supplied by a 210 H.P., 2 stage, oil free, carbon ring, reciprocating compressor. Its capacity was 600 cf.m of saturated free air at a maximum supply pressure of 250 psig. and average temperature 350°F.

The compressor output was passed via an after cooler with mechanical extraction of water vapour and a "Birlec", twin-pass drier incorporating hot air regeneration, into a 1500 ft<sup>3</sup>. capacity receiver. The system was capable of a sustained 0.75 lb/sec of clean air at 250 psig. and was built for use with a

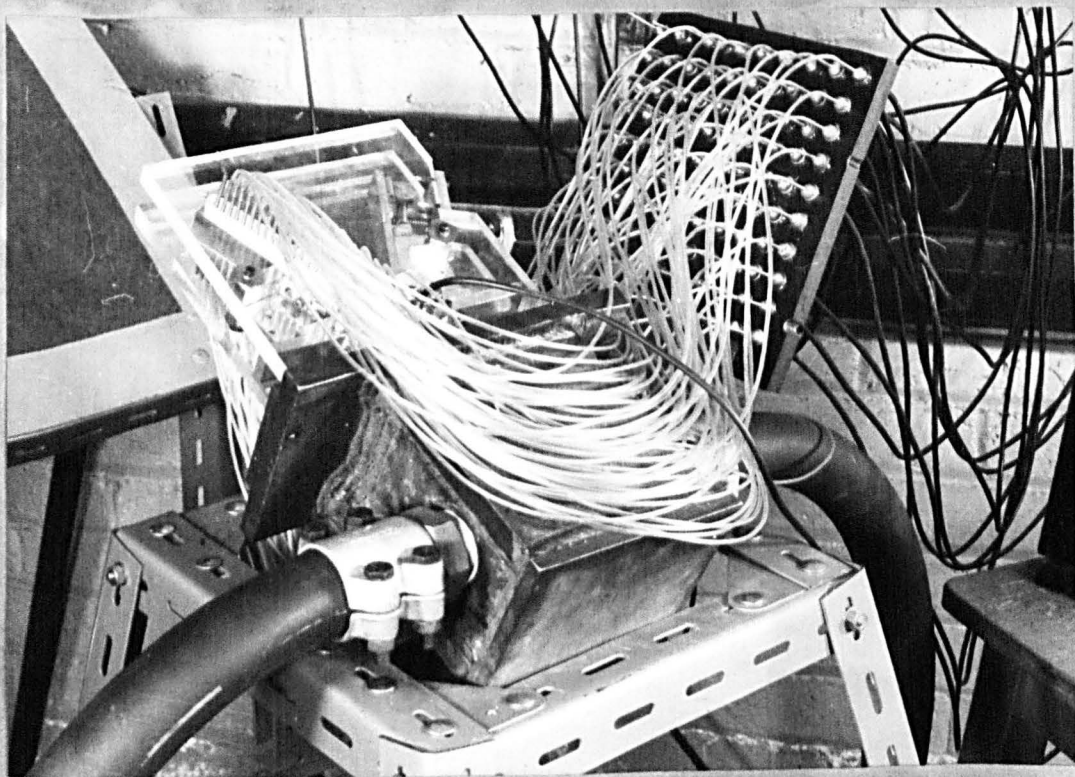


Fig. 4.10a. The Local Assembly.

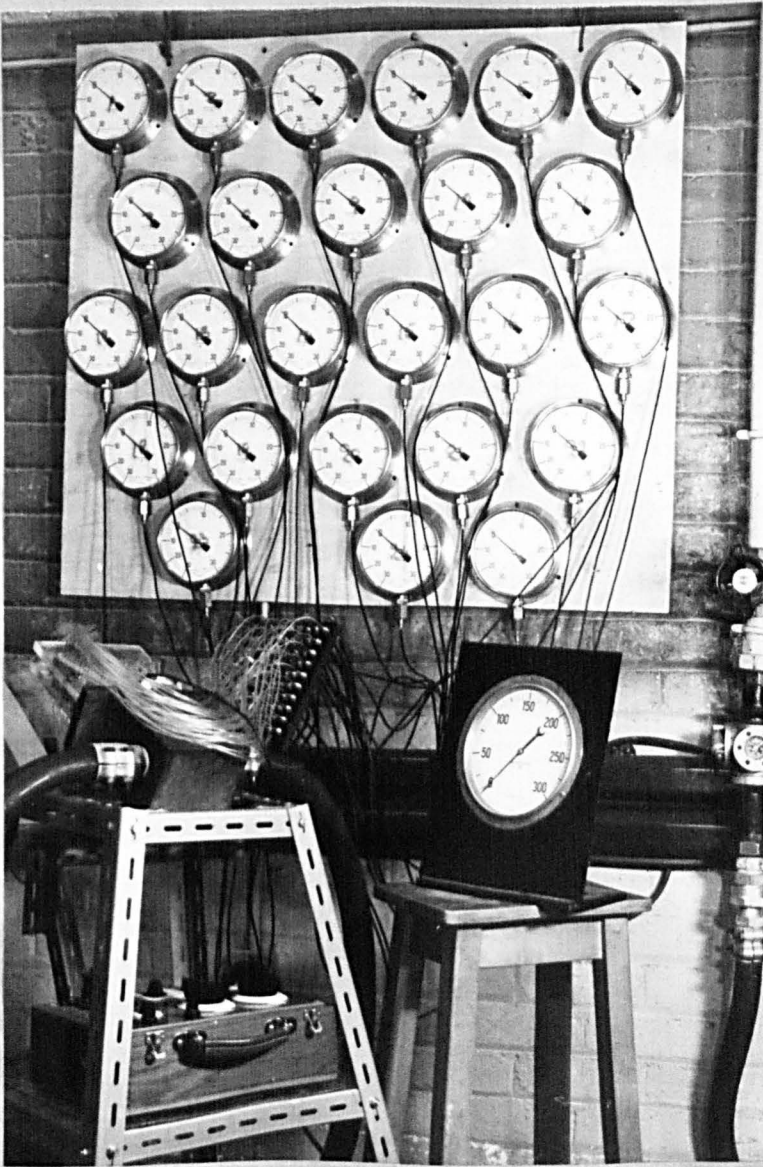


Fig. 4.10b The Total Test Assembly.

supersonic wind tunnel situated in the Aerodynamics Laboratory of the University.

#### 4.4 Test procedure.

Measurements were taken of the pressure distribution in the boundary layer at supply pressures of 50 psig. to 200 psig. in increments of 25 psi. for a range of aspect ratios (3.75 to 37.5). No splitter was used and offset was maintained at zero. The initial intention was to measure temperature during each test but the results were so consistent it was only necessary to make spot checks at frequent intervals. The tests were repeated for three included wall angles  $30^{\circ}$ ,  $40^{\circ}$  and  $50^{\circ}$ .

As with the visual test programme, results were taken to determine, qualitatively, the effect of offset on the pressure distribution in the boundary layer; they are discussed in Chapter 5 dealing with analysis.

#### 4.5 Experimental results.

##### 4.5.1 Schlieren results.

The prime function of the Schlieren process in this investigation was to obtain some visual indication of the flow process involved and hence determine the areas of potential interest. However, to promote useful comparison with subsequent pressure distribution results a large number of measurements were taken, from photographic prints, of the position of separation and reattachment. All results were limited to a wall divergent angle of  $30^{\circ}$ .

Figure 4.11 shows a typical photograph obtained with the test apparatus. The dark areas in the main flow stream indicate expansion and the light areas compression. Separation of the flow stream can be seen on both walls of the duct, occurring earlier (i.e. further upstream) and quite distinctly when not followed by reattachment. The position of separation on the opposite wall, however, is somewhat indistinct and for consistency in measurement was assumed to be taking place at the point where the projected oblique shock wave intersected the adjacent wall. Comparison with the measured pressure distribution suggests that

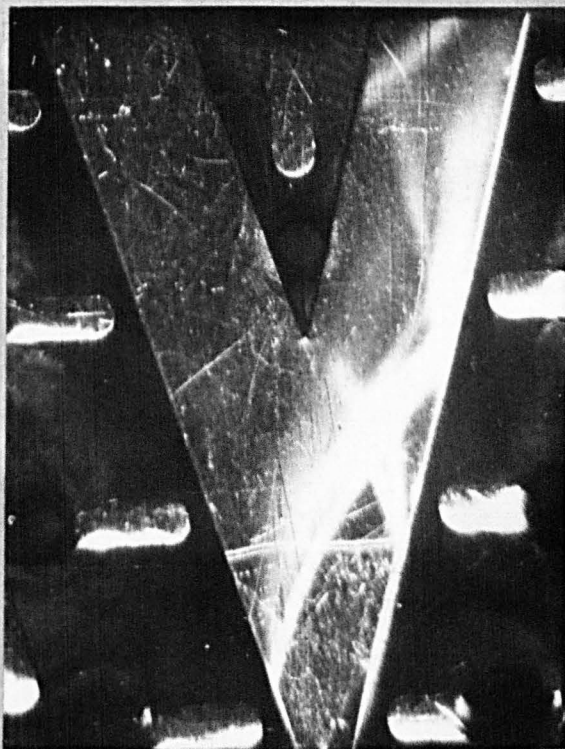


FIG. 4. 11. TYPICAL SCHLIEREN PHOTO SHOWING SEPARATION AND REATTACHMENT.



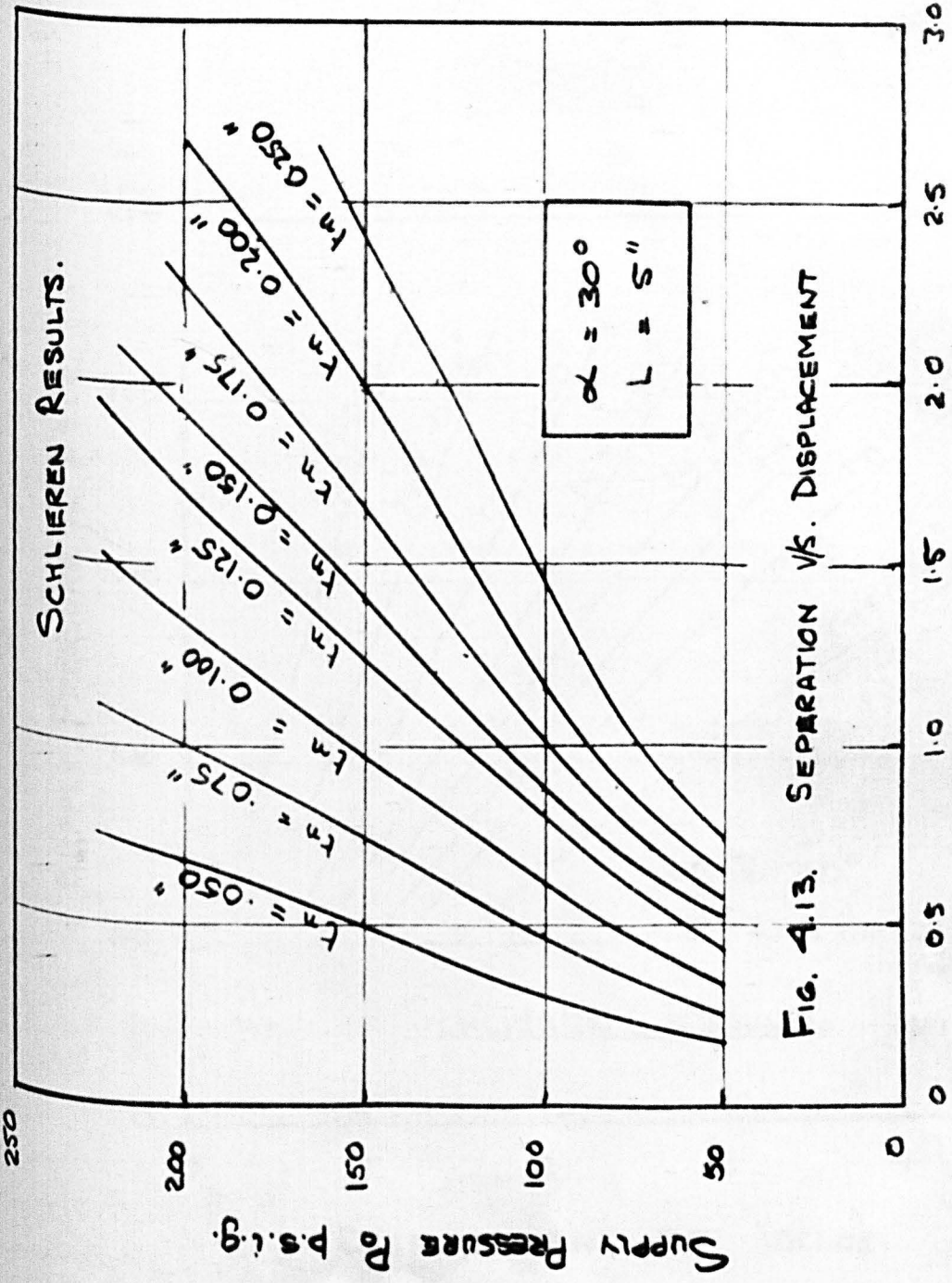
separation was, in practice, occurring a little before this point. A similar approximation was necessary to determine the position of reattachment.

Figure 4.12 shows, pictorially, the advancement of the reverse flow region along the wall to which the jet is attached with increase in supply pressure at a constant throat width of 0.125 inches (aspect ratio of 6). Figures 4.13 and 4.14 indicate the measured position of separation and reattachment respectively at various throat widths with variation of supply pressure,  $P_0$ , and are shown plotted nondimensionally, with respect to throat width, in Figure 4.15. The shaded area between the two characteristics is assumed to be the reverse flow region and in practice determines the useful working range of a supersonic bistable switch.

Figure 4.16 is a photograph of the flow situation when large asymmetric offset has been set in the duct, (offset equals throat width). Figure 4.17 indicates the effect of splitter position on the flow situation.



FIG. 4. 12. ADVANCEMENT OF REVERSE FLOW REGION WITH SUPPLY PRESSURE  $P_0$ .



SCHLIEN RESULTS.

FIG. 4.13. SEPARATION V/S. DISPLACEMENT

DISPLACEMENT 24 inches.

Supply Pressure p.s.i.g.

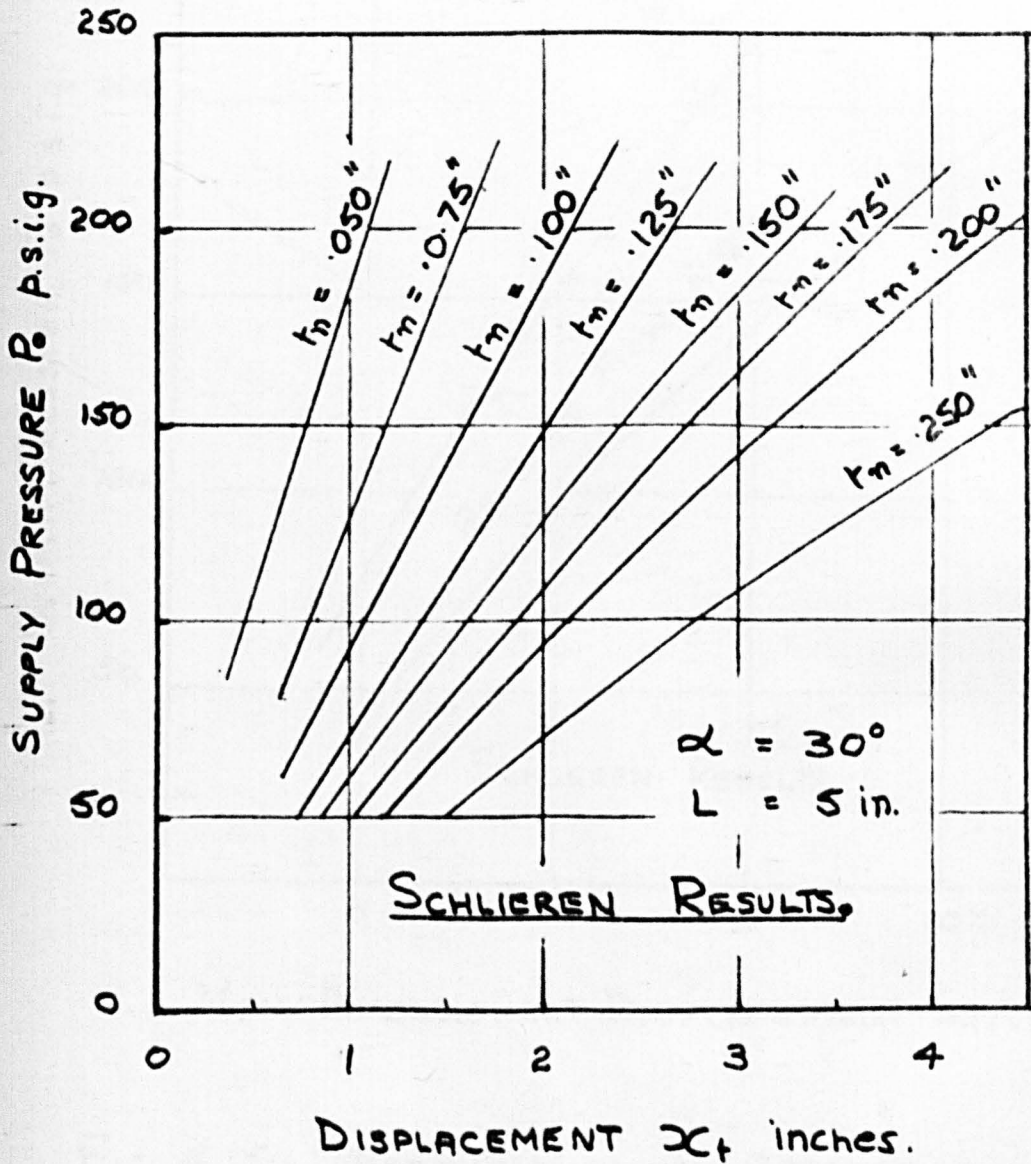
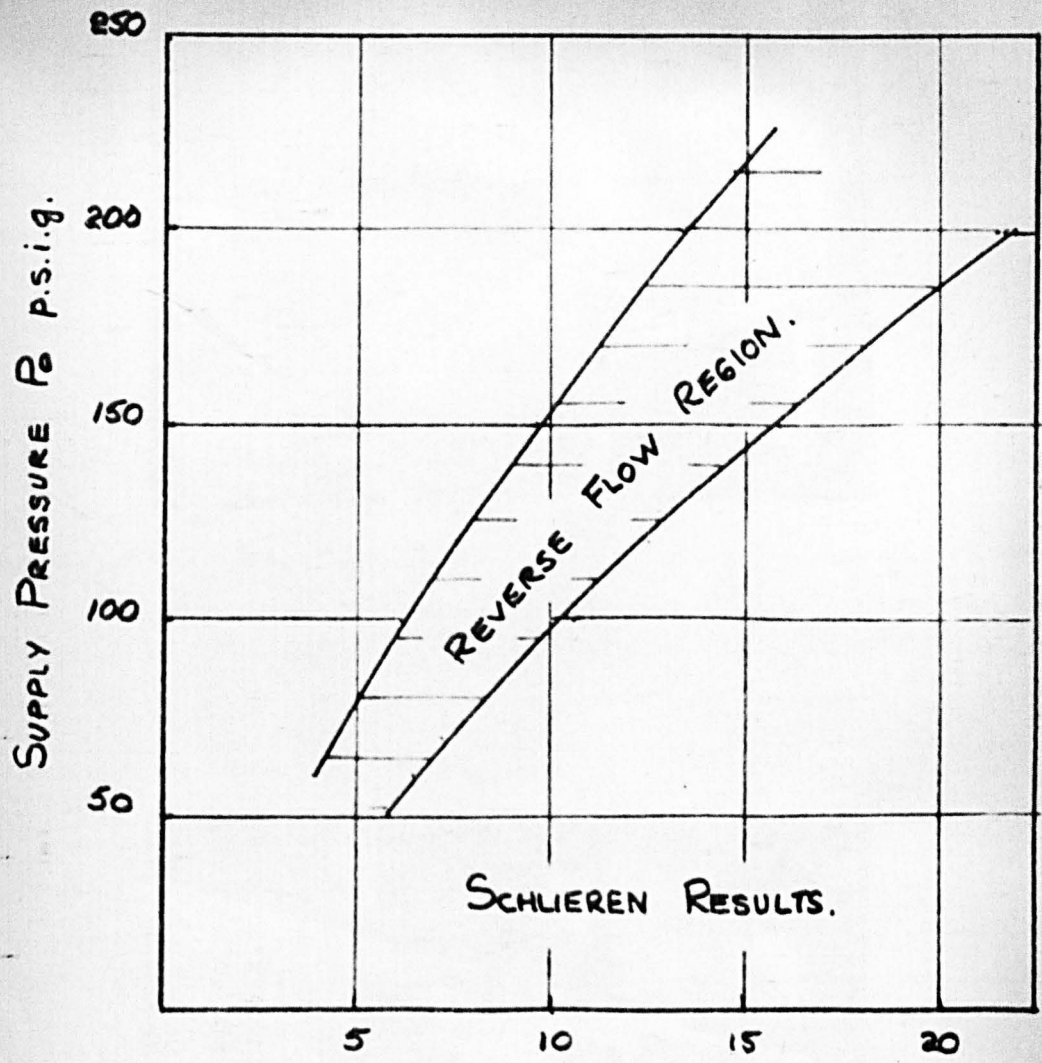


FIG. 4.14 RE-ATTACHMENT VS DISPLACEMENT.



NON-DIMENSIONAL DISPLACEMENT  $x_r/t_n$ .

FIG. 4.15. NON-DIMENSIONAL SEPARATION -  
- REATTACHMENT CHARACTERISTIC.

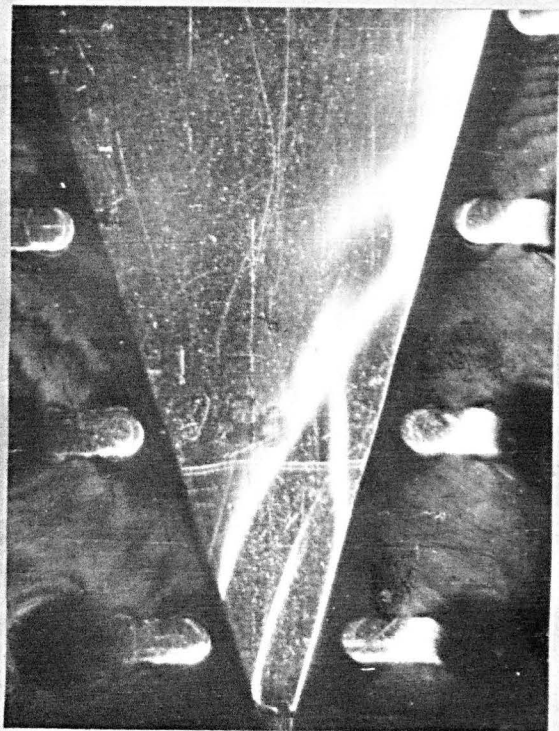


FIG. 4. 16. THE EFFECT OF OFFSET.

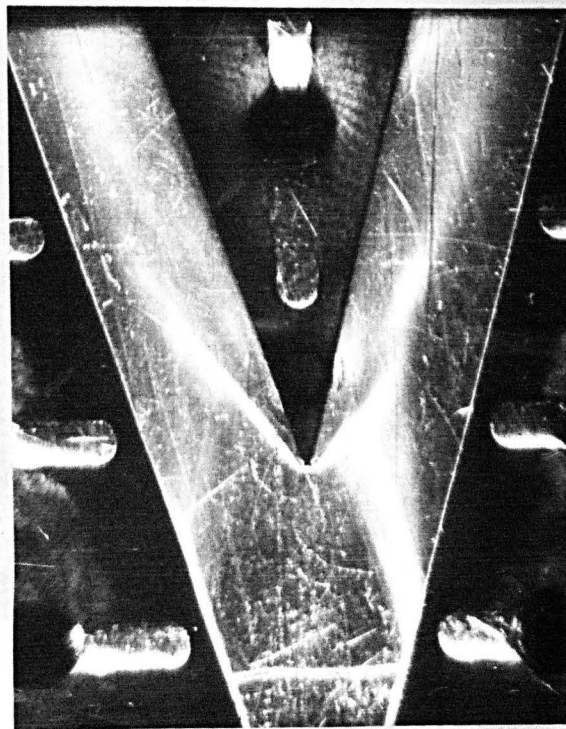


FIG. 4. 17. SPLITTER / FLOW INTERACTION.

An analysis of these results is given, together with those below, in the following chapter;(5).

#### 4.5.2 Measurement of pressure distribution.

As indicated in paragraph 4.4 measurements were made of the pressure distribution occurring along both walls (attached, non-attached) at three distinct divergent angles  $30^{\circ}$ ,  $40^{\circ}$  and  $50^{\circ}$  for a range of aspect ratios and supply pressures. As may be expected the results so obtained were largely repetitive in nature and in consequence have been relegated to Appendix (4)(page ). in the interests of clarity. Fortunately the results may be condensed into one series of curves for each included angle by nondimensionalising the displacement with respect to throat width and measured absolute pressure with respect to supply pressure. The resulting graphs are shown in Figures 4.18, 4.19 and 4.20 respectively. For ease of comparison each figure shows both the reattached and non-reattached measured pressure distribution. The displacement values ( $x_t$ ) also plotted, correspond to a throat width ( $t_n$ ) of 0.200 inches



## **ETHOS**

Boston Spa, Wetherby  
West Yorkshire, LS23 7BQ  
[www.bl.uk](http://www.bl.uk)

The text for the following three pages is bound into the spine.



**OVEREXPANSION EXPERIMENTS.**

FREE SEPARATION WITH  
SUBSEQUENT REATTACHMENT  
BOUNDARY LAYER PRESSURE RATIO  $P/P_0$   
vs.  
NONDIMENSIONAL DISPLACEMENT  $\frac{x}{t}$

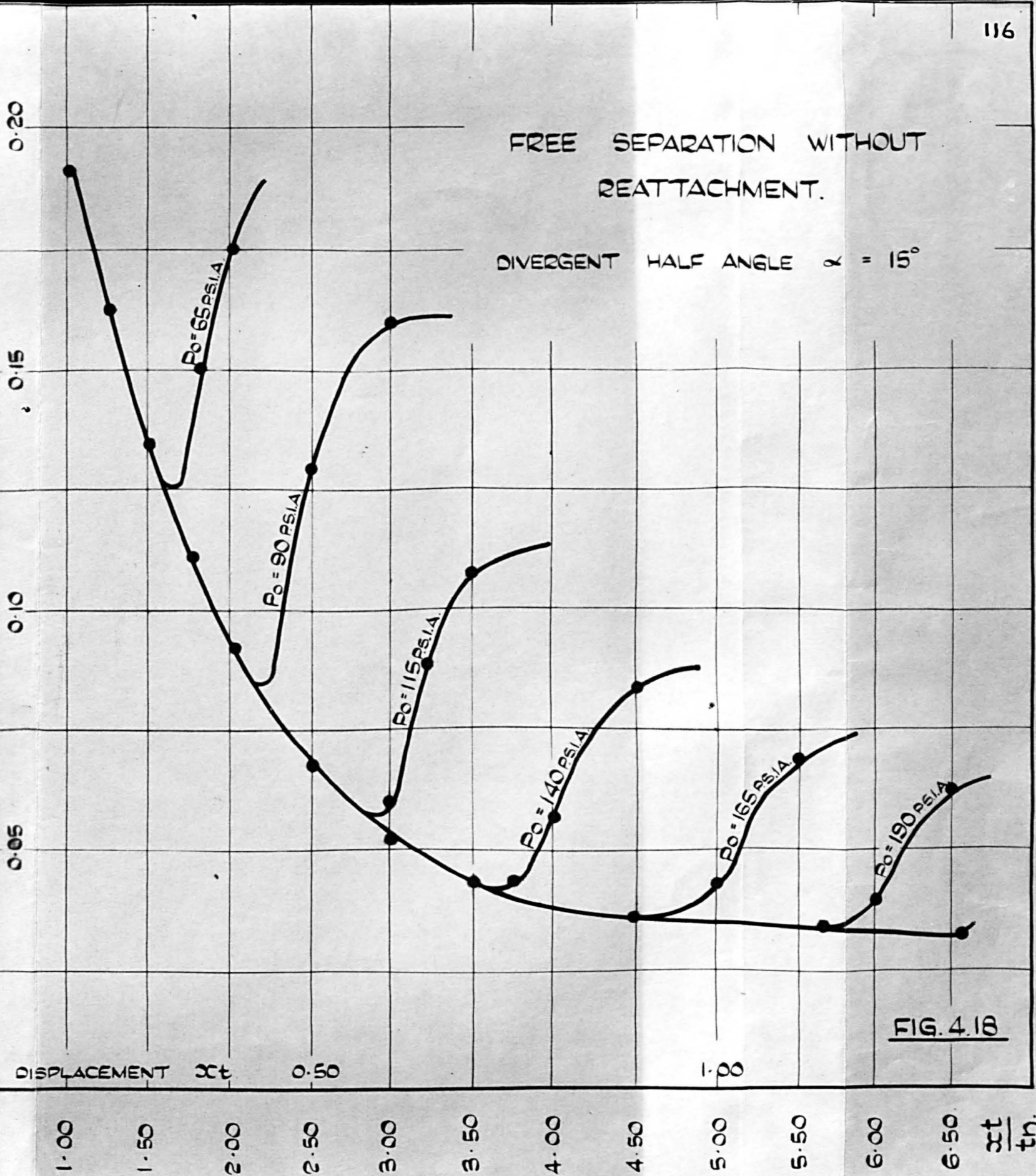
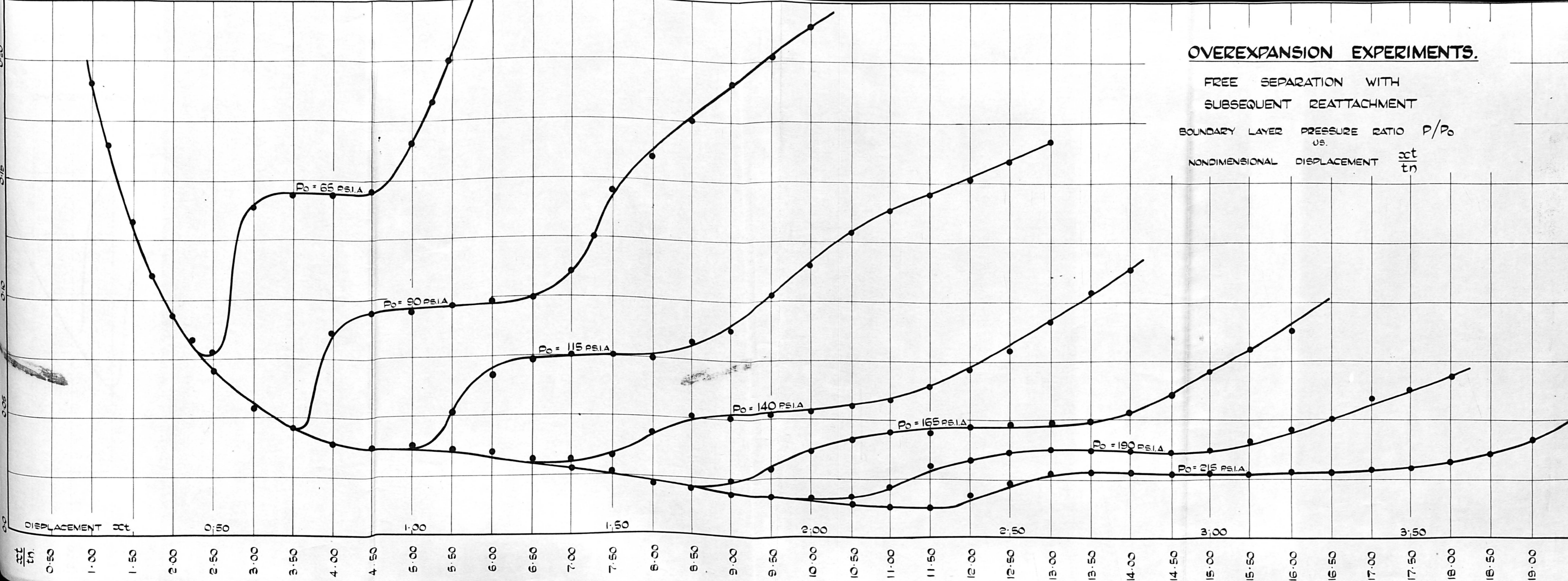
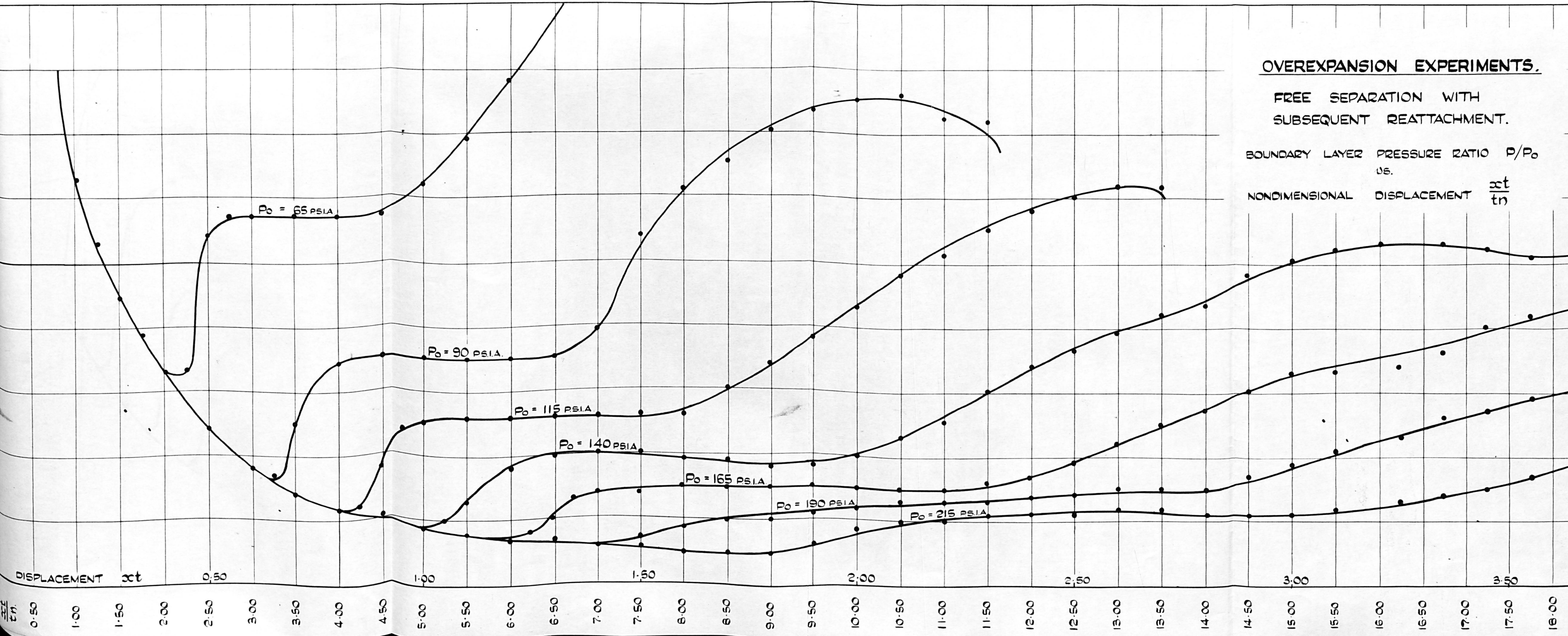


FIG. 4.18

OVEREXPANSION EXPERIMENTS.

FREE SEPARATION WITH  
SUBSEQUENT REATTACHMENT.

BOUNDARY LAYER PRESSURE RATIO  $P/P_0$   
VS.  
NONDIMENSIONAL DISPLACEMENT  $\frac{x}{t_n}$



FREE SEPARATION WITHOUT  
REATTACHMENT.

DIVERGENT HALF ANGLE  $\alpha = 20^\circ$

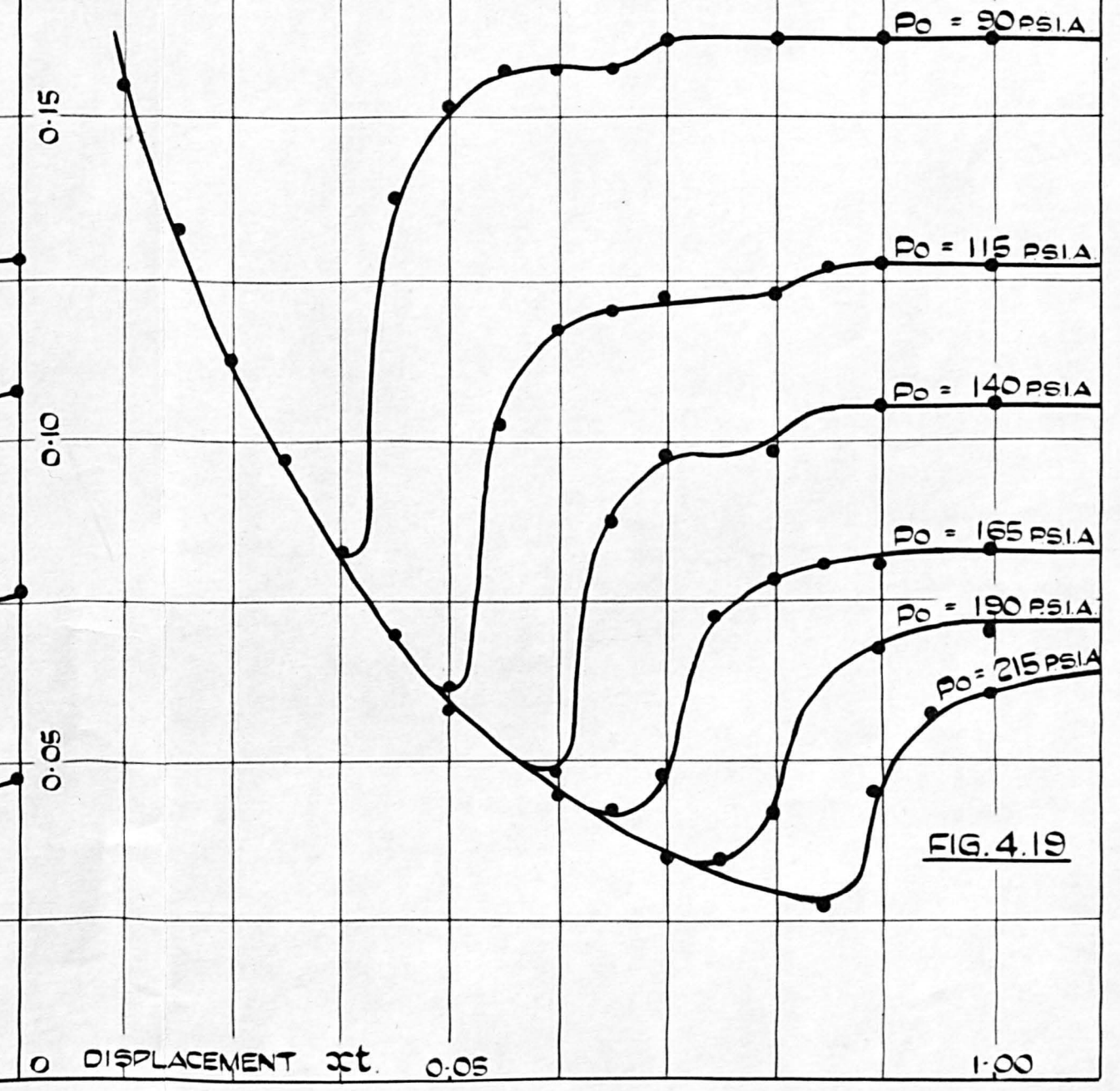
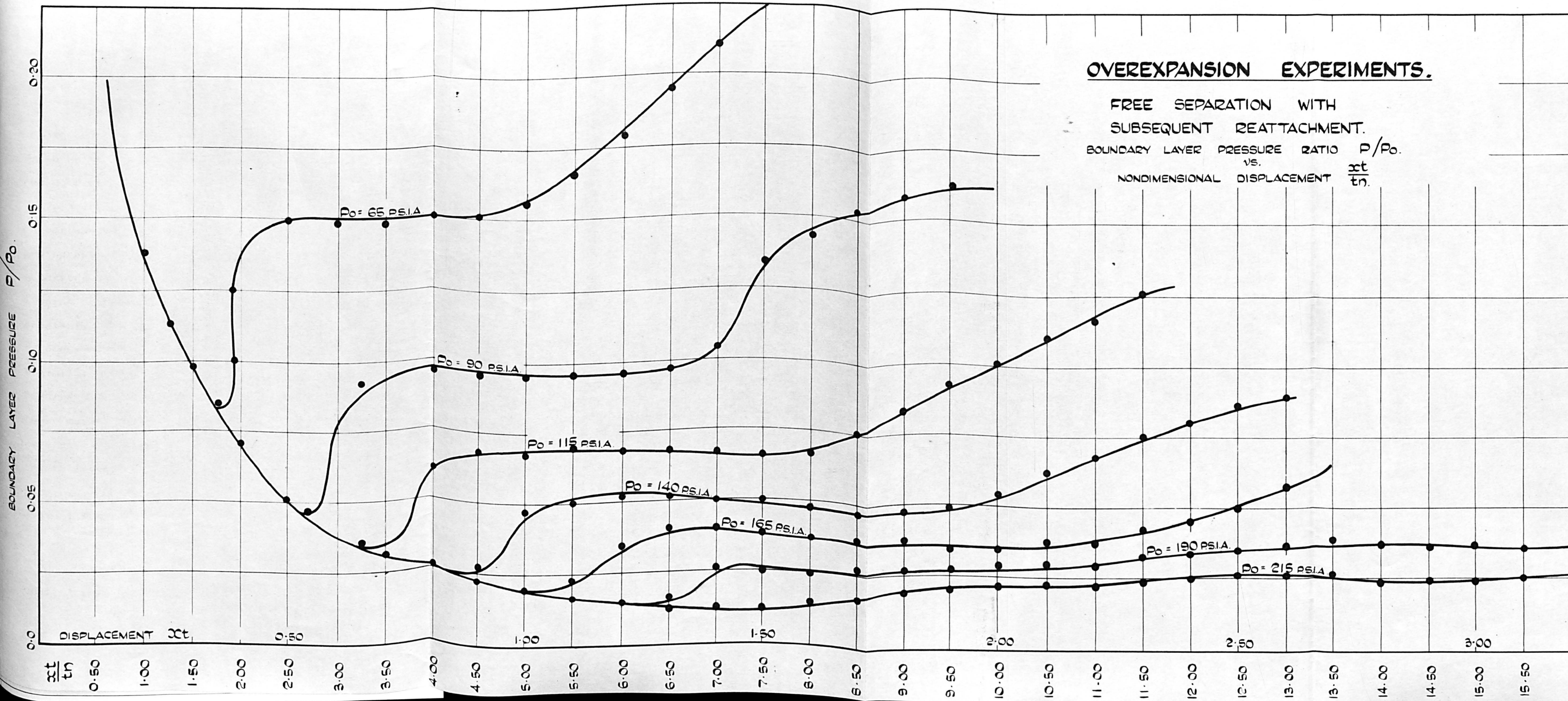


FIG. 4.19

### OVEREXPANSION EXPERIMENTS.

FREE SEPARATION WITH  
 SUBSEQUENT REATTACHMENT.  
 BOUNDARY LAYER PRESSURE RATIO  $P/P_0$   
 vs.  
 NONDIMENSIONAL DISPLACEMENT  $\frac{x}{t_n}$



FREE SEPARATION  
 WITHOUT REATTACHMENT.

DIVERGENT HALF ANGLE  $\alpha = 25^\circ$

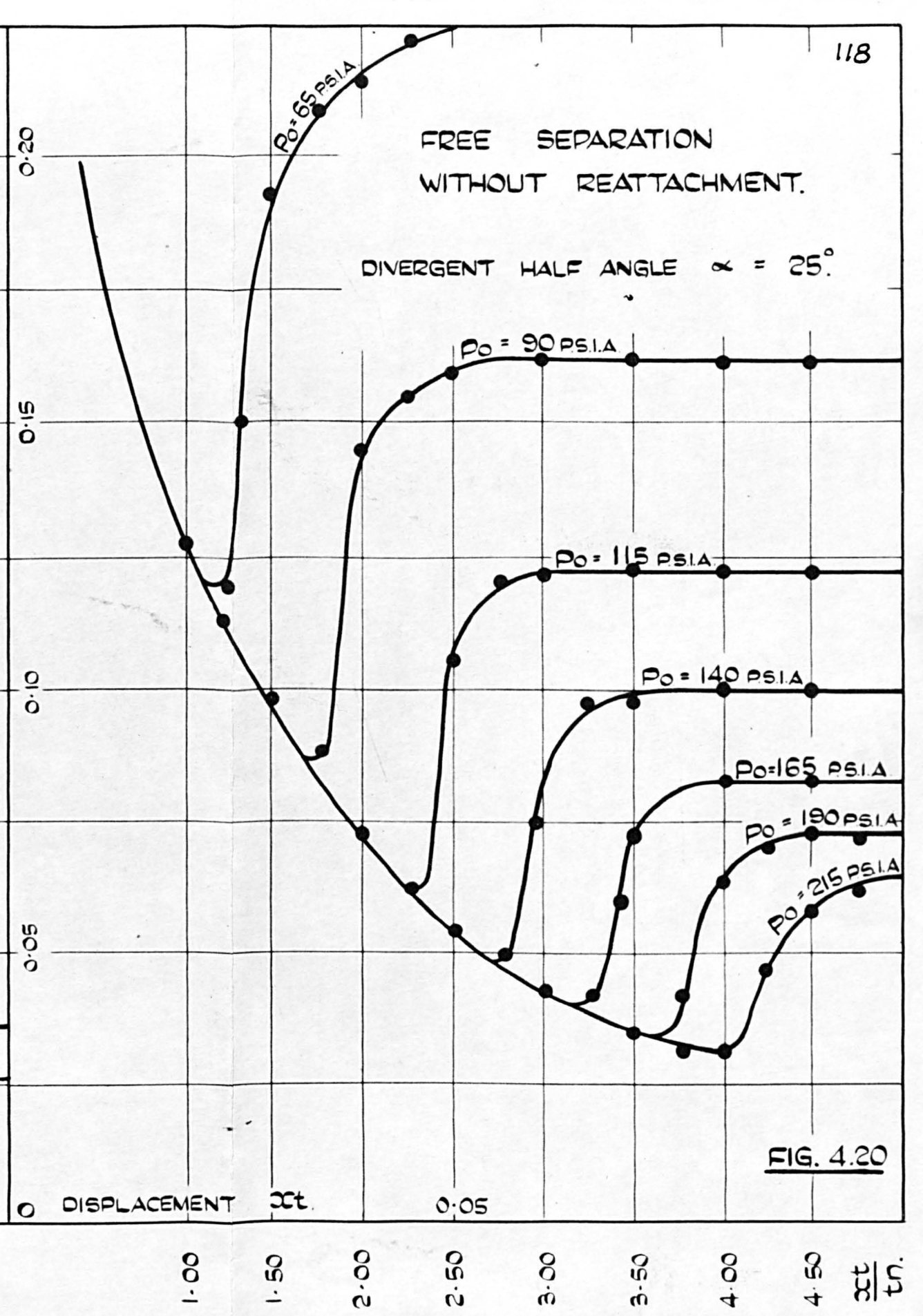


FIG. 4.20

(aspect ratio 3.75) and are included to give some indication of scale.

The position of minimum pressure (i.e.  $dp/dx = 0$ ) occurring at the end of isentropic expansion is shown in Figures 4.21, 4.22 and 4.23, together with the corresponding values computed by equations 3.17, 3.18, 3.19 and 3.20 derived in Chapter 3 (page ). Comparison of pressure distribution with Schlieren photographs indicated that separation was not occurring at this position of minimum pressure but at a point somewhere along the following abrupt pressure gradient. For expediency, separation was assumed to occur midway along this adverse pressure gradient. A similar approximation was made for reattachment. Figures 4.24 and 4.25 show the curves resulting from these measurements. Figure 4.26 shows the average reverse flow pressure characteristics for the separation-reattachment condition.

#### 4.5.3 The effect of control port aspect ratio on switching.

Attempts were made to determine the effect of control port position and width on jet attachment

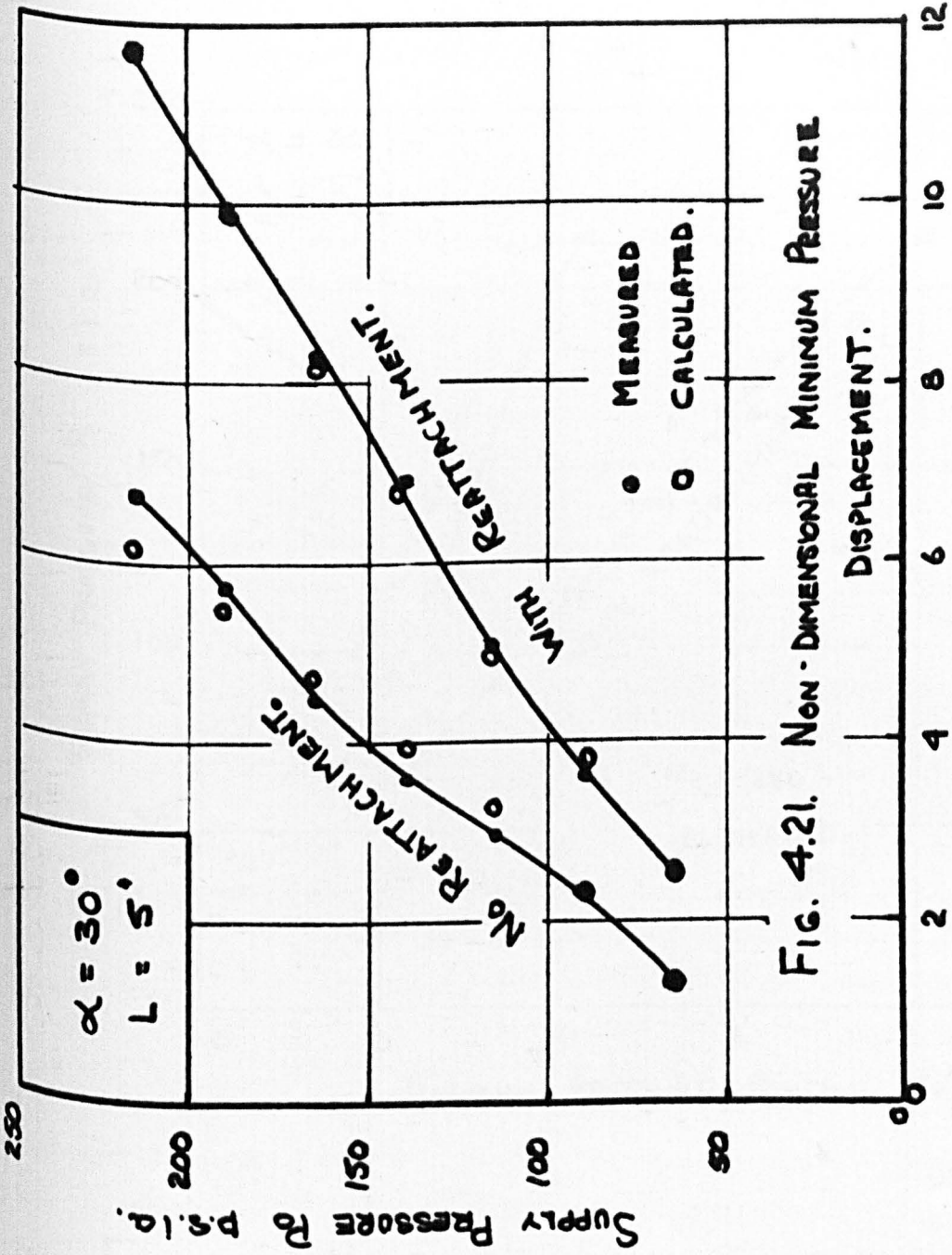


FIG. 4.21. Non-DIMENSIONAL MINIMUM PRESSURE

MINIMUM PRESSURE POSITION  $x_1'/L$ .

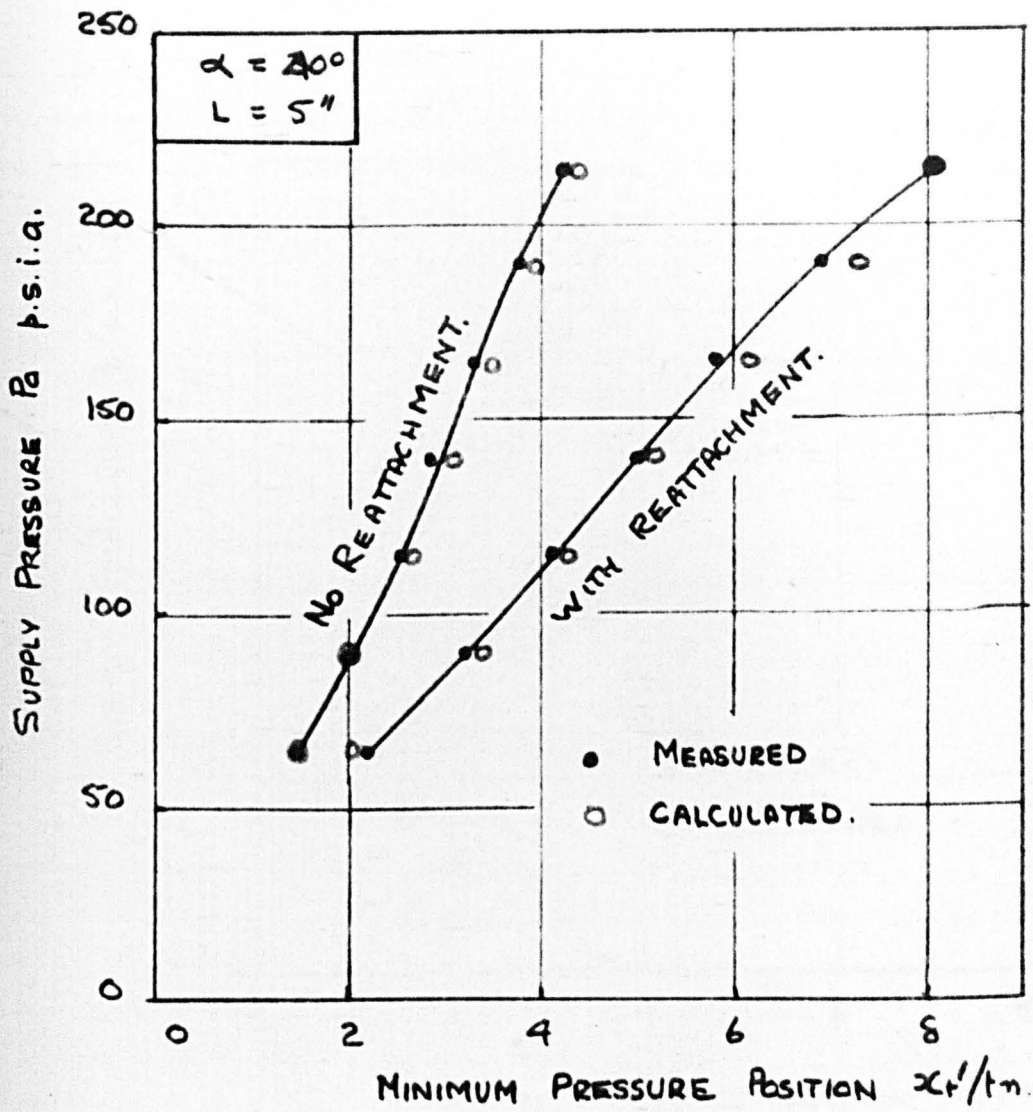


FIG. 4.22. NON DIMENSIONAL MINIMUM PRESSURE DISPLACEMENT.

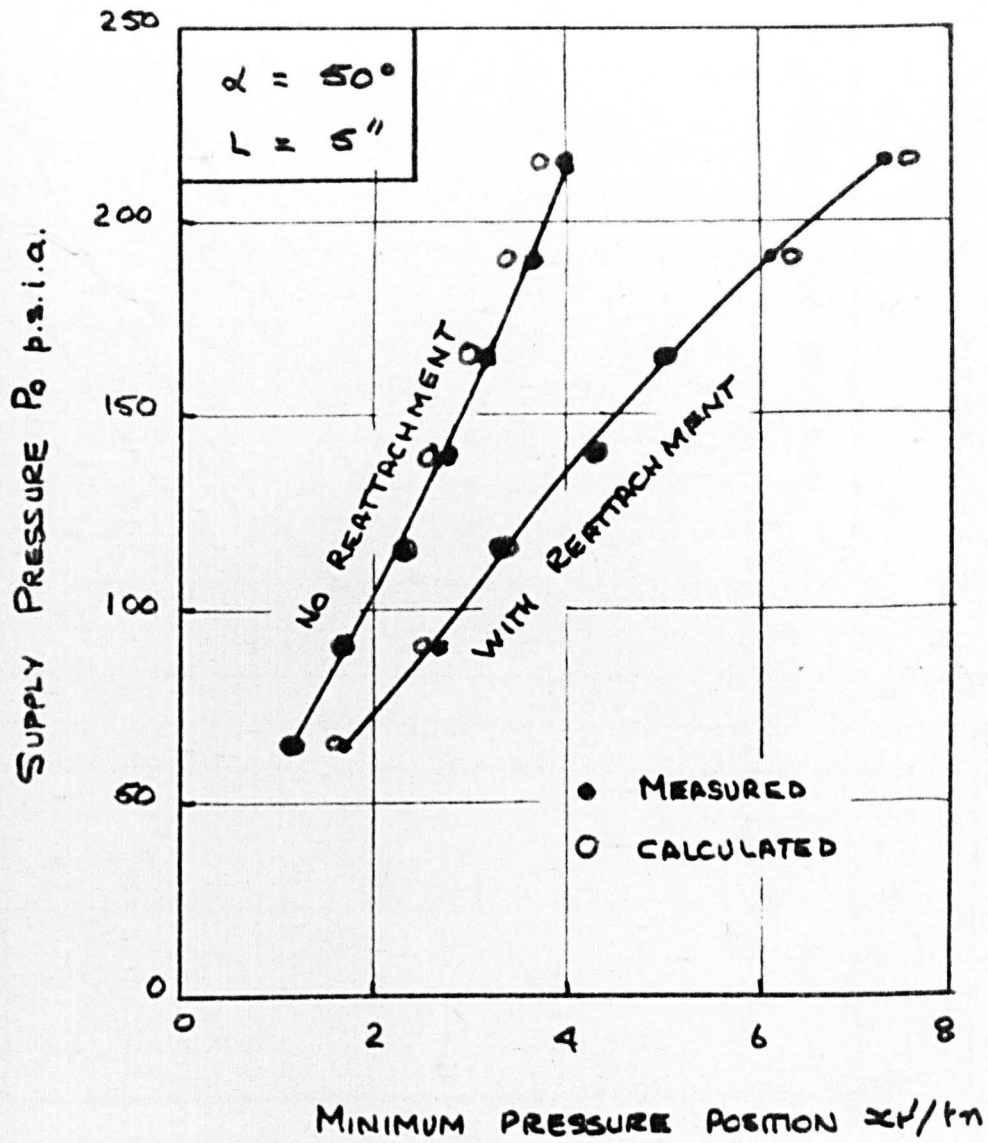
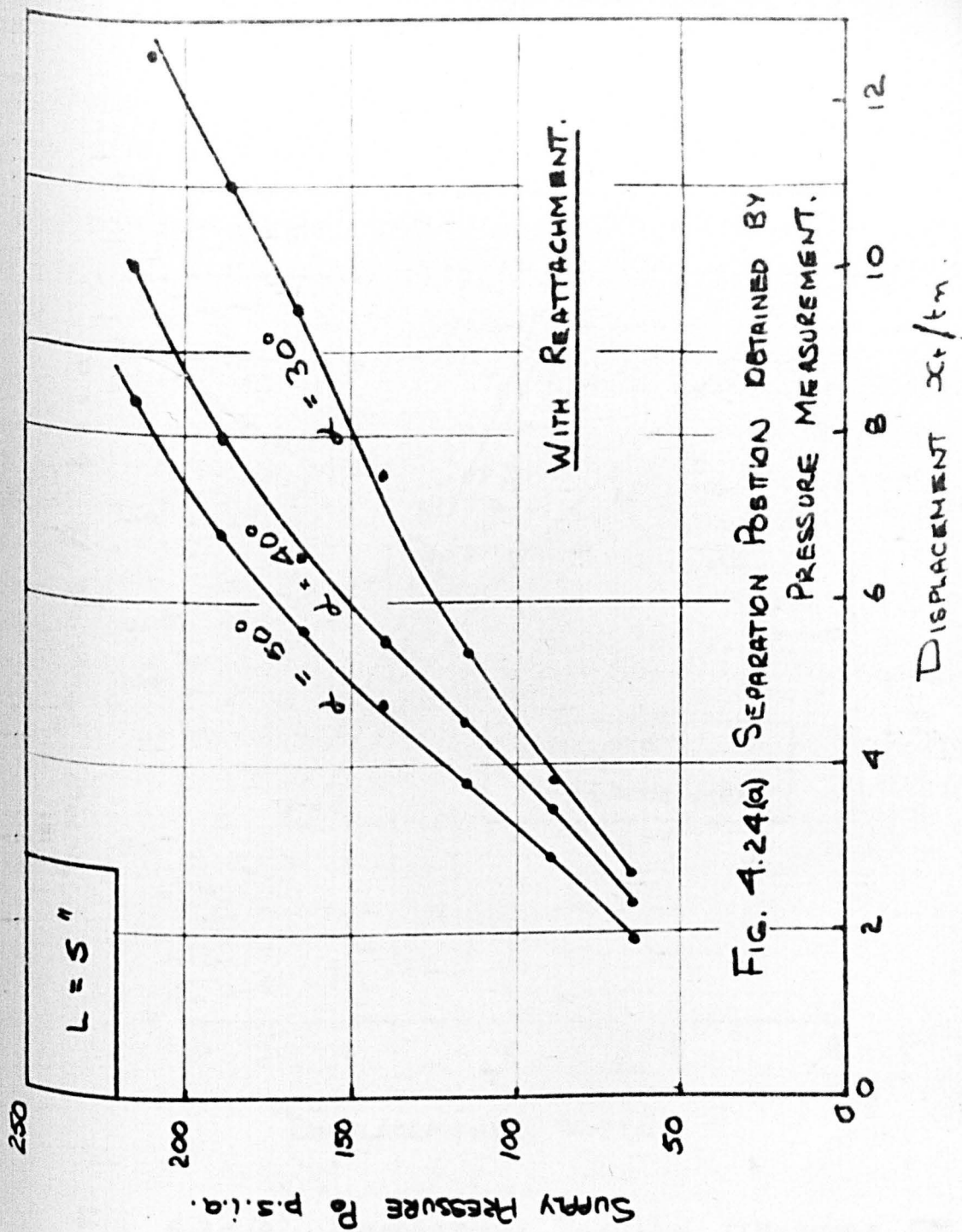


FIG. 4.23. NON DIMENSIONAL MINIMUM PRESSURE DISPLACEMENT.





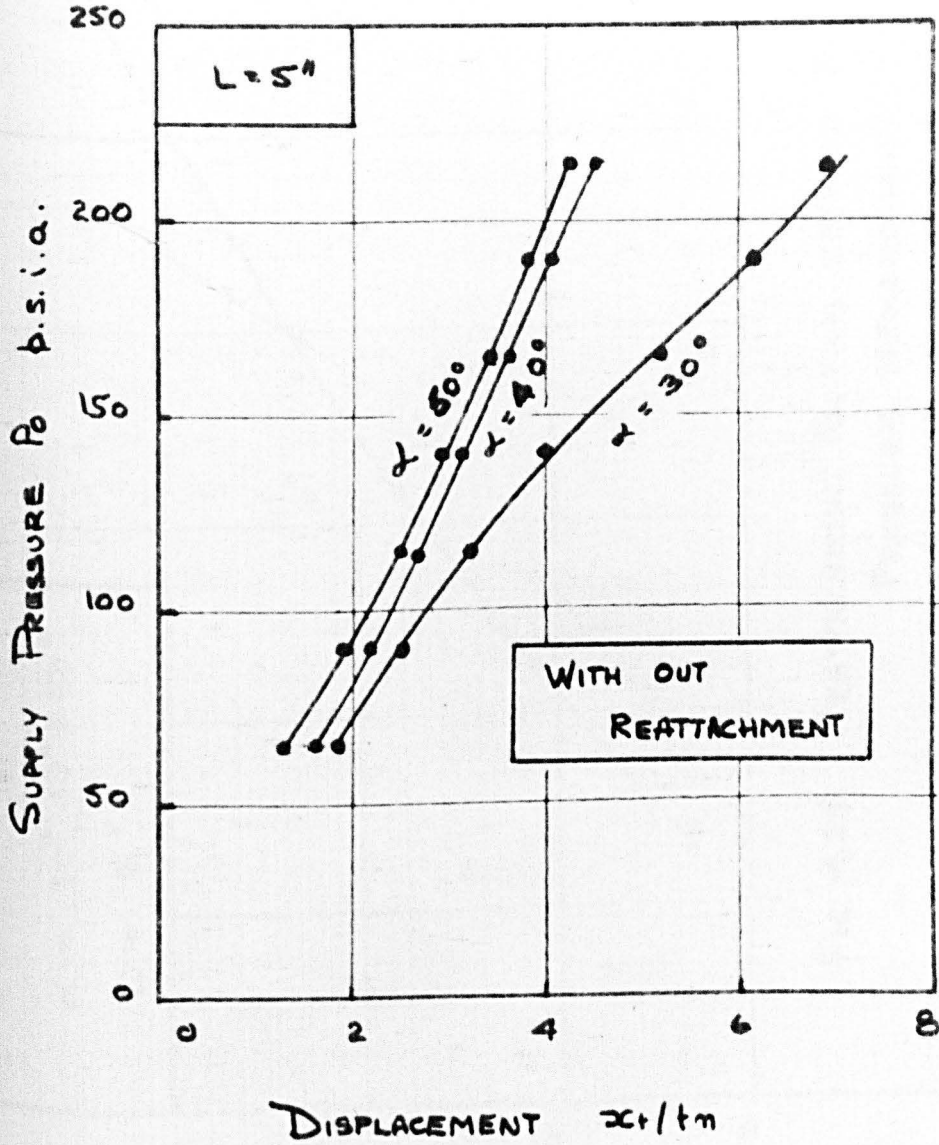
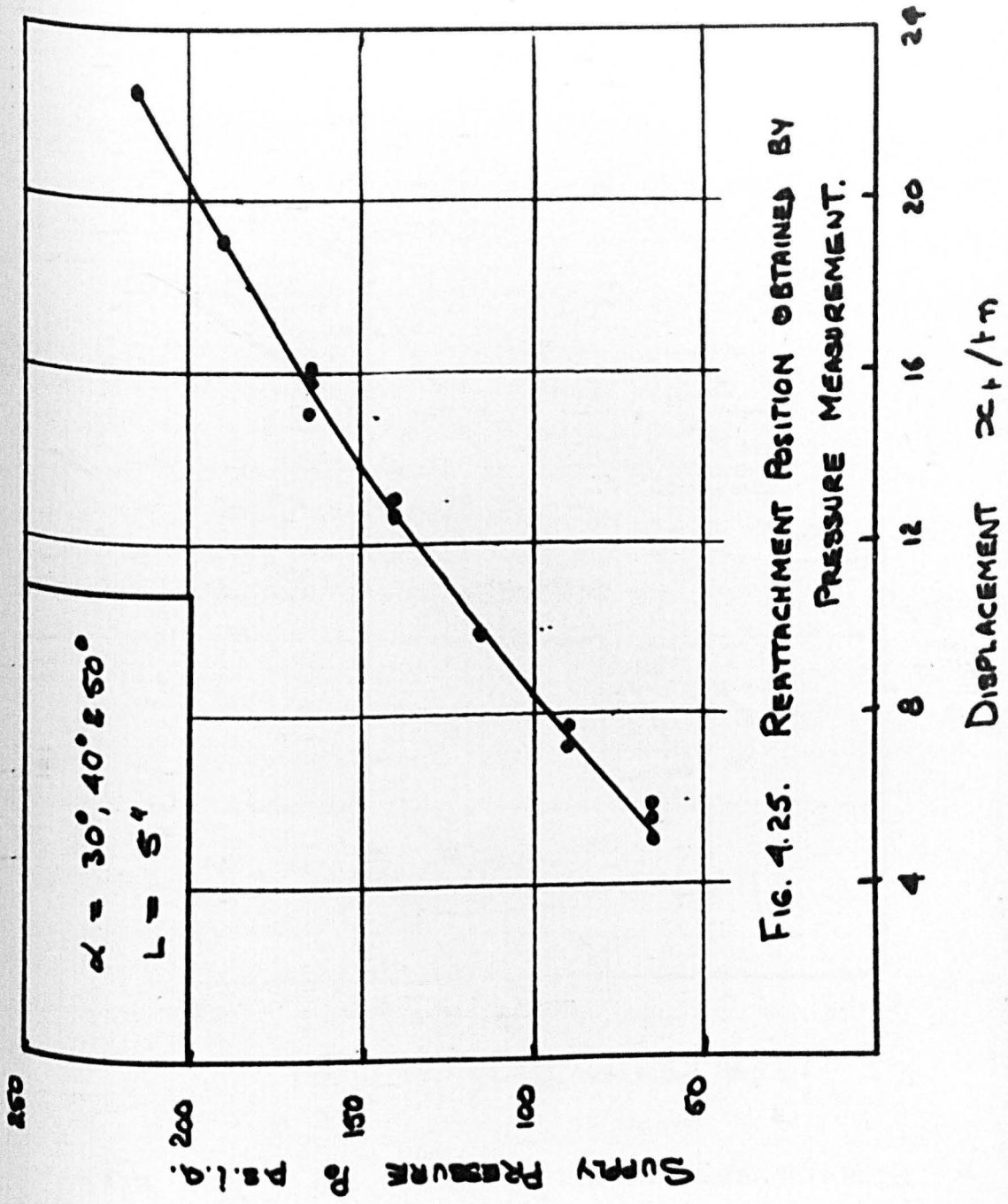


FIG. 4.24 (b) SEPARATION POSITION OBTAINED BY PRESSURE MEASUREMENT.



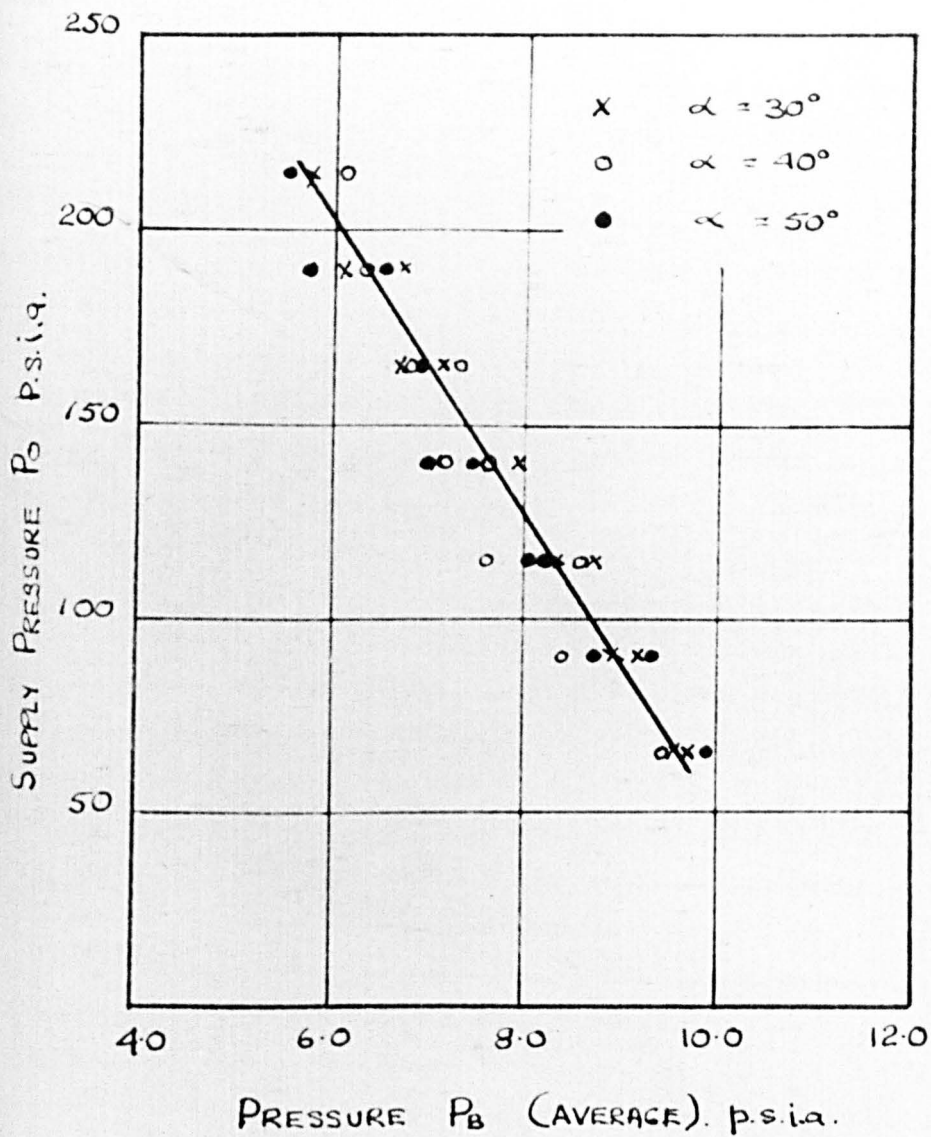


FIG. 4.26. THE AVERAGE PRESSURE CHARACTERISTIC OF THE REVERSE FLOW REGION.

stability. The main flow was forced to attach to the wall with the moveable control aperture closed and the supply pressure increased to maximum to check for stability. Assuming that no switching occurred the pressure was reduced to approximately 25 psia. and the control vent opened to a maximum of 0.300 inches. Supply pressure was then increased gradually until switching occurred. The process was repeated with decreasing values of control port width until switching could not be obtained in this way; the corresponding port width and supply pressure were noted. All tests were repeated for differing wall angles and main port widths.

Figure 4.27 shows the supply pressure obtained just on the point of switching plotted against aspect ratio for all three divergent angles. It was found that a similar limiting control port width was required to just prevent switching in all cases the main valve being 0.085 inches (aspect ratio 8.8).

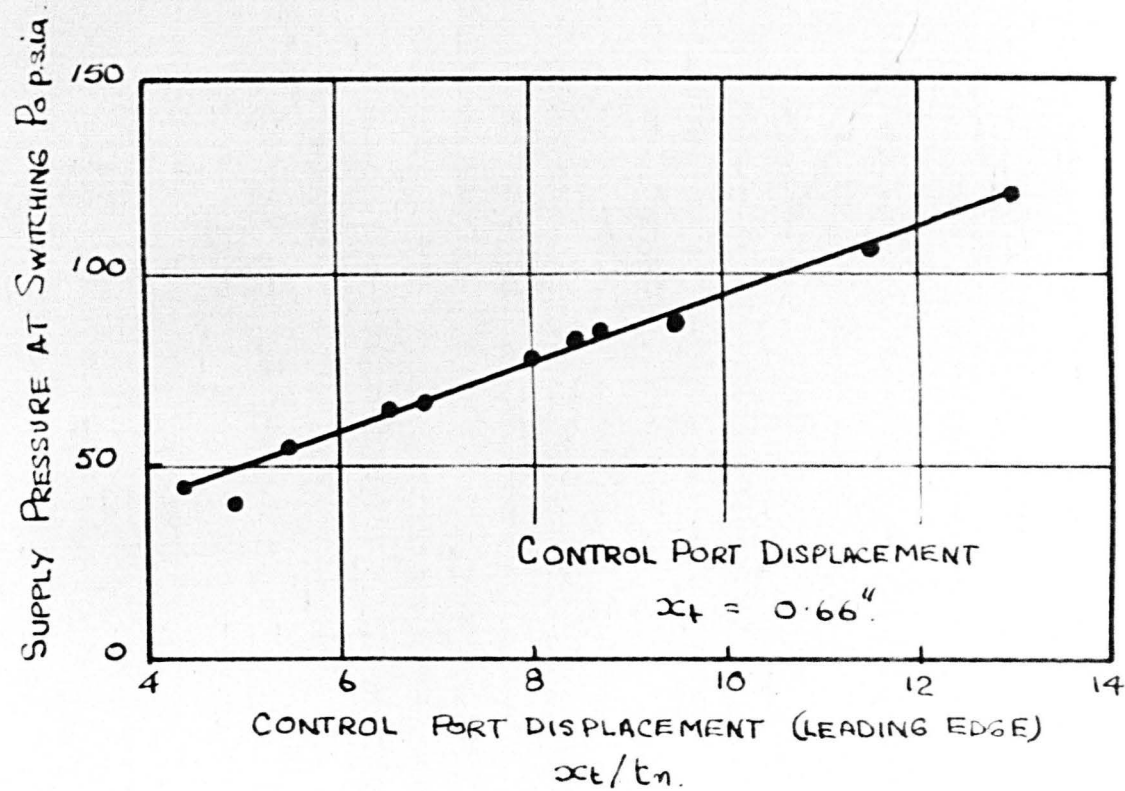


FIG. 4.27. CONTROL PORT - SWITCHING CHARACTERISTIC.

CHAPTER V

ANALYSIS OF RESULTS

5. ANALYSIS OF RESULTS.

5.1. The general situation.

The process of events leading to the flow situation indicated in the Schlieren photographs illustrated in Chapter 4 is as follows.

At the instant flow is introduced to the test duct separation occurs, to all intents and purposes axisymmetrically. Due to a turbulent jet mixing process along the jet boundaries a pressure drop occurs immediately after each separation point. Asymmetry caused, either by manufacture or the general flow situation permits the entrainment process to be more vigorous on one wall causing, in turn, progressive reorientation of the jet toward that wall until reattachment occurs. Enclosed, is a region of reverse flow, the average pressure of which is somewhat lower than ambient but higher than the static pressure of the main stream.

Reference to the results contained in Appendix 4 , and also Figures 4.18, 4.19 and 4.20 (Chapter 4) indicates that separation begins at a

particular pressure ratio, i.e. the minimum pressure prior to separation to that immediately after is virtually constant for any assumed flow situation. Because of the drop in pressure due to vorticity, etc., this ratio occurs further downstream with the reattached flow condition - isentropic expansion occurring for a longer period. The net result is a transverse pressure gradient across the jet reinforcing unilateral attachment. Destruction of the operating vortex by venting to the prevailing ambient pressure causes the jet to transfer allegiance to the opposite wall where attachment takes place by a similar process of entrainment.

Referring again to Figures 4.18, 4.19 and 4.20, the pressure distribution at attachment can be seen to divide into four principle regions, i.e. those of,

- (1) Initial expansion
- (2) Adverse pressure gradient
- (3) Constant pressure distribution
- (4) Positive pressure gradient.



These may be related to

- (1) Normal supersonic acceleration of the gas
- (2) Boundary layer back pressure interaction terminating in separation
- (3) Mean reverse flow region
- (4) Reattachment.

The nondimensional curves appertaining to conditions on the opposite wall, included in Figures 4.18, 4.19 and 4.20, show similar tendencies but do not terminate in reattachment.

Of interest, to the successful operation of the proposed switch are the positions of separation, reattachment and minimum pressure and for analytical purposes the reverse flow pressure characteristic. These are detailed below.

#### 5.2. The position of separation.

Comparison of the results obtained by the Schlieren method with those of pressure measurement (Figures 4.15 and 4.24a) show that the approximation used to measure, from photographs, the position of

separation overestimated the related distance to such an extent (approximately 30%) that it would appear to occur in the reverse flow region. Obviously, the apparent "bending" effect known to occur with shock wave interaction/generation etc. has been neglected, the pressure rise in the boundary layer being considerably less steep than that occurring in the main stream. Also separation cannot be expected to occur instantaneously at the minimum pressure situation but occurs gradually due to turbulent mixing - drag effects obtaining to the assumed sonic stream line. Therefore, a seemingly sensible approximation is to assume that separation occurs somewhere along the positive pressure gradient and probably at the point where  $d^2P/dx^2 = 0$ . From Figures 4.18, 4.19 and 4.20 this appears at an approximate pressure occurring midway between the minimum and that of the mean reverse flow. Figure 4.24 is plotted at this situation.

With reattached flows, separation occurs at a point approximately 10% further downstream than the minimum pressure

i.e. 
$$x_{ts} = 1.1 x_{tr}$$

For free separation without subsequent reattachment a value of 5% would appear more applicable for the range considered.

### 5.3. Reverse flow pressure.

The position of separation depends on the pressure fed back along the boundary layer and therefore is dependent on the reverse flow pressure condition. Reference to pressure distribution characteristics (4.18, 4.19 and 4.20) shows that the pressure of the reverse flow region may only be considered constant at the lower supply pressures, i.e.  $P_0 < 115$  psia. Beyond this the pressure experiences small negative and positive gradients until approaching the reattachment position where the pressure gradient once again becomes large and positive.

This is thought to be due to the non-symmetrical formation of the enclosed vortex; the asymmetries becoming more noticeable with increase in vortex length which is itself a function of supply pressure.

#### 5.4. The position of reattachment.

As with separation, some difficulty in predicting exactly the position of reattachment from Schlieren photographs was experienced and therefore a similar approximation was made, i.e. the  $d^2P/dx^2 = 0$  position was considered appropriate in the reattachment positive pressure gradient. Comparison of the position so predicted from the pressure characteristics (Figure 4.25) with those from the Schlieren process (Figure 4.15) suggests that the latter process tended to overestimate reattachment displacement. However, comparison with the control port switching characteristic (Figure 4.27) shows strong agreement with the results obtained by visual means, indicating that Figure 4.15 may be used to give the minimum wall length requirement for reattachment to take place, having the advantage of extended range over Figure 4.27.

Surprisingly, the reattachment position appears to be independent of wall angle for the test range considered, being a function of supply pressure and throat area only.

### 5.5. Minimum pressure situation.

As indicated in para. 5.2, the minimum pressure position occurs in close proximity to that of separation and has the advantage of being relatively easy to determine both in theory and practice. Analysis of the results shown in Figures 4.18, 4.19 and 4.20 indicates that, in this two-dimensional flow situation, the minimum pressure position occurs at a distinct pressure ratio ( $P/P_b$  or  $P/P_a$ ) of average value 0.49 for the range of Reynolds number,  $R_x = 2 \times 10^6$  to  $6 \times 10^6$ . For flow rates with Reynolds number between  $1.2 \times 10^6$  and  $2 \times 10^6$  the pressure ratio appears to increase, presumably because of a change in the assumed velocity profile. Actual physical measurement at these conditions (small nozzle widths and low  $P_o$  values, 65 psia) however, was difficult due to the  $dP/dx = 0$  situation occurring very near to the throat; the first pressure tapping point being physically limited to a distance of 0.200 inches ( $x_t$ ).

The position of minimum pressure prior to separation can be seen to increase with increase in

supply pressure and throat area but decrease with increase in wall angle and back pressure as shown in Figures 4.21, 4.22, and 4.23 of Chapter 4.

### 5.5.1 Comparison with theory.

Figure 5.1 shows the theoretical position of the minimum pressure prior to separation for the condition of no reattachment when the main flow is exhausting into an ambient pressure of 14.7 psia, i.e. assuming zero pressure drop due to turbulent jet mixing etc. Figure 5.2, reproduced from Figures 4.21, 4.22 and 4.23, shows the measured position of minimum pressure together with the theoretical values modified to include the effect of pressure drop due to entrainment without subsequent reattachment. Comparison of the two characteristics shows an interesting tendency. At total included wall angles of  $30^{\circ}$  and  $50^{\circ}$  pressure drop due to entrainment is large, particularly with the former but at  $\alpha = 40^{\circ}$  the curves of Figures 5.1 and 5.2 show fair agreement. It would appear, therefore, (from these experiments) that there is an optimum wall angle at which the entrainment process may be minimised.

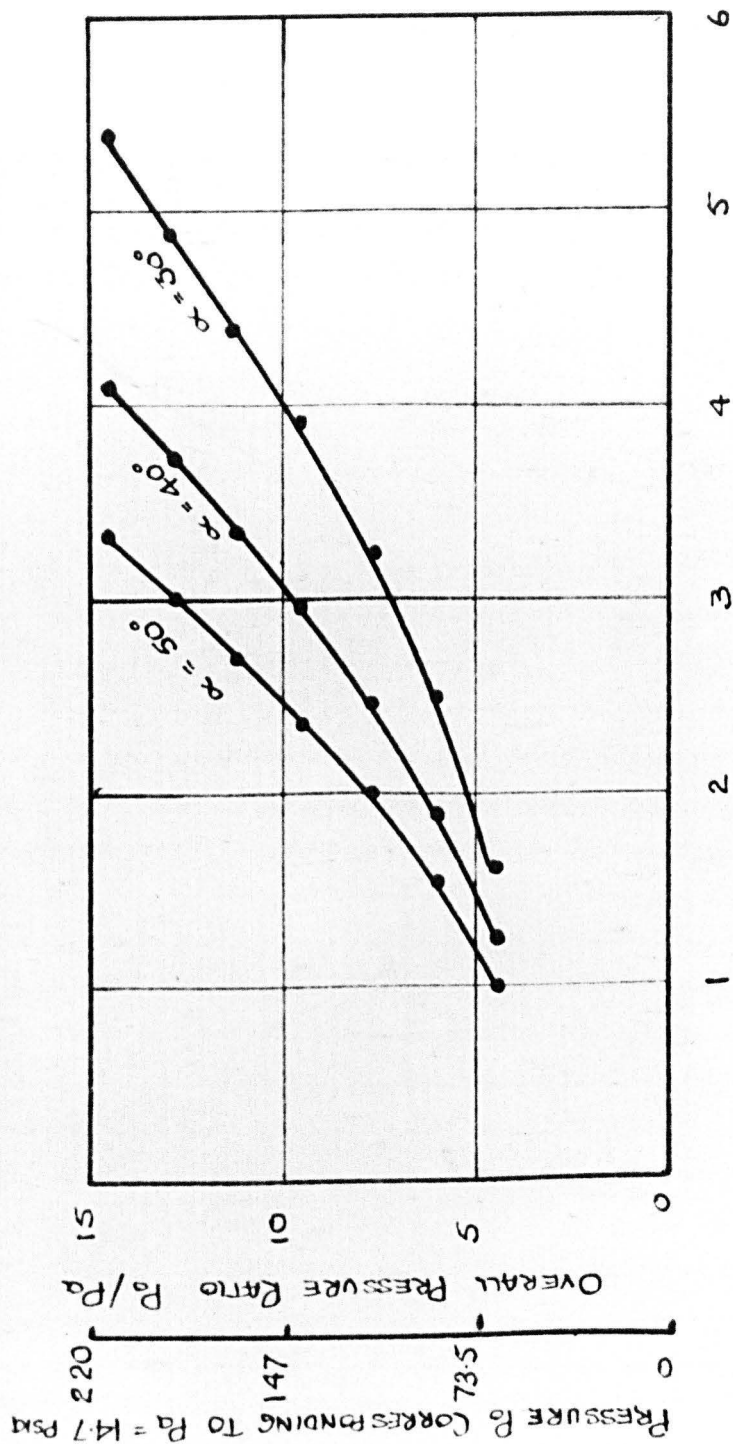


FIG. 5.1. THEORETICAL MINIMUM PRESSURE POSITION WHEN EXHAUSTING INTO A BACK PRESSURE OF 14.7 P.S.I.A. (NO REATTACHMENT)

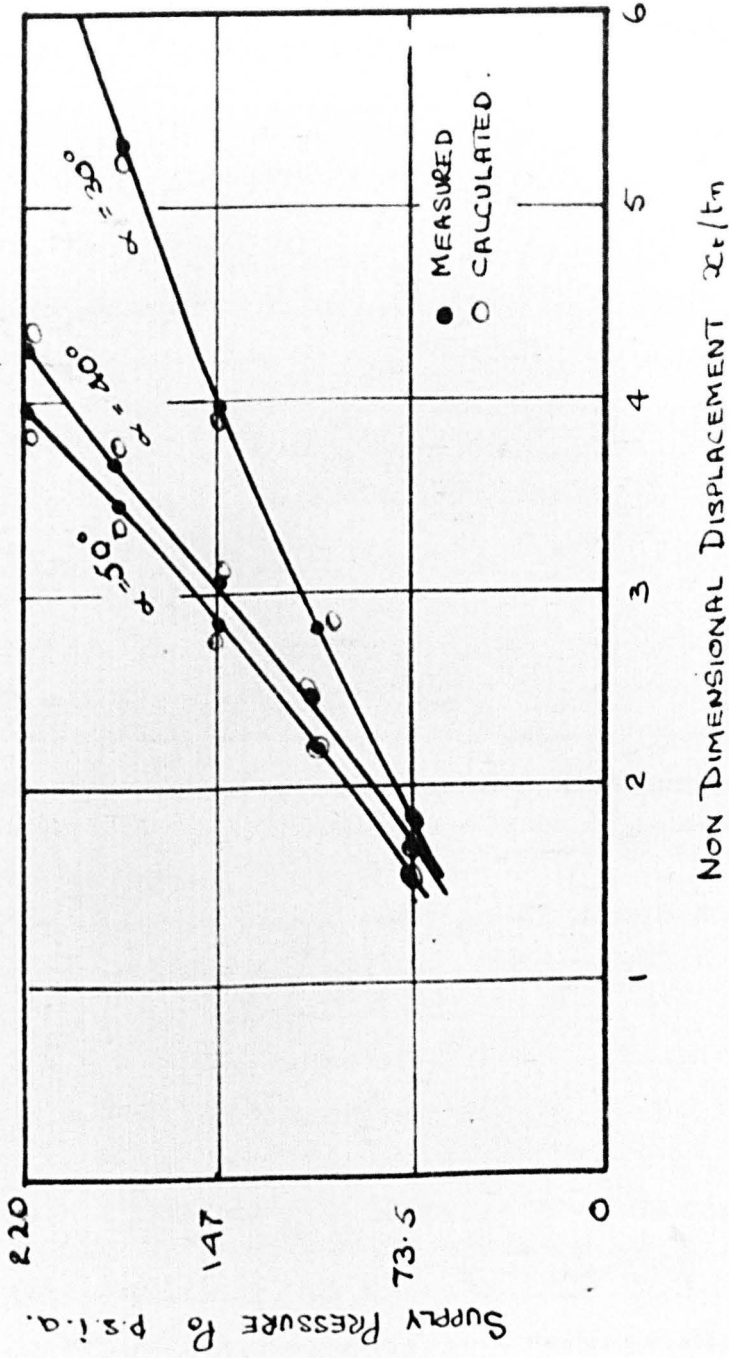


FIG. 5.2. MEASURED & CALCULATED POSITION OF MINIMUM PRESSURE WITHOUT REATTACHMENT.



Figures 4.21, 4.22 and 4.23 show the accuracy of the theory detailed in Chapter 3 when compared with experimental data - generally within a positional tolerance of 6%. Experimental results could be measured within a tolerance of  $\pm 1.5\%$ . It should be noted that the method used to obtain theoretical and experimental comparison was to insert in equation (3.17) the measured value of  $P_a$  or  $P_b$  to obtain the overall pressure ratio necessary for the solution of equation (3.20), p. as no satisfactory theoretical means of obtaining these values is known to the author.

#### 5.6. The design approach.

The net results of this research programme are shown in Figure 5.3 and are presented in a form particularly useful to the design of a supersonic bistable switch.

##### 5.6.1. Control port position.

The shaded portion between the characteristics showing wall angle,  $\alpha = 50^\circ$ ,  $40^\circ$  and  $30^\circ$ , and the reattachment curve represents the reverse flow or the

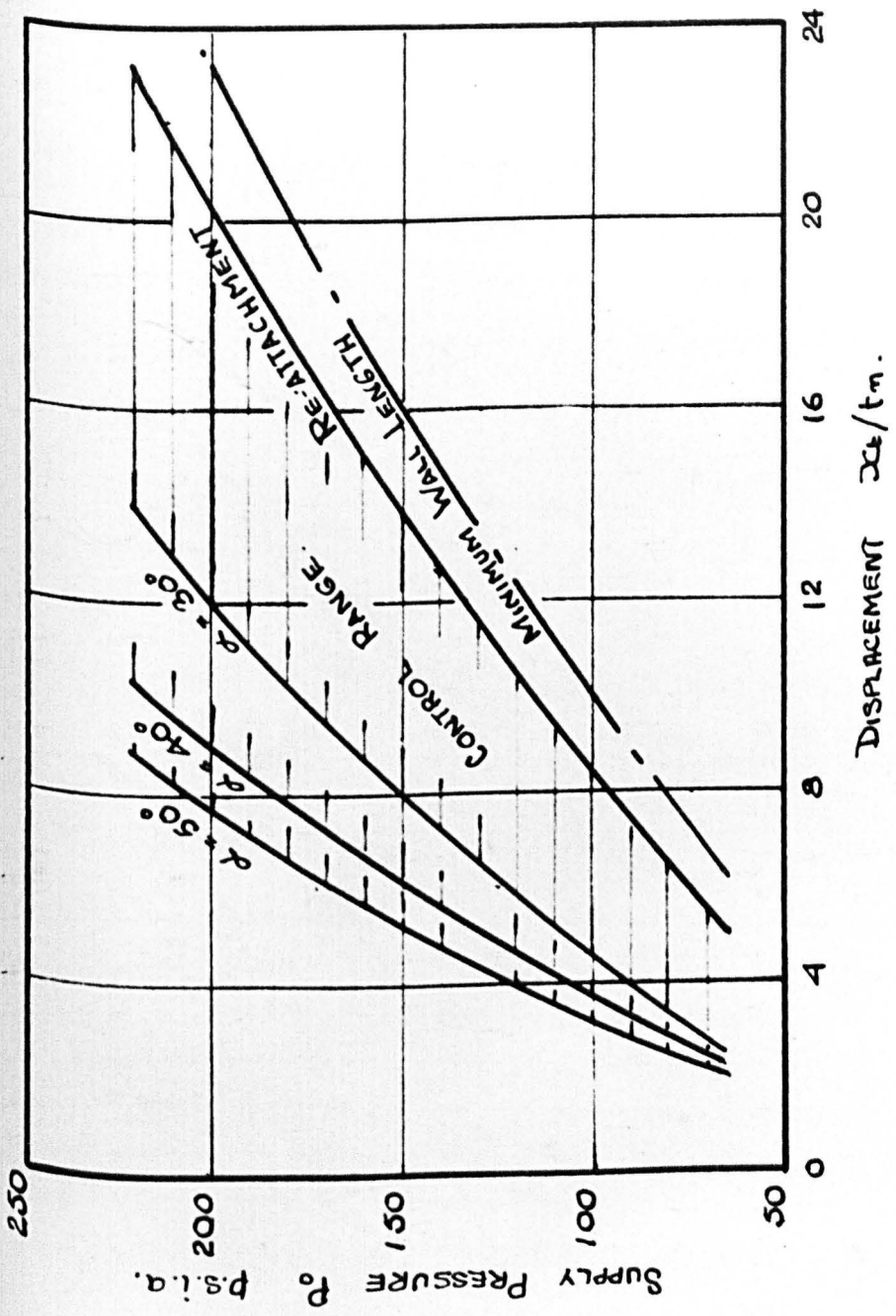


FIG. 5.3. SUPERSONIC BISTABLE SWITCH : BASIC DESIGN CRITERIA.

optimum range of control port position when operating with air as the control medium.

For example, if control ports are situated at an  $x_t/t_n$  ratio of 8 then switching of the main jet by atmospheric venting could be expected within the range of supply pressure,  $p_o$ , 100 to 150 psia, for  $\alpha = 30^\circ$ . Increase of divergent angle increases the effective operating range, i.e. for  $\alpha = 40^\circ$  and  $50^\circ$  the above working range becomes 100 - 180 psia. and 100 - 205 psia. respectively.

#### 5.6.2. Control port width.

As suggested in Chapter 4, para. 4.5.3, a limiting value of control port width (.085 inches) was determined to promote jet switching experimentally.

It is concluded, therefore, that to ensure effective switching at all operating conditions, control port width should not be less than 0.085 inches and as a rough design guide should be approximately equal to inlet width  $t_u$ , providing  $t_n \geq 0.085$  inches.

### 5.6.3. Effect of divergent angle on operation.

As indicated in para. 5.6.2 above, the basic effect of increase of divergent angle on operation is to increase the effective working range for any given position of control port. The most stable operating angle is  $40^{\circ}$  due to its free separation entrainment characteristic.

### 5.6.4. Wall length.

The minimum wall length may be determined from Figure 5.3 and will always exceed reattachment distance by 20%.

### 5.6.5. Splitter position.

If the switch is not to be used for simple thrust vector control but requires two distinct output channels the "splitter" position may be determined as follows.

Determine either by Figure 4.24 or by theory the position of separation on the non-attached wall for the maximum main jet pressure (if theory is preferred assume that a 1 or 2 psia. pressure drop occurs between end of duct and separation position). The outer

streamline of the jet separating on the free wall may then be assumed to be parallel to the opposite (reattached) wall. The splitter must be positioned tangential to this flow as shown below in Figure 5.4 and at an apex distance greater than the centre line distance  $Z$  to reattachment. A blunt nose splitter is to be preferred.

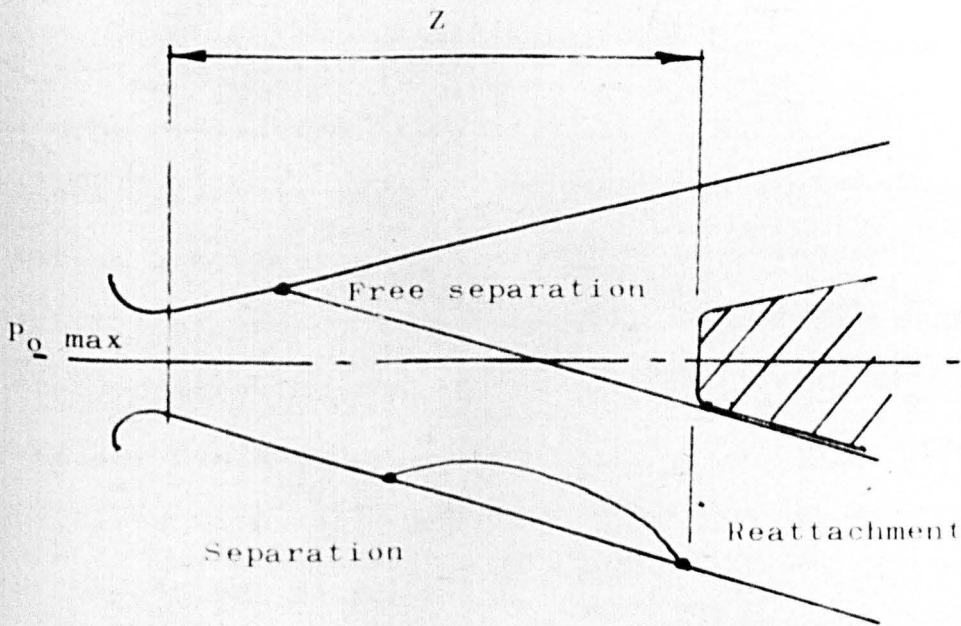


FIGURE 5.4 DETERMINATION OF SPLITTER POSITION.

### 5.6.6 The effect of offset.

No direct experimental or theoretical values can be given for the effect of offset on the flow situation but, in view of the qualitative results obtained (viz. Figure ) the following points may be made.

Offset should be limited to the throat situation if effective switching is to be maintained and only has advantages where high pressure operation is to be considered, i.e.  $P_0$  greater than 250 psia. Its net effect is to move the position of separation upstream and if excessive the flow will have insufficient energy to expand into the offset region thereby destroying the operating characteristic necessary for successful operation. As with subsonic amplifiers with large offset the device may be expected to act as a momentum interaction device rather than a bistable switch.

Small differential offset will cause instability in the flow situation. Initially, the jet will attach to the wall without offset but as supply pressure is increased it will have the tendency to spread toward

the wall with offset until, at some critical pressure, it will switch.

With regard to a theoretical approach to offset, the prediction of separation becomes more difficult as isentropic expansion can no longer (by) <sup>be</sup> assumed to occur to that position, as a shock wave is normally formed in the offset corner (see Figure ).

It is concluded that offset is generally an unnecessary complication for switches operating in the range of parameters dealt with in this research programme and should be avoided where possible.

CHAPTER VI

SUMMARY AND CONCLUSIONS



6. SUMMARY AND CONCLUSIONS.

The bistable switching of supersonic gas jets by atmospheric venting of the control ports has been shown to be a relatively simple process providing the mode of operation is fully understood. The advantages of this form of actuation are obvious, viz. no moving parts in the power stream, control system/main stream isolation, ease of manufacture, increased reliability over conventional thrust vector control systems and operating simplicity.

Operation has been shown to depend on the phenomenon of boundary layer separation followed by asymmetric reattachment enclosing a region of reverse flow of average pressure midway between that of the main stream and ambient condition. Destruction of the enclosed reverse flow region by access to ambient pressure via strategically positioned control ports causes a change in the thrust vector of the main jet.

Separation position, relative to main jet throat, has been shown to increase proportionally with throat width and some function of supply pressure but

decrease with increase in back pressure and divergent wall angle.

The ratio of the minimum pressure experienced by the flow stream immediately before separation to that immediately after has been shown to be almost constant for the operating range considered. A dependence of Reynolds number, however, is indicated.

The new theory evolved to predict the condition appertaining to this minimum pressure situation gives close agreement with the corresponding values obtained experimentally. It is equally applicable to both laminar and turbulent boundary layers at supersonic velocities acting under the duress of an adverse pressure gradient and has the advantages of being simple to use and independent of any empirical coefficient. Indications are that the pressure ratio considered decreases with increase in Reynolds number until a definite minimum value is experienced - slightly in excess of 0.4.

Reattachment position appears to be independent of wall angle for the test range considered and is a function of overall pressure ratio ( $P_o/P_a$ ) and throat

area only. Wall length must exceed reattachment distance by 20% to promote satisfactory stable jet attachment.

Indications are that the entrainment activity of a separated jet passes through a minimum at a definite divergent wall angle near to  $40^\circ$ , suggesting that this value be accepted as the optimum for jet attachment stability.

Providing that the control port is positioned somewhere between the points of separation and reattachment for the required working range and exceeds a clearly defined minimum area its effect on switching is minimised.

Splitter position also is not too critical but must be placed such that no interference with the main flow occurs at the asymmetric attachment condition.

Offset is generally considered to be detrimental to the stable operation of supersonic bistable switches.

Before the design of such a switch may be fully described theoretically, an accurate model of the

reattachment process is required and is therefore considered to be the principal objective for further research. Dynamic switching characteristics are also of vital interest.

Finally, it may be said that, this research programme has been rewarding, in that it has provided a fairly complete understanding of the process involved in the directional control of supersonic jets together with the formulation of a new theory applicable to the separation of supersonic laminar and turbulent boundary layers under the duress of an adverse pressure gradient.

CHAPTER VII

REFERENCES.

REFERENCESCHAPTER 1.

- (1) METRAL, M. "L'effet Coanda", Proc. Fifth International Congress on Applied Mechanics, 1938, p. 258.
- (2) THOMPSON, R.V. Contribution to the paper by Kadosch "The Curved Wall Effect", Second Cranfield Fluidics Conference, 3rd - 5th January, 1967, paper A.4.
- (3) MULLER, H.R. "A Study of the Dynamic Features of a Wall-reattachment Amplifier", Fluids Engineering Conference, Philadelphia, Pa, 18th - 21st May, 1964.
- (4) SHER, N.C. "Jet Attachment and Switching in Bistable Amplifiers", Fluids Engineering Conference, Philadelphia, Pa. 18th - 21st May, 1964.
- (5) MUELLER, T.J. "An Experimental Investigation of the Re-attachment of Compressible Two-dimensional Jets", Fluids Engineering Conference, Philadelphia, Pa. 18th - 21st May, 1964.

- (6) THOMPSON, R.V. "A Fresh Approach to Fluid Power Switching", Process Control and Automation, February, 1966, p. 33.
- (7) DUNAWAY and AYRE. "A Status Report on the Experimental Development of a Hot Gas Valve", Proc. of the Fluid Amplification Symposium, H.D.L. (Washington D.C., 1964), p. 459.
- (8) HOLMES and FOXWELL. "Supersonic Fluid Amplification with Various Expansion Ratio Nozzles", Proc. of the Fluid Amplification Symposium, H.D.L. (Washington D.C.), 1965.
- (9) CAMPAGNUOLO, C.J. and HOLMES, A.B. "Experimental Analysis of Digital Fluidic Amplifiers for Proportional Thrust Control", Second Cranfield Fluidics Conference, 3rd - 5th January, 1967, Cambridge, Paper K.3.
- (10) DAHLEN, G. (In Swedish). "Further Developments of a Fluidic Injection Valve for Thrust Vector Control of a Rocket Motor", Svenska Flygmotor, A.B., report no. RF. 5:1997, 15th June, 1966.

- (11) British Aircraft Corporation, Filton,  
Bristol, Unpublished report.
- (12) WARREN, R.W. "Some Parameters Affecting  
the Design of Bistable Fluid Amplifiers",  
A.S.M.E., paper no.
- (13) HACKER, R. Weapons Division, Royal  
Aircraft Establishment, Farnborough, Hants,  
Unpublished report.
- (14) FEHRMANN Technische Hochschule,  
Institut f. Regelungstechnik, Karl Marx  
Stadt, Deutsche Democtatische Republic,  
March, 1967.
- (15) ROSIC, R. Communications, Thompson  
Manufacturing Company, Los Angeles,  
California 90023, U.S.A.



REFERENCESCHAPTER II.

- (1) GRUSCHWITZ, E. Calcul approche de la couche limite laminaire du ecoulement compressible sur une paroi non conductrice de la chaleur. ONERA (Office national d'etudes et de recherche aeronautiques) publication No. 47, Paris 1950.
- (2) POHLHAUSEN, K. Zur naherungsweise Integration der Differentialgleichung der laminaren Reibungsschicht ZAMM, 1, 252(1921).
- (3) HOLSTEIN, H. and BOHLEN, T. Ein einfaches Verfahren zur Berechnung laminares Reibungsschichten, die dem Naherungsansatz von K. Pohlhausen genugen. Lilienthal-Bericht S.10. p.5, (1940).
- (4) SCHLICHTING Boundary Layer Theory, Chapter XV, p.295, Pergamon Press, 1955.
- (5) HOWARTH, L. Ibid, 194. 16. 1948.
- (6) YOUNG, A.D. 1949. Aero Quart. 1, 137.

- (7) LUXTON, R.E. and YOUNG, A.D. 1960,  
ARCR & M. 3233.
- (8) STEWARTSON, K. 1949, Proc. Royal Soc. A.,  
200, 84.
- (9) ILLINGWORTH, C.R. 1949, Proc. Royal Soc. A.,  
199, 533.
- (10) ROTI, N. 1953. J. Aero. Sci., 20, 67.
- (11) OSWATITSCH and WOIGHARDT, K. 1943,  
Lil-Ges. fur Luft, S. 13, 7.
- (12) ILLINGWORTH, C.R. 1946. ARCR & M., 2590,
- (13) FRANKL, F.I. 1934, Trans. CAHL, 176, p.3.
- (14) EMMONS, H.W. and BRAINARD, J.G. 1941,  
J. Appl. Mech. E., 105.
- (15) GADD, G.E. Journal Aero. Sci., Vol. 20,  
November, 1953, No. 11, p. 729.
- (16) STRATFORD, B.E. Journal of Fluid Mechanics  
Vol. 5, 1959, p.1 and p. 17.
- (17) GOLDSTEIN, S. (Ed.) 1938. Modern Developments  
in Fluid Dynamics, Vols. I and II, Oxford  
University Press.

- (18) SCHLICHTING, H. 1941. Tech. Mem. Nat. Adv. Comm. Aero. Wash., No. 1218(transl.)  
see also reference (4) above, p. 432.
- (19) von DOENHOFF and TETERLIN. 1943,  
Rep. Nat. Adv. Comm. Aero., Washington, No.772.
- (20) KALIKHMANN. 1943. Dokl. Akad. Nauk. S.S.S.R., 38, 165.
- (21) ROTTA, J. 1953, Rep. no. 8, University of Göttingen.
- (22) SPENCE 1956(a) Aero. Res. Coun. Lond. Unpublished paper No. 18, 261. (Modified method by Spence; also a review of methods including those of Garner, Schuh, Truckenbradt and Zaat). (b) 1956, J. Aero. Sci., 23, 3.
- (23) SQUIRE and YOUNG. 1937, Rep. and Mem. Aero. Res. Coun., Lond., No. 1838.
- (24) MASKELL, E.C. 1951, Aero. Res. Coun., Lond., Unpublished paper no. 14, 654.
- (25) TOWNSEND, A.A. The behaviour of a turbulent boundary layer near separation. Journ. Fluid Mechs., vol. 12, 1962.

- (26) SCHUBAUER, G.B. and KLEBANOFF. P.S. 1951.,  
Nat. Adv. Comm. Aero., Wash., Rep. no. 1030.
- (27) ARENS and SPIEGLER. A.I.A.A. Journ.  
March 1963, p. 581.
- (28) SHAPIRO, A.F. The Dynamics and  
Thermodynamics of Compressible Fluid Flow.  
(Ronald Press. N.Y., 1953), vol. 1, p. 140-141.
- (29) FRASER, R.P., EISENKLAM, P., and WILKIE, D.  
J. Mech. Sci. 1, 267 - 279 (1959).
- (30) McKENNEY, J.D. Ae. E. Thesis, Calif. Inst.  
Tech. (1949).
- (31) FOSTER, C.R. and COWLES, F.B. "Experimental  
Study of Flow Separation in overexpanded  
nozzles for pocket motors". Calif. Inst.  
Tech., Progr. Report 4 - 103 (1949).
- (32) CAMPBELL, C.E. and FARLEY, J.M. Reference of  
several conical convergent-divergent  
type exhaust nozzles. NASA T.N. D-467 (1960).
- (33) AHLBERG et al. Truncated perfect nozzle  
in optimum nozzle design. ARS J. 31,  
614 - 620 (1961).

- (34) FARLEY, J.M. and CAMPBELL, C.E. Performance of several method of characteristic exhaust nozzles. NASA T.N. D-293 (1960).
- (35) BLOOMER, H.E. et al. Experimental study of effects of geometric variables on performance of conical rocket engine exhaust nozzles. NASA T.N. D-846 (1961).
- (36) ARENS and SPIEGLER. Separated flow in overexpanded nozzles at low pressure ratios. Bull Research Council, Israel, 11C, 45 - 55, (1962).
- (37) MAGER, A. Journal of the Aero Sciences, February, 1966, p. 181.
- (39) VAN LEE, N. Transformation between Compressible and incompressible boundary layer equations. Journal of the Aero Sciences, Vol. 20, No. 8, pp. 583-584, August 1953.
- (40) SCHUH, H. On Determining Turbulent Boundary Layer Separation in incompressible and compressible Flow, Journal of the Aero Sci., vol. 22, no. 5, pp. 343 - 345, May, 1955.

- (41) TRUCKENBRODT, E. Ein Quadraturverfahren zur Berechnung der laminaren und turbulenten Reibungsschicht bei ebener und rotationssymmetrischer Strömung. Ing. Arch. 20, 211 (1952).
  
- (42) GARNER, H.C. The Development of turbulent boundary layers. ARC Rep. and Memo. No. 2133 (1944).

REFERENCESCHAPTER III.

- (1) BRINICH, P.F. Boundary layer measurements in 3.84 by 10 inch Supersonic Tunnel.  
N.A.C.A. T.N. 2203, 1950.
- (2) TUCKER, M. Approximate Turbulent Boundary layer development in Plane Compressible Flow along Thermally Insulated Surfaces with application to Supersonic Tunnel Contour Correction, N.A.C.A. T.N. 2045, 1950.
- (3) RUPTASH, J. Boundary Layer Measurements in the UTIA 5 - by 7 inch Supersonic Wind Tunnel, UTIA Rep. no. 16, 1952.
- (4) TUCKER, M. Approximate Calculation of Turbulent Boundary Layer Development in Compressible Flow by the Similarity Theory.  
N.A.C.A. T.N. 2543, 1951.
- (5) SHEN, S.F. Investigation of Turbulent Layer over a Flat Plate in Compressible Flow by the Similarity Theory, N.A.C.A. T.N. 2543, 1951.

- (6) WILSON, R.E. Turbulen Boundary Layer Characteristics at Supersonic Speeds - Theory and Experiment. Jour. Aero. Sci., Vol. 17, No. 9, September, 1950.
- (7) NIKURADSE, J. Gesetzmabigkeit der turbulentum Stromung in glatten Rohren. Forschungsheft 359 (1932).
- (8) NIKURADSE, J. Turbulente Reibungsschichton an der Platte. Ed. by Zentr. wiss. Ber Wesen Obtainable from R. Oldenbourg, Munich and Berlin, 1942.
- (9) SCHUBAUER, G.B. and KLEBANOFF, P.S. Contributions on the Mechanics of Boundary Layer Transition. N.A.C.A. T.N. 3489 (1955) and N.A.C.A. Rep. no. 1289 (1956). see also Proc. Symp. on Boundary Layer Theory Nat. Phys. Lab. England, 1955.
- (10) BLASIUS, H. Grenzsichten in Flussigkeiten mit kleiner Reibung Z. Math. u. Phys. 56, 1 (1908). English Translation N.A.C.A. Memo no. 1256.



- (11) CURLE, N. The Laminar Boundary Layer Equations. p. 88, Oxford Mathematical Monographs, 1962.
- (12) BOURQUE and NEWMAN. Reattachment of a Two-dimensional Incompressible jet to an adjacent Flat Plate. Aero. Quart., vol. X 1, August, 1960.
- (13) SAWYER, R.A. The Flow due to a Two-dimensional Jet issuing parallel to a Flat Plate. J. Fluid Mech. vol. 9, p.4, December, 1960.
- (14) COPE and HARTREE. 1948. Phil. Trans. Roy. Soc. A., 241, 1.
- (15) SHER, N.C. Jet Attachment and Switching in Bistable Fluid Amplifiers, ASME paper, 64-FE-19, March 1964.
- (16) OLSON, R.E. Reattachment of a Two-dimensional Jet to an Adjacent Plate. Symp. on Fluid Jet Devices, ASME, 1962.

- (17) SAWYER, R.A. Two-dimensional Reattaching Jet Flows Including the Effects of Curvature on Entrainment, J. Fluid Mech., vol. 17, pt. 4, December, 1963.
- (18) MULLER, H.R. A Study of the Dynamic Features of a Wall-Reattachment Fluid Amplifier. ASME paper no. 64-FE-10.
- (19) MUELLER, T.J. An Experimental Investigation of the Reattachment of Compressible Two-dimensional Jets. 64-FE-18.
- (20) GREBER, I. Bubble Pressures under Reattaching Laminar Jets and Boundary layers. Symposium on Fluid Jet Devices. ASME 1962.

CHAPTER VIII

APPENDICES

APPENDIX 1.

The Method of Pohlhausen applied to  
Laminar Incompressible Boundary Layers.

The original approach of K. Pohlhausen\* later amended by Holstein and Bohlen\* was to select a suitable velocity profile to satisfy the imposed boundary conditions such that incorporation in the momentum equation gave an ordinary differential equation in terms of the boundary layer thickness.

To satisfy the various boundary conditions he selected the profile

$$\frac{u}{U} = f(\eta) = a\eta + b\eta^2 + c\eta^3 + d\eta^4 \quad (\text{A.1})$$

in the range  $0 \leq \eta \leq 1$ , for  $\eta \geq 1$ ,  $u/U$  assumes unity where  $\eta = y/\delta(x)$

Assuming  $dP/dx = 0$ , the four constant coefficients can be determined for the boundary conditions.

$$\begin{aligned} y=0 : u=0 \quad \nu \frac{\partial^2 u}{\partial y^2} &= \frac{1}{\rho} \frac{dP}{dx} = -U \frac{dU}{dx} \\ y=\delta \quad u=U \quad ; \quad \frac{\partial u}{\partial y} &= 0 \quad \frac{\partial^2 u}{\partial y^2} = 0 \end{aligned} \quad (\text{A.2})$$

By successive differentiation and substitution

\* (see References 2 & 3.

of the boundary conditions the coefficients become;

$$a = 2 + \frac{A}{6} ; \quad b = -\frac{A}{2} ; \quad c = -2 + \frac{A}{2} ; \quad d = 1 - \frac{A}{6}$$

where 
$$A = \frac{\delta^2}{\nu} \frac{dU}{dx} \quad (A.3)$$

Substitution of these values in (A.1) and rearranging gives:

$$\frac{u}{U} = F(\eta) + A G(\eta) \quad (A.4)$$

where 
$$F(\eta) = 1 - (1-\eta)^3(1+\eta)$$

$$G(\eta) = \frac{1}{6} \eta (1-\eta)^3$$

Obviously equation (A.4) constitutes a parametric set of velocity profiles with  $A$  as the shape factor. Note that:

$$A = \frac{\delta^2}{\nu} \cdot \frac{dU}{dx} = -\frac{dP}{dx} \cdot \frac{\delta}{\mu U/\delta}$$

which may be interpreted as the ratio of pressure forces to viscous forces.

It is to be expected that the shape factor will have a particular value at separation which may

be determined by invoking the condition

$$\left. \frac{\partial u}{\partial y} \right|_0 = 0 \quad \text{at separation}$$

i.e. differentiating (A.4) and equating zero gives,  
at  $y = 0$ ,

$$U \left[ \frac{a}{\delta} + \frac{2by}{\delta^2} + \frac{3cy^2}{\delta^3} + 4 \frac{dy^3}{\delta^4} \right]_{y=0} = 0$$

i.e.  $a = 0$

which, in turn, suggests

$$a = 0 = 2 + \frac{\Lambda_{SEP}}{6}$$

i.e.  $\Lambda_{SEP} = -12$  (A.5)

or in terms of pressure gradient becomes

$$\frac{dP}{dx} = \frac{12 \mu U}{\delta^2} \quad (A.6)$$

The shape factor is limited to the range

$$-12 \leq \Lambda \leq +12$$

as for values greater than +12, values of  $u/U > 1$  occur.

Substituting the velocity profile equation (A.4) into the respective equations for displacement and momentum equations (Appendix 3) results in

$$\frac{\delta^*}{\delta} = \frac{3}{10} - \frac{\Lambda}{120} ; \quad \frac{\theta}{\delta} = \frac{37}{315} - \frac{\Lambda}{945} - \frac{\Lambda^2}{9072} \quad (\text{A.7})$$

Similarly the viscous stress at the wall becomes

$$\frac{\tau_0 \delta}{\mu U} = 2 + \frac{1}{6} \Lambda \quad (\text{A.8})$$

Multiplying the momentum equation (Appendix 3) by  $\delta/\sqrt{U}$  is obtained

$$\frac{U \theta \theta'}{\nu} + (2 + \frac{\delta^*}{\theta}) K = \frac{\tau_0 \theta}{\mu U} \quad (\text{A.9})$$

$$\text{where } K = \frac{\theta^2}{\nu} \cdot \frac{dU}{dx} = z \frac{dU}{dx} \quad (\text{A.10})$$

The object now, is to obtain expressions involving  $K$  and  $\Lambda$  only such that for any assumed value of the shape factor,  $K$  or some function of  $K$ , may be obtained and re-related to the defined boundary layer thicknesses, which by successive iteration provide solutions to the form of the boundary layer at any value of  $x$ .

Eliminating  $\frac{dU}{dx}$  between equations (A.10) and (A.3)

$$K = \frac{\theta^2}{\delta^2} \Lambda \quad (\text{A.11})$$

Using the momentum thickness equation, (A.7)

becomes

$$K = \left[ \frac{37}{315} - \frac{\Delta}{945} - \frac{\Delta^2}{9072} \right]^2 \Delta \quad (\text{A.12})$$

Scrutiny of the momentum equation (A.9) suggests that expressions for  $\delta^*/\theta$  and  $U\theta\theta'$  will be required, preferably in terms of  $K$  and  $\Delta$  if a simple linear equation is to be obtained.

Therefore, as  $\delta^*/\delta \cdot \delta/\theta = \delta^*/\theta$  equations

(A.7) and (A.9) provide (as  $K = f(\Delta)$ );

$$\frac{\delta^*}{\theta} = \frac{\frac{3}{10} - \frac{\Delta}{120}}{\left[ \frac{37}{315} - \frac{\Delta}{945} - \frac{\Delta^2}{9072} \right]^2} = f_1(K) \quad (\text{A.13})$$

Similarly (A.8) becomes

$$\begin{aligned} \frac{\tau_0 \theta}{\mu U} &= \frac{\tau_0 \delta}{\mu U} \cdot \frac{\theta}{\delta} \\ &= \left[ 2 + \frac{\Delta}{6} \right] \left[ \frac{37}{315} - \frac{\Delta}{945} - \frac{\Delta^2}{9072} \right] \end{aligned}$$

i.e.

$$\frac{\tau_0 \theta}{\mu U} = f_2(K) \quad (\text{A.14})$$



Substitution of these derived functions in the momentum equation (A.9) provides;

$$\frac{U\theta\theta'}{\sqrt{}} + [2 + f_1(K)]K = f_2(K) \quad (\text{A.15})$$

also 
$$z = \theta^2/\sqrt{}$$

$$\frac{dz}{dx} = \frac{z\theta}{\sqrt{}} \cdot \frac{d\theta}{dx}$$

$$\therefore \theta \frac{d\theta}{dx} = \frac{\sqrt{}}{2} \frac{dz}{dx} = \theta\theta'$$

giving

$$\frac{U}{2} \cdot \frac{dz}{dx} + [2 + f_1(K)]K = f_2(K)$$

Multiplying by 2 and gathering the K terms the finalised expression becomes

$$U \frac{dz}{dx} = F(K) \quad (\text{A.16})$$

where 
$$F(K) = 2f_2(K) - 4K - 2f_1(K)K.$$

$$= 2 \left( \frac{37}{315} - \frac{\Lambda}{945} - \frac{\Lambda^2}{9072} \right) \left[ 2 - \frac{116}{315} \Lambda + \left( \frac{2}{945} + \frac{1}{120} \right) \Lambda^2 + \frac{2}{9072} \Lambda^3 \right]$$

(A.17.)

Summarising

$$\frac{dz}{dx} = \frac{F(K)}{U} ; \quad K = z U'$$

For a general method of solution to the above equations the reader is referred to Schlichting\*. The interest, in this research programme, is mainly limited to the point of separation and a general solution to the condensed momentum equation at this point may be obtained as follows.

Using expression (A.10)

$$K = z U'$$

$$\frac{dz}{dx} = -K (U')^{-2} \frac{dU'}{dx}$$

$$= -\frac{K U''}{U'^2}$$

giving 
$$U \frac{dz}{dx} = -\frac{K U U''}{U'^2} \quad (A.18)$$

which, from (A.16), becomes a function of  $K$  and  $U$  only, i.e.

$$\frac{F(K)}{K} = -\frac{U U''}{U'^2} = -\sigma \quad (A.19)$$

\* (Schlichting, "Boundary Layer Theory, p. , McGraw Hill Co., 1962).

where

$$\sigma = \frac{U U''}{U'^2}$$

At separation  $\Lambda = -12$  and  $K = -0.1567$ ;

$$F(K) = 1.7241$$

hence  $\sigma \doteq 11$  at the limit of attachment.

Therefore, to predict the position of separation by this method, it is necessary to obtain an expression for main stream velocity  $U$  in terms of  $x$ , which has distinct first and second derivatives. Substitution of the expression for main stream velocity and its derivatives in  $\sigma = 11$  gives an expression in  $x$  at the point of separation. Note that  $x$  is measured along the contour of the boundary layer.

APPENDIX 2.

Theoretical prediction of the point of separation in a convergent divergent duct assuming incompressible flow.

As suggested in Chapter 1, the method of Pohlhausen may be used to determine the position of separation in a flow situation similar to that occurring in a subsonic 'Fluidic Switch'. The method is as follows.

Assume that the duct in the vicinity of its throat may be represented by two cylinders as shown below (Figure A.1).

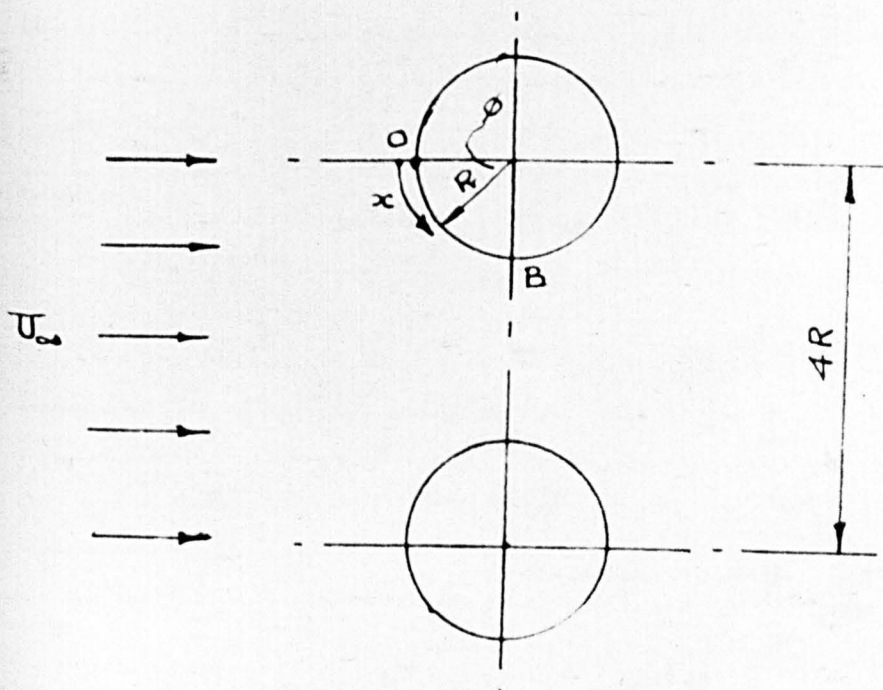



FIG. A.1.

Assuming that  $O$  is the stagnation point then

tangential flow at  $O = \text{zero}$

tangential flow at  $B = 2 U_{\infty}$

Assuming a sine function for main stream flow, 

i.e.

$$U_x = 2U_{\infty} \sin \phi \quad (\text{A.20})$$

Then

$$\frac{dU_x}{dx} = 2U_{\infty} \cos \phi \frac{d\phi}{dx} \quad (\text{A.21})$$

$$\frac{d^2U_x}{dx^2} = 2U_{\infty} \cos \phi \frac{d^2\phi}{dx^2} - \frac{d\phi}{dx} \cdot 2U_{\infty} \sin \phi \frac{d\phi}{dx}$$

However,  $\phi$  is proportional to  $x$  therefore

$$\frac{d^2\phi}{dx^2} = 0$$

hence

$$\frac{d^2U_x}{dx^2} = - \left( \frac{d\phi}{dx} \right)^2 \cdot 2U_{\infty} \sin \phi \quad (\text{A.22})$$

which, on substituting (A.20), (A.21) and (A.22) in expression (A.19), Appendix 1, gives

$$\sigma = \frac{2U_{\infty} \sin \phi \times 2U_{\infty} \sin \phi \cdot \left( \frac{d\phi}{dx} \right)^2}{- (2U_{\infty} \cos \phi \frac{d\phi}{dx})^2}$$

$$\sigma = \tan^2 \phi$$

which, for the limit of attachment, i.e.  $\sigma^* = 11$ , provides

$$\beta = 106.4^\circ \quad (\text{A.23})$$

Suggesting that separation will occur approximately  $16^\circ$  after the throat. Obviously, with offset, it may be assumed to occur at the throat.

To the author's knowledge, the solution offered above to flow past two cylinders is original, the usual method ( ) being to assume the Blasius series for velocity distribution containing six terms in  $x$  up to the power eleven, providing a solution of  $109.5^\circ$ . (see Schlichting, p. 253 and p. 153, 2nd Edition). This approach, in the author's opinion, seems unnecessarily complicated.

APPENDIX 3.Some Definitions.

The following includes quantities referred to in the test.

Displacement Thickness.

$$\delta^* = \int_0^{\delta} \left(1 - \frac{eu}{e_1 U}\right) dy \quad (\text{A.24})$$

Momentum Thickness.

$$\theta = \int_0^{\delta} \frac{eu}{e_1 U} \left(1 - \frac{u}{U}\right) dy \quad (\text{A.25})$$

Energy Dissipation Thickness.

$$\theta_E = \int_0^{\delta} \frac{eu}{e_1 U} \left(1 - \frac{u^2}{U^2}\right) dy \quad (\text{A.26})$$

Enthalpy Thickness.

$$\theta_h = \int_0^{\delta} \frac{eu}{e_1 U} \left(\frac{h}{h_1} - 1\right) dy \quad (\text{A.27})$$

where  $h = g C_p T$ .

Velocity Thickness.

$$\delta_u = \int_0^{\delta} \left(1 - \frac{u}{U}\right) dy \quad (\text{A.28})$$

Continuity Equation.

$$\frac{\partial u}{\partial x} + \frac{\partial v}{\partial y} = 0 \quad (\text{A.29})$$

The Momentum Integral Equation.

$$\int_0^{\delta} \frac{\partial}{\partial x} [u(\tau - u)] dy + \frac{\partial \tau}{\partial x} \int_0^h (\tau - u) dy = \frac{\tau_0}{e} \quad (\text{A.30})$$

which, on substitution of the displacement thickness and momentum thickness equations becomes;

$$\frac{\tau_0}{e} = \frac{d\tau^2 \theta}{dx} + \delta^* \tau \frac{d\tau}{dx} \quad (\text{A.31})$$

The Energy Equation.

(a) turbulent flow

$$\frac{d\tau^3 \delta^{**}}{dx} = 2 \int_0^{\infty} \frac{\tau}{e} \cdot \frac{\partial u}{\partial y} \cdot dy \quad (\text{A.32})$$

(b) laminar flow

$$\frac{d\tau^2 \delta^{**}}{dx} = 2 \nu \int_0^{\infty} \left( \frac{\partial u}{\partial y} \right)^2 dy \quad (\text{A.33})$$

Energy Thickness.

$$\delta^{**} = \int_0^{\infty} \frac{u}{\tau} \left( 1 - \frac{u^2}{\tau^2} \right) dy \quad (\text{A.34})$$



APPENDIX 4.Experimental Results.

The following Figures show the measured pressure distribution occurring in the convergent-divergent, two-dimensional duct. Figures (A.4.1) to (A.4.25) correspond to boundary layer separation followed by reattachment, and Figures (A.4.26) to (A.4.43) to the separation condition only.

The supply pressure ( $P_0$ ) appertaining to each test curve is indicated by the following numerals

- |               |               |
|---------------|---------------|
| (1) 65 psia.  | (2) 90 psia.  |
| (3) 115 psia. | (4) 140 psia. |
| (5) 165 psia. | (6) 190 psia. |
| (7) 215 psia. |               |

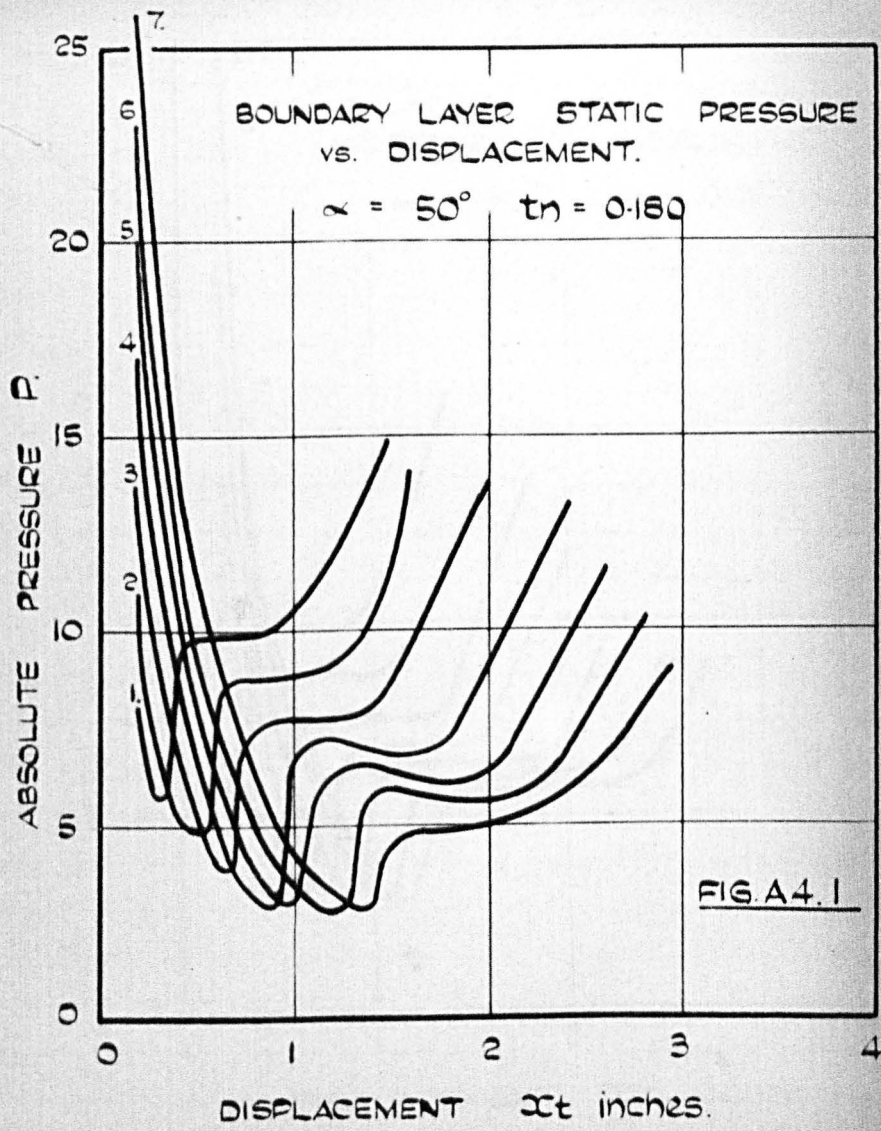
Where the minimum pressure situation occurred before the first pressure tapping position the characteristic has been omitted.

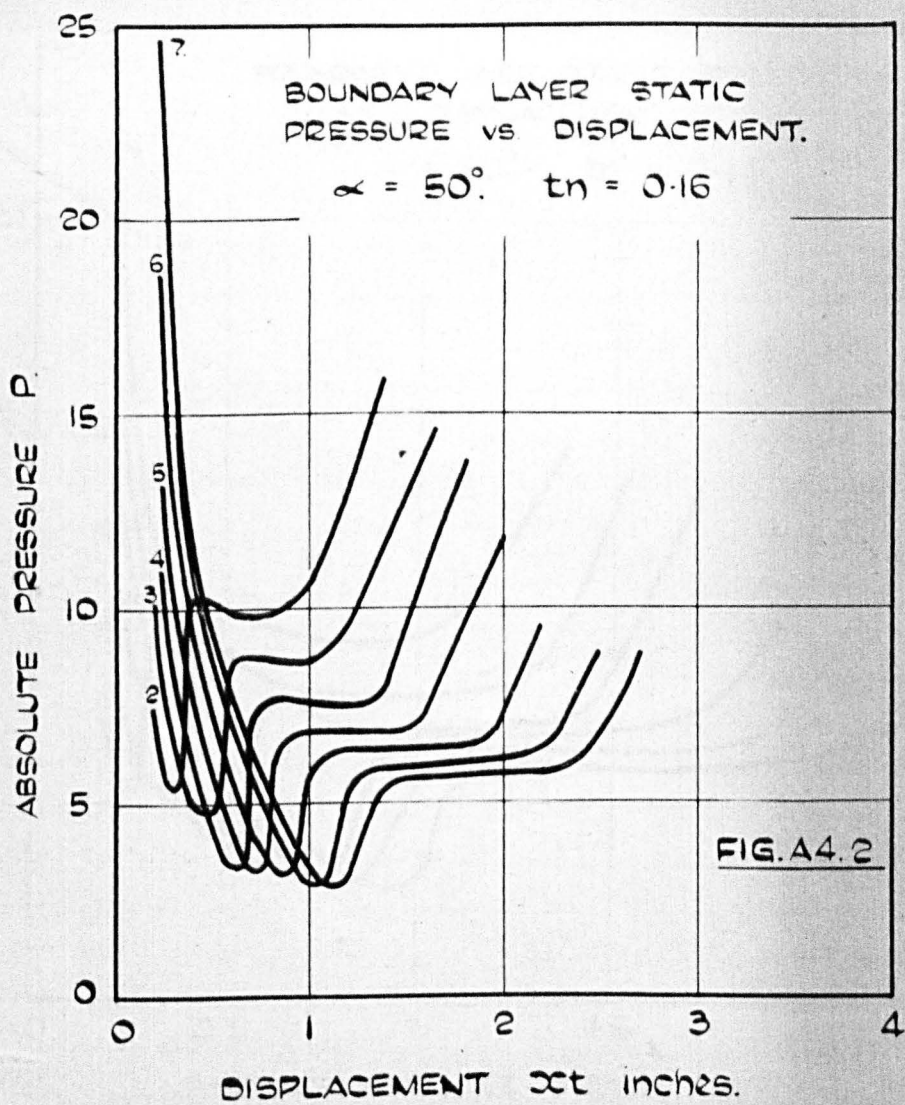
NOTE.

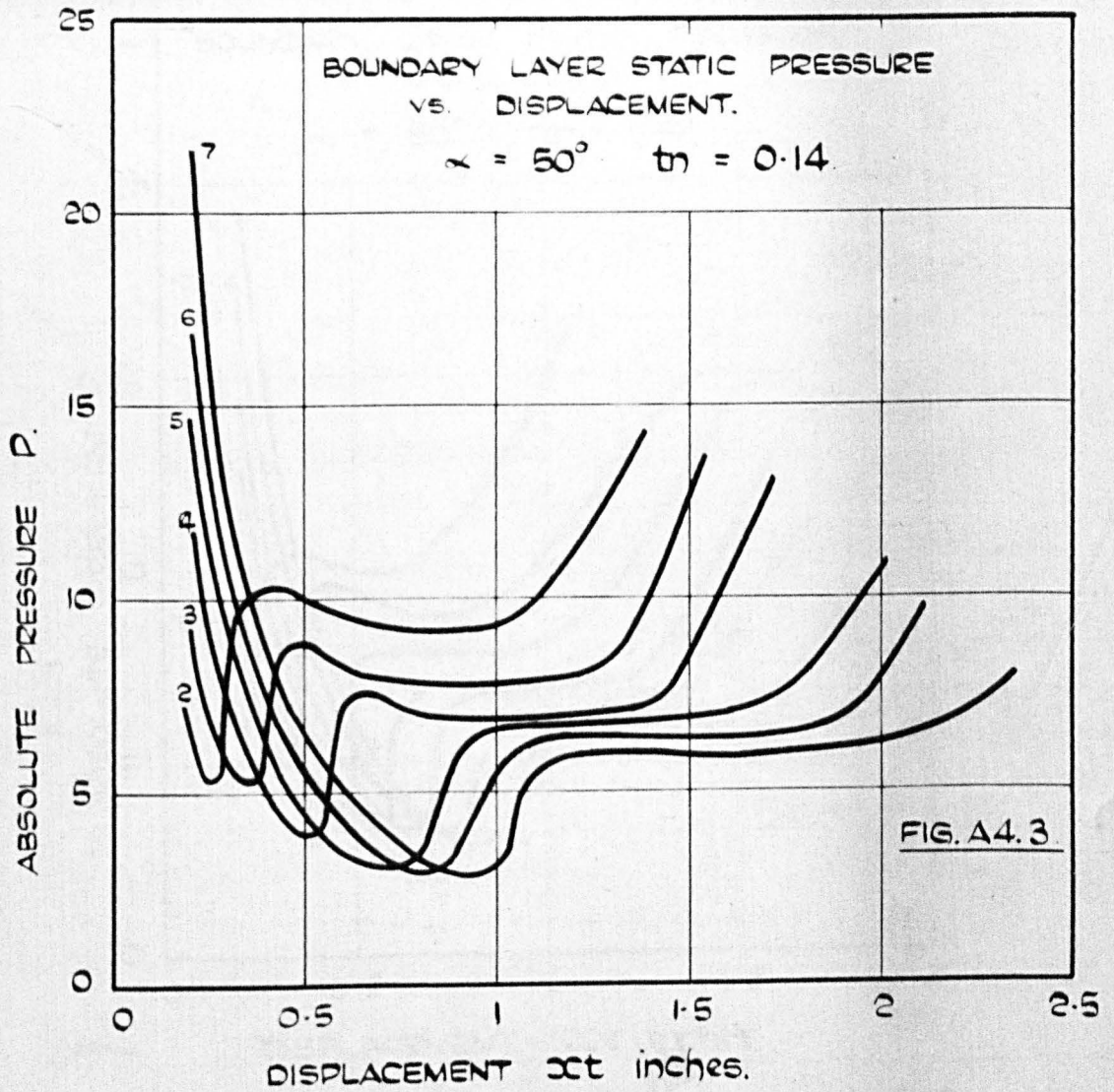
$\alpha$  = included wall angle

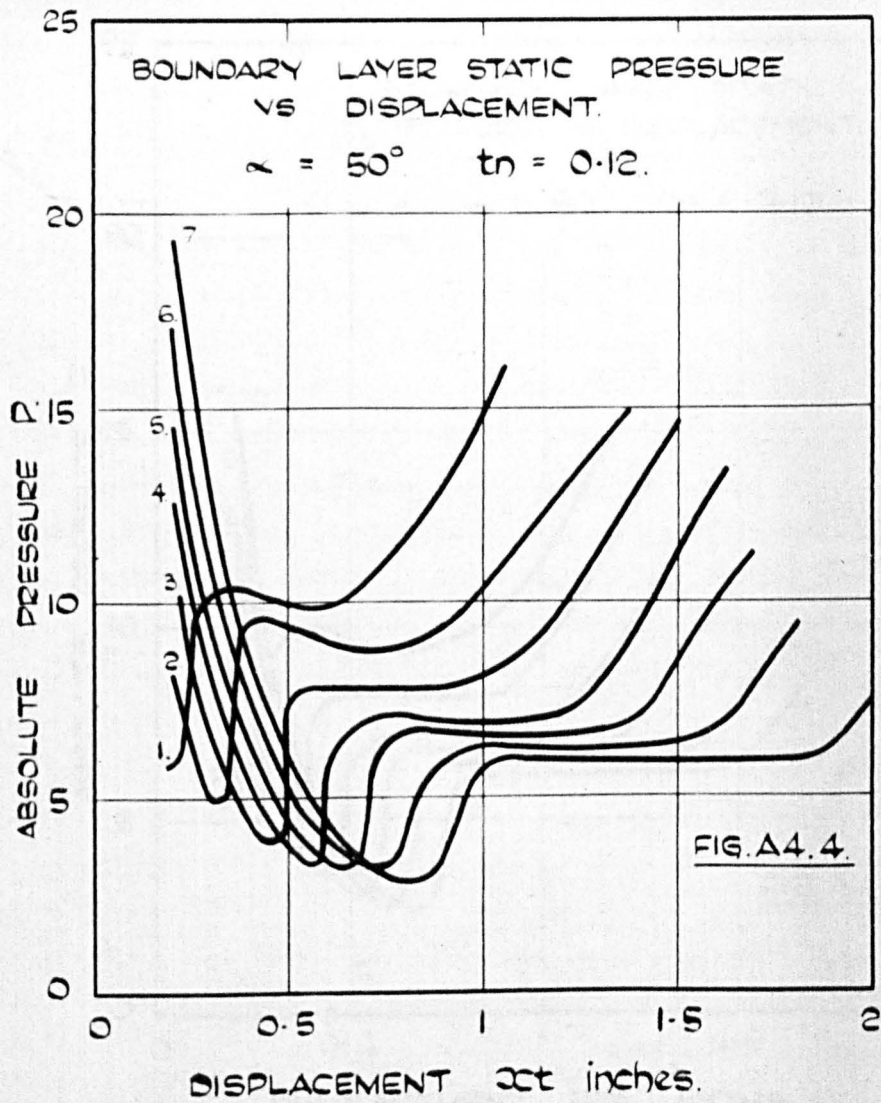
$t_n$  = measured throat width.

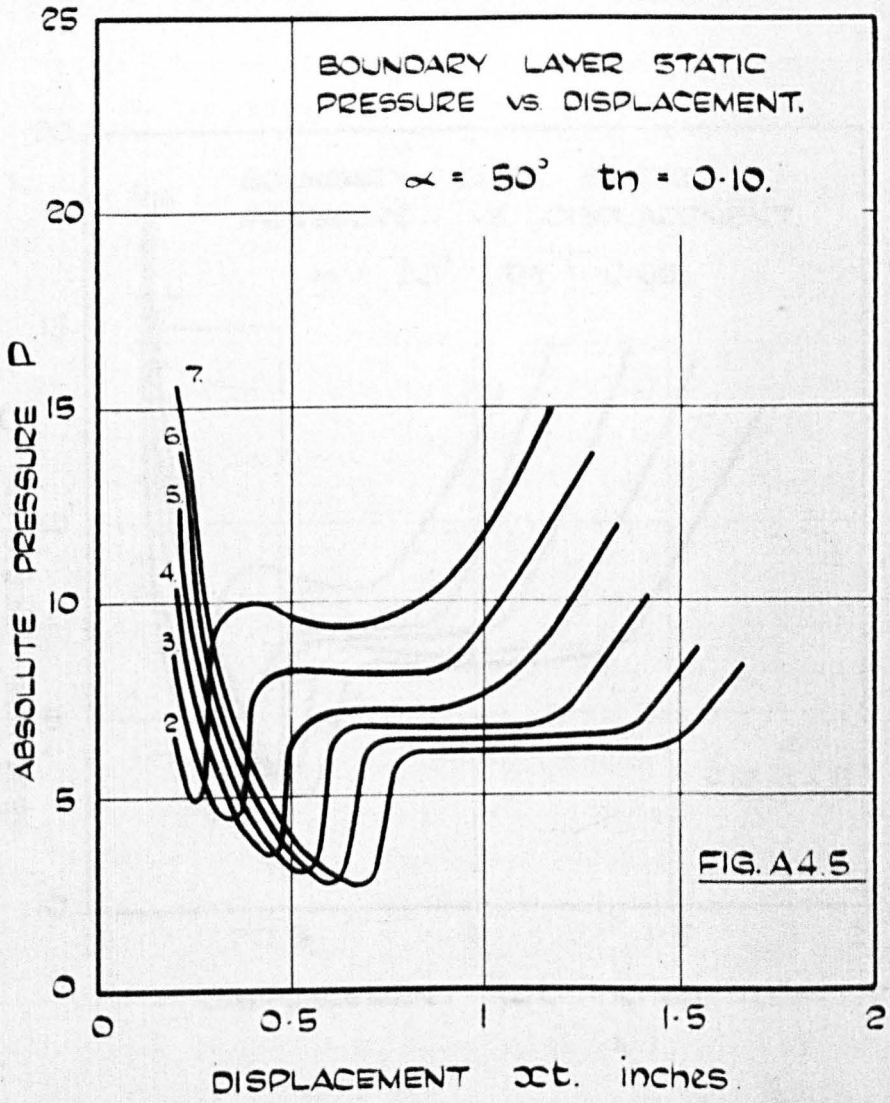
**PRESSURE CHARACTERISTICS SHOWING BOUNDARY  
LAYER SEPARATION FOLLOWED BY REATTACHMENT**

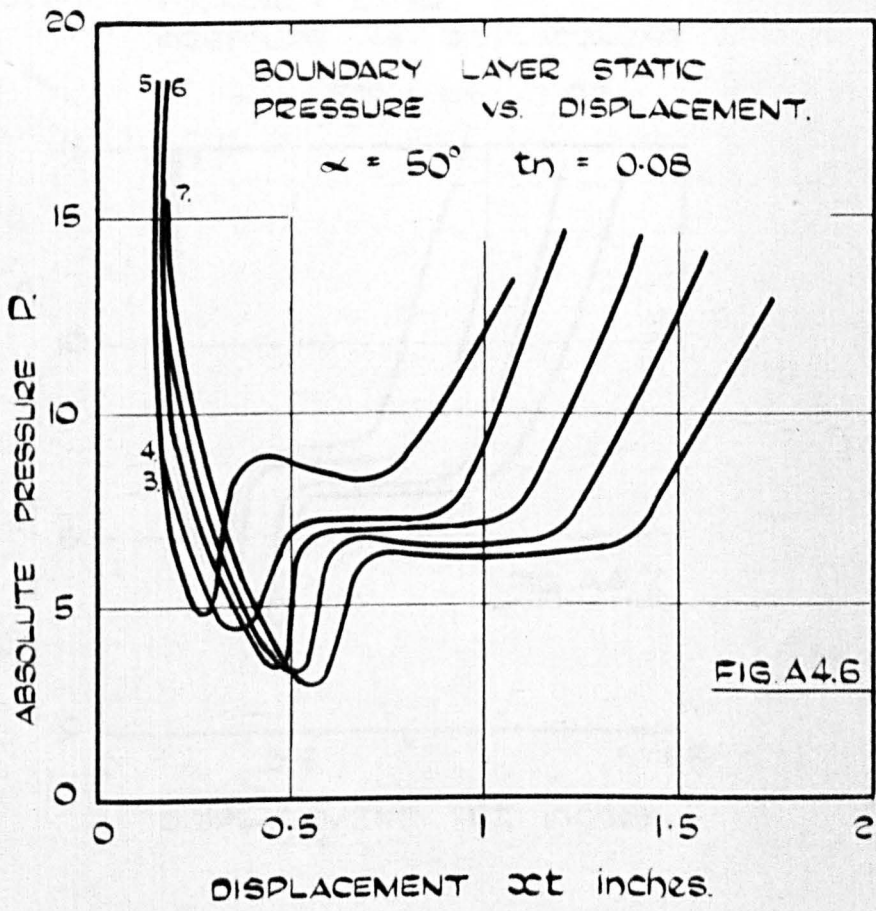








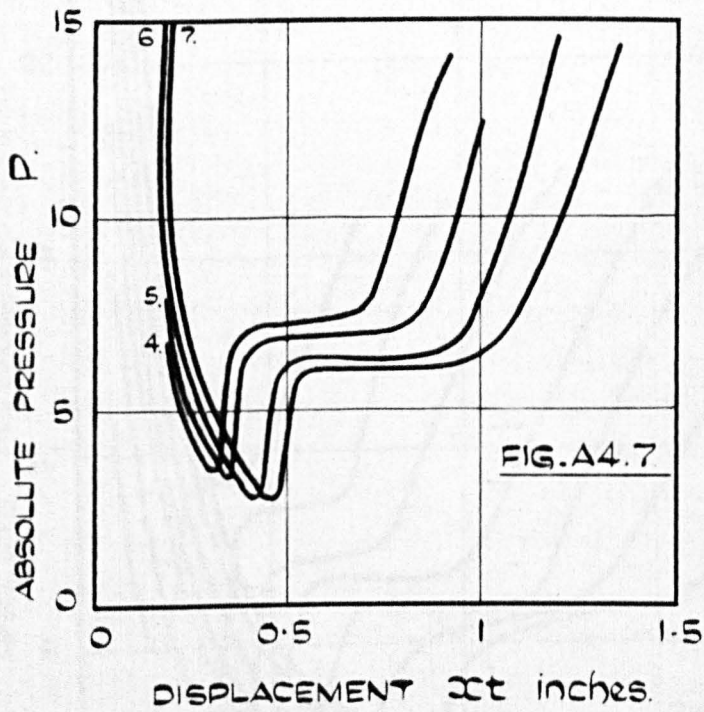


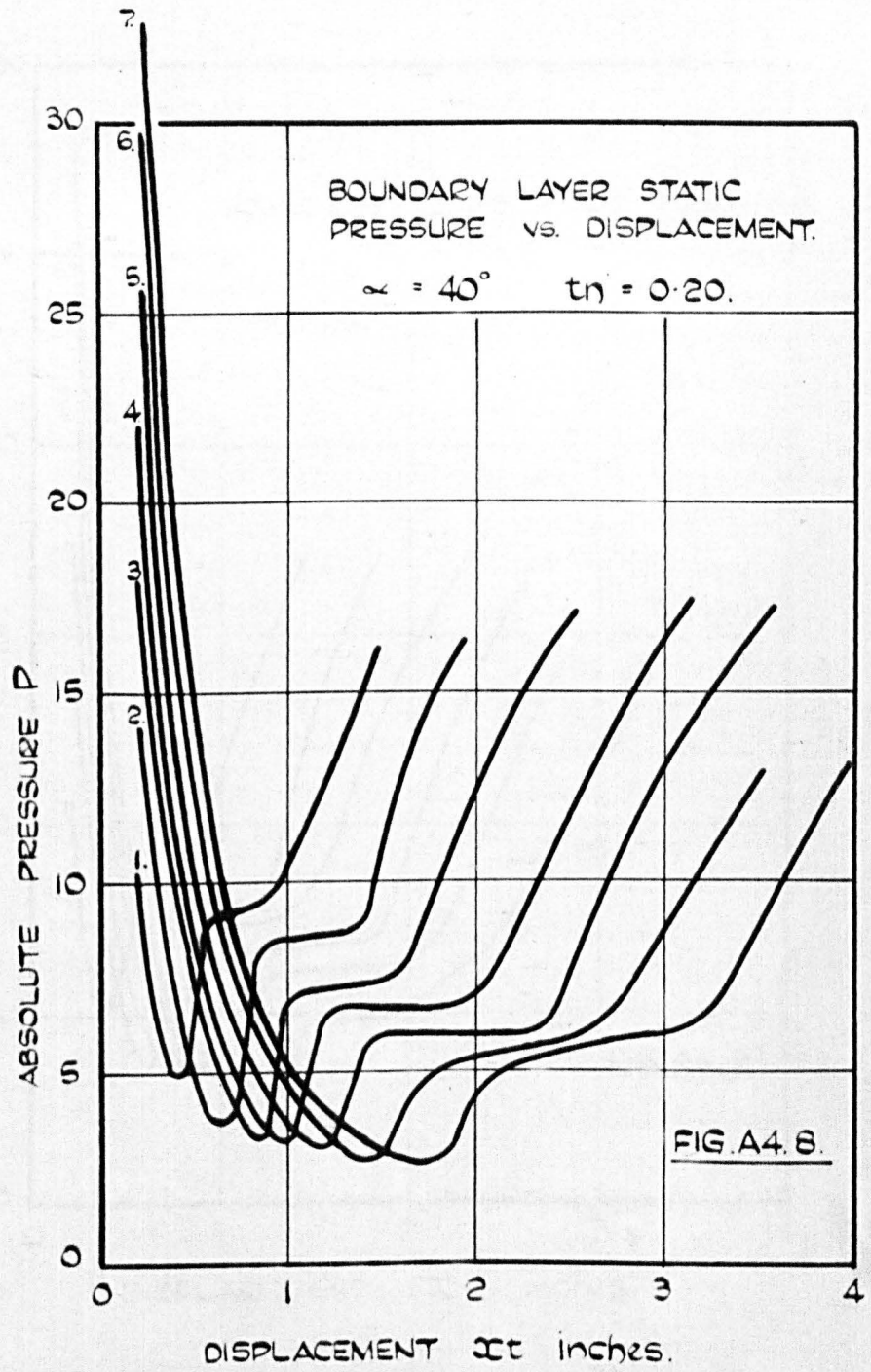


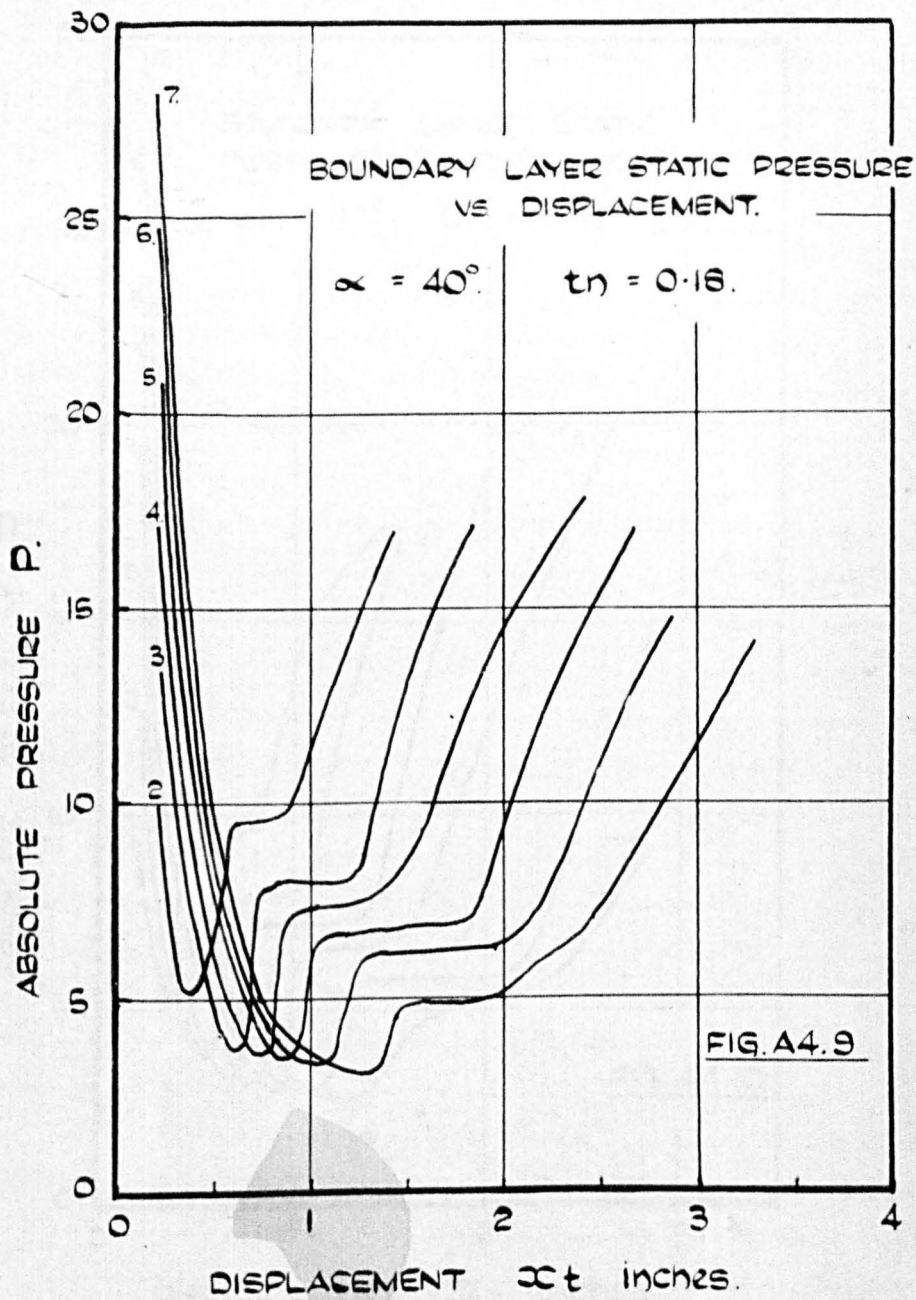


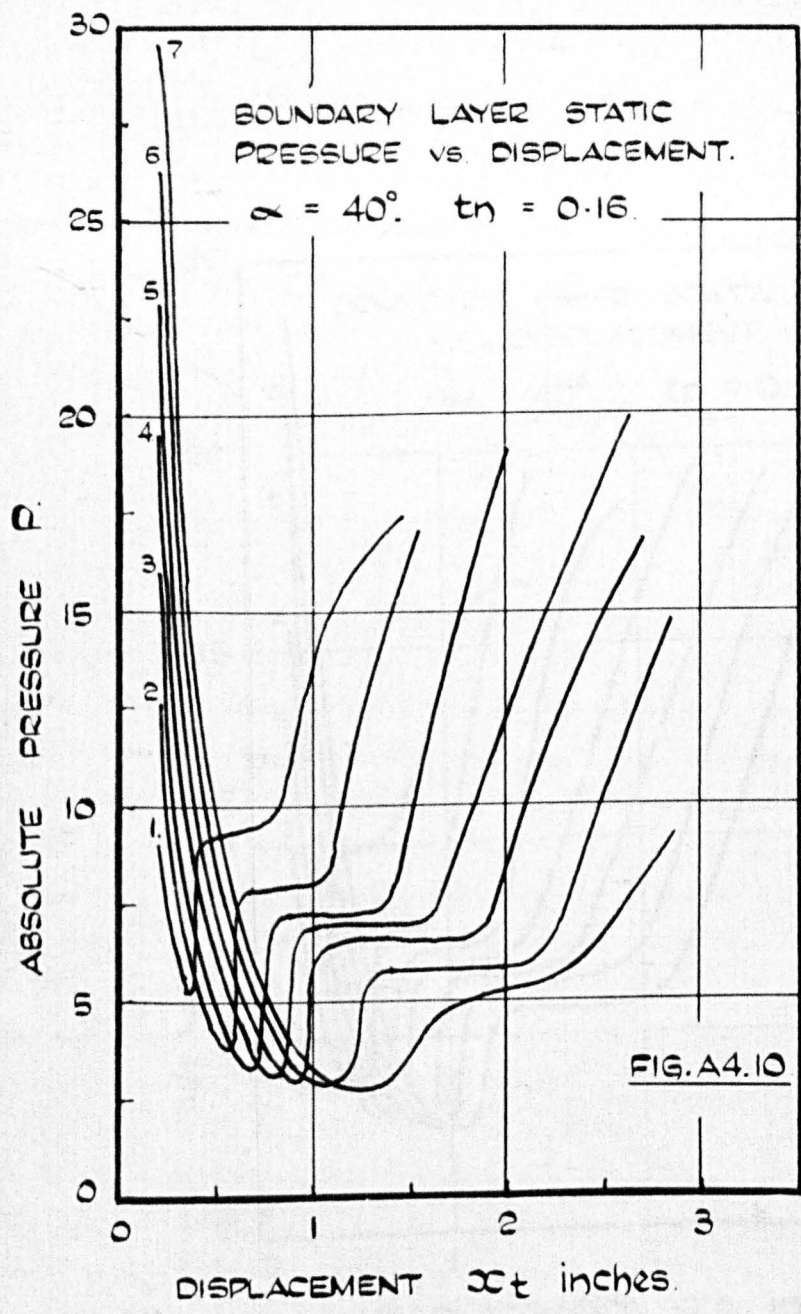
BOUNDARY LAYER STATIC  
PRESSURE VS. DISPLACEMENT.

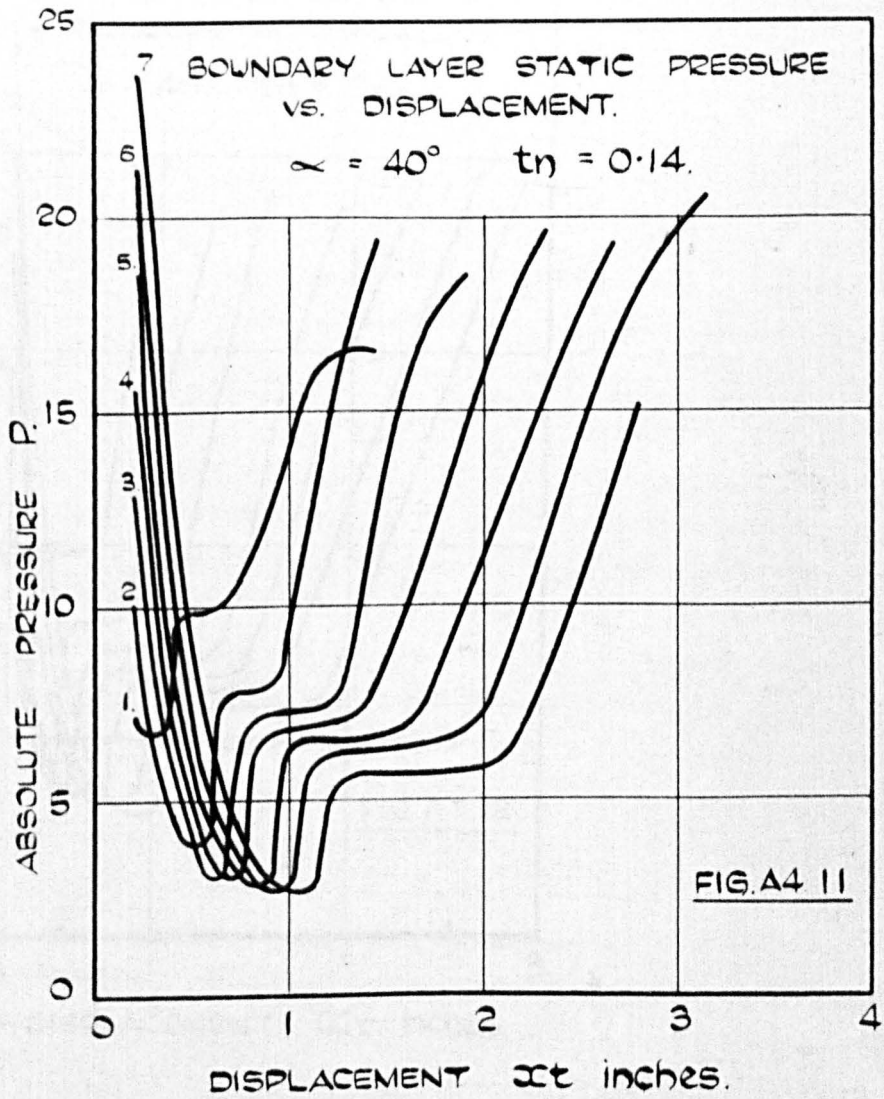
$$\alpha = 50^\circ \quad t_n = 0.06.$$

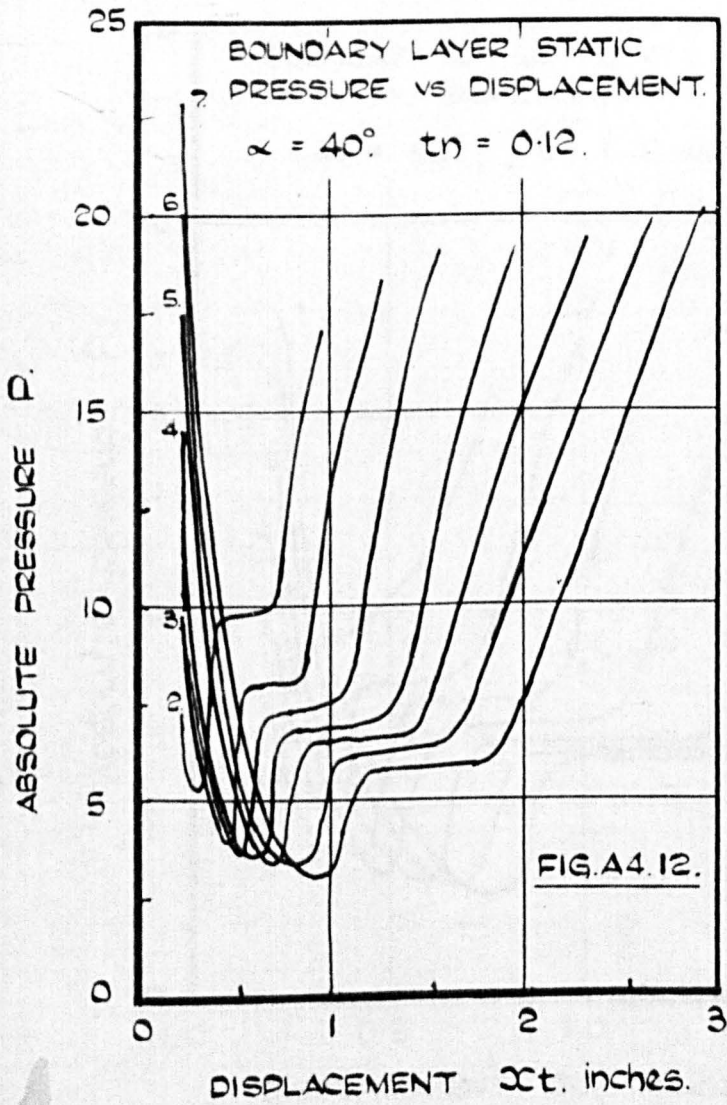


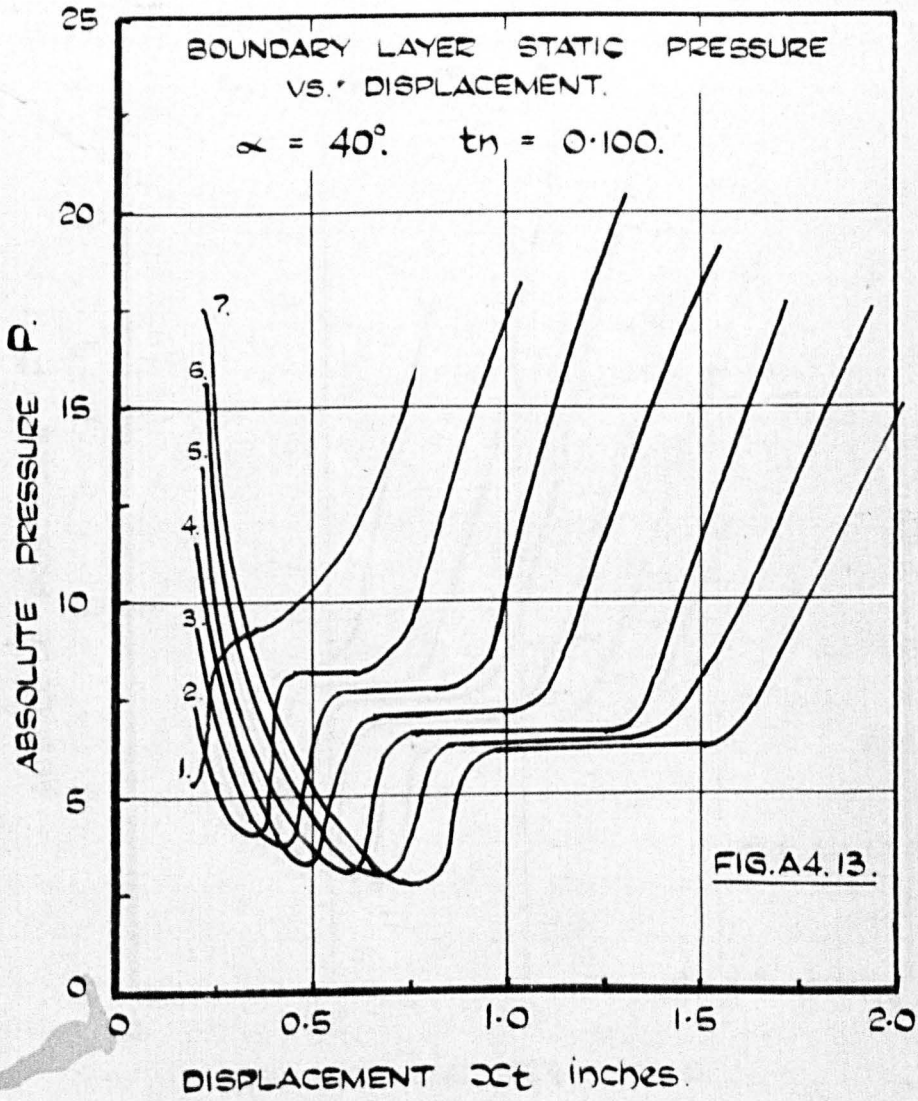




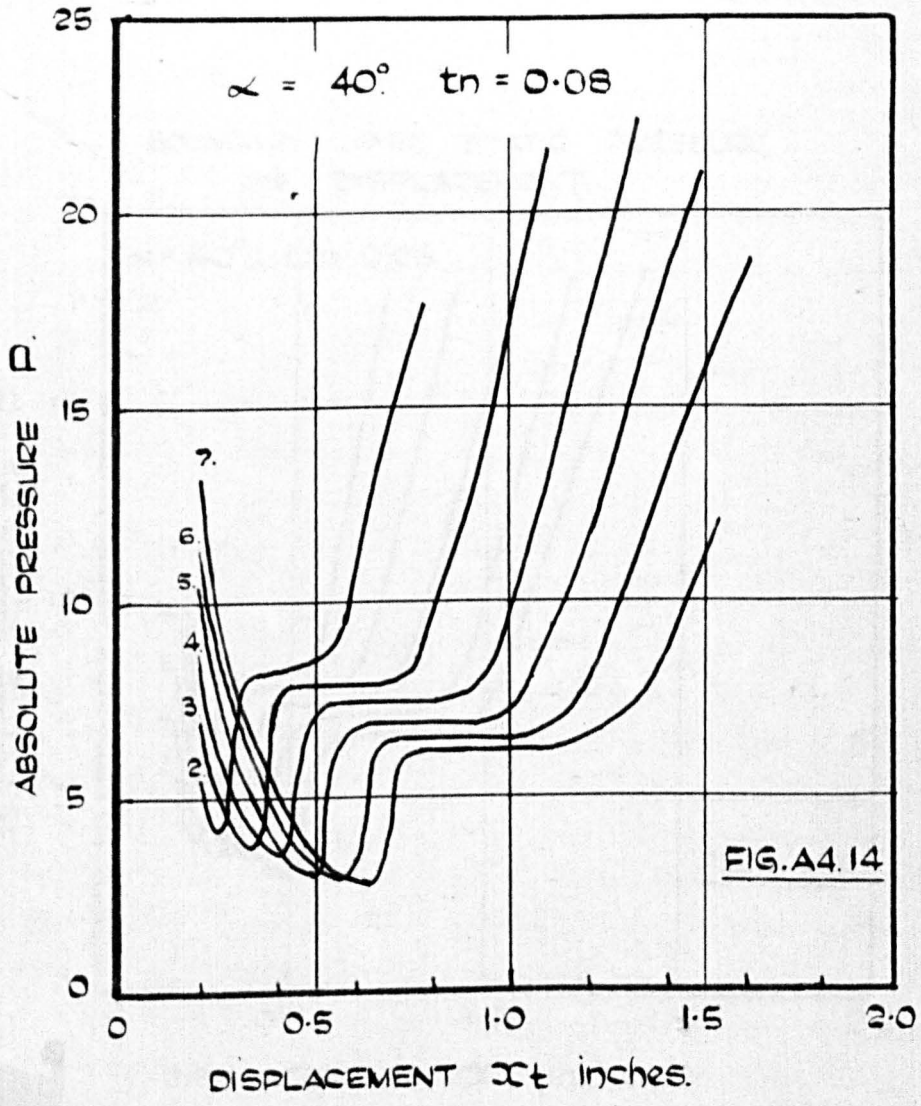






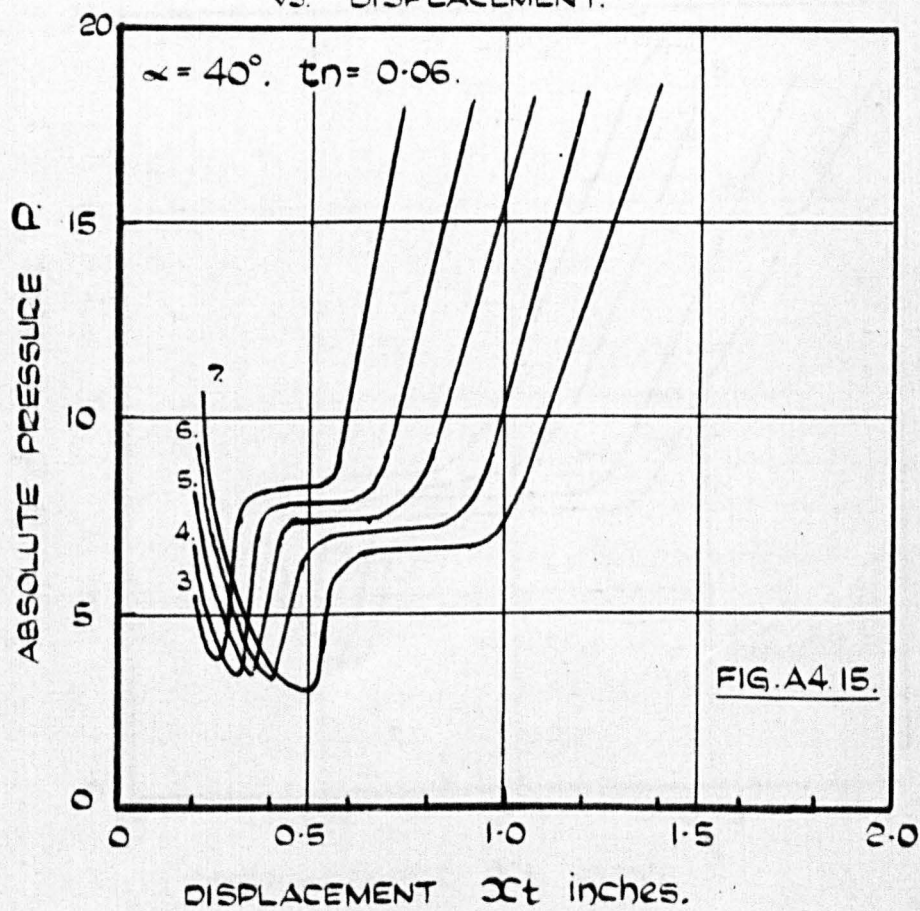


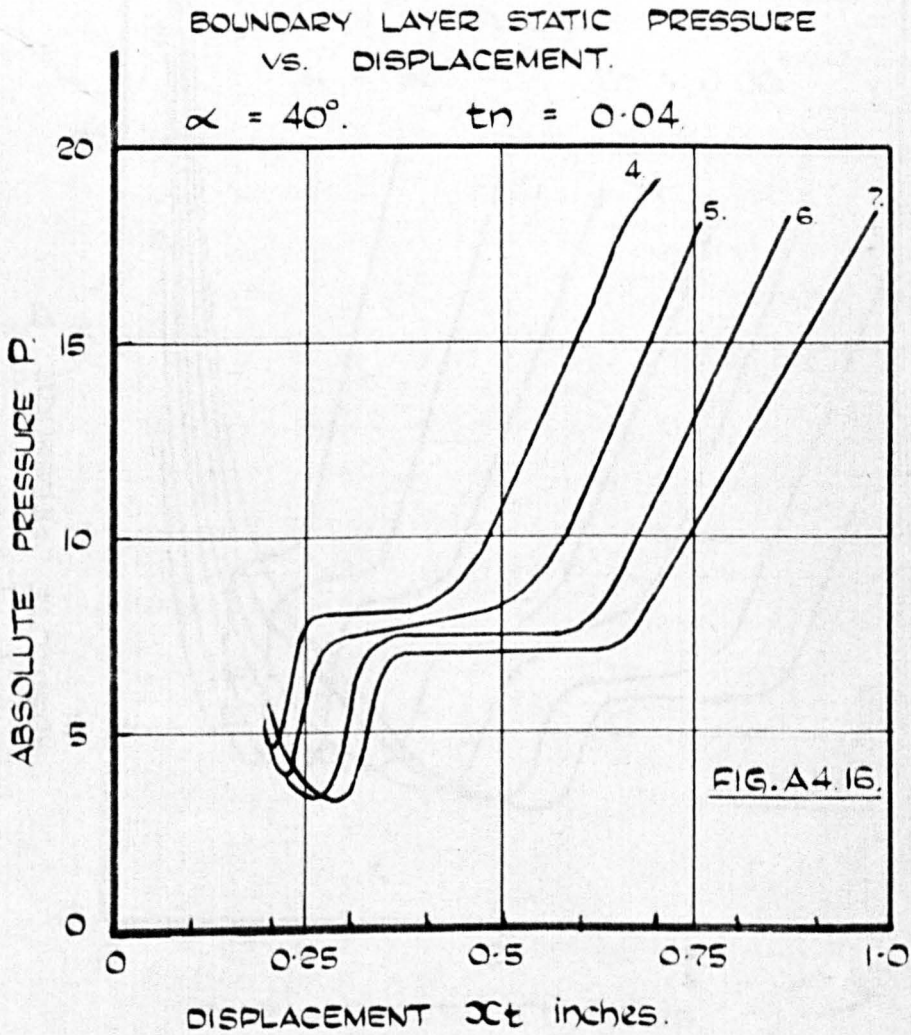
BOUNDARY LAYER STATIC PRESSURE  
VS. DISPLACEMENT.

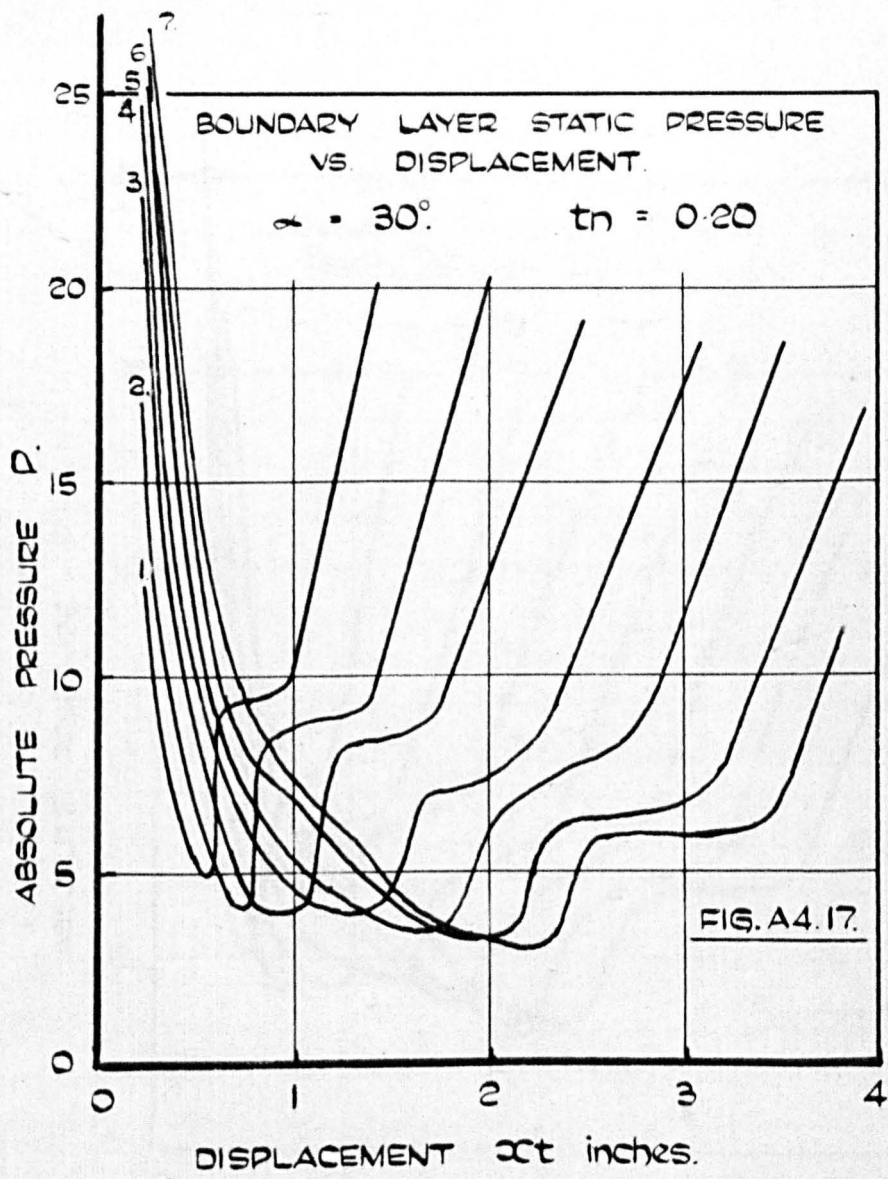


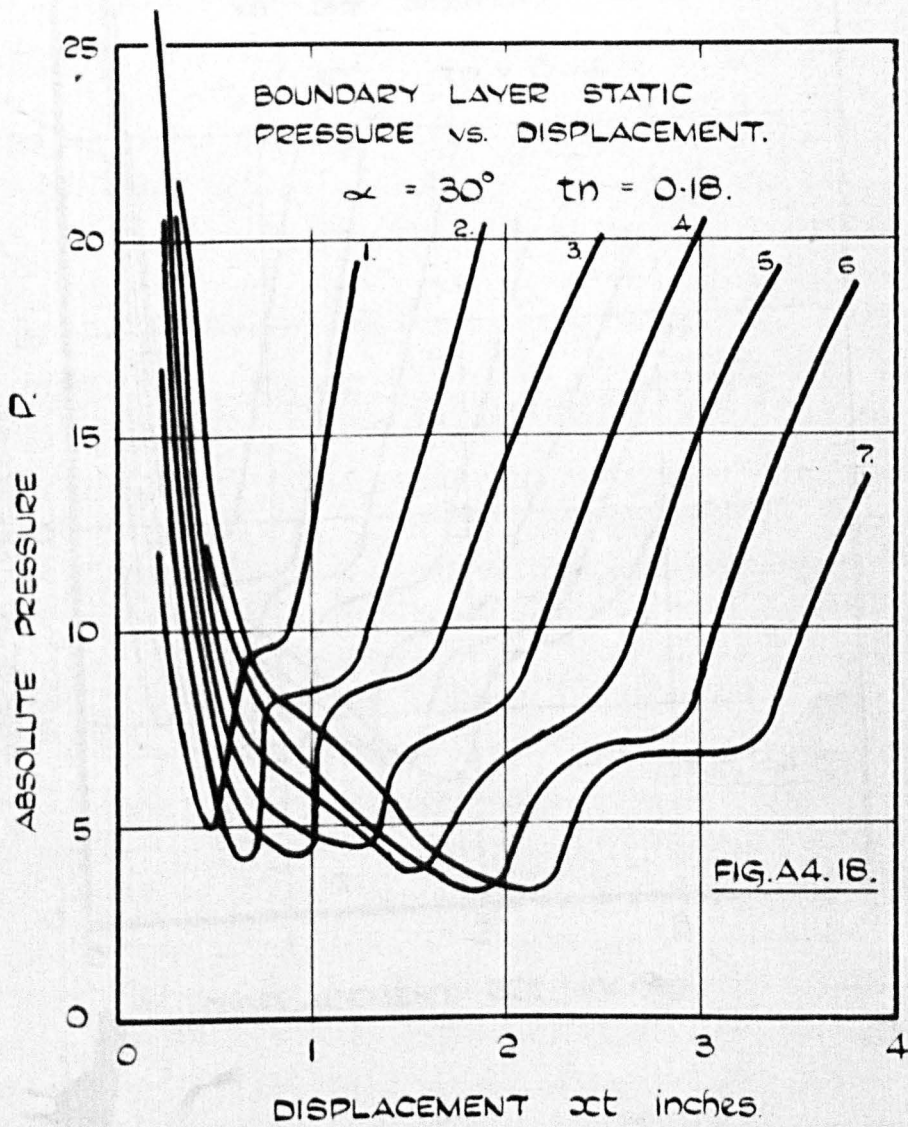


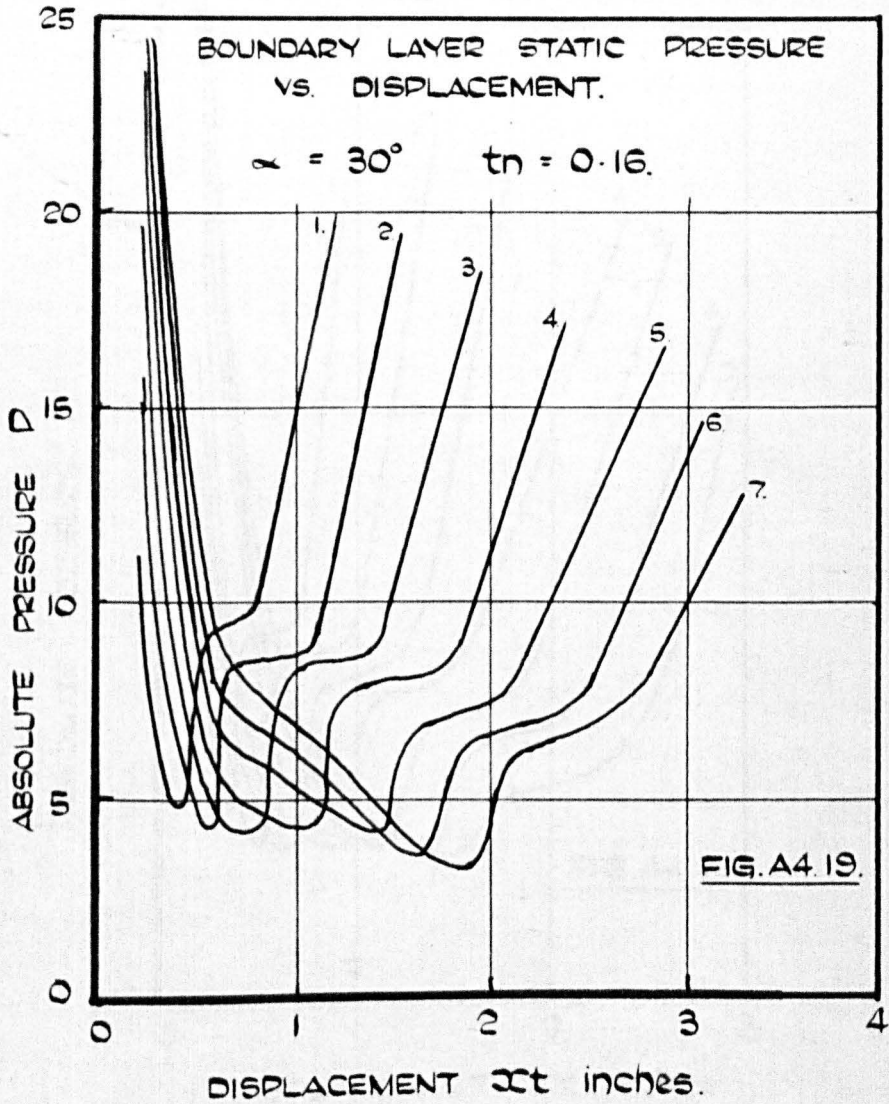
BOUNDARY LAYER STATIC PRESSURE  
VS. DISPLACEMENT.





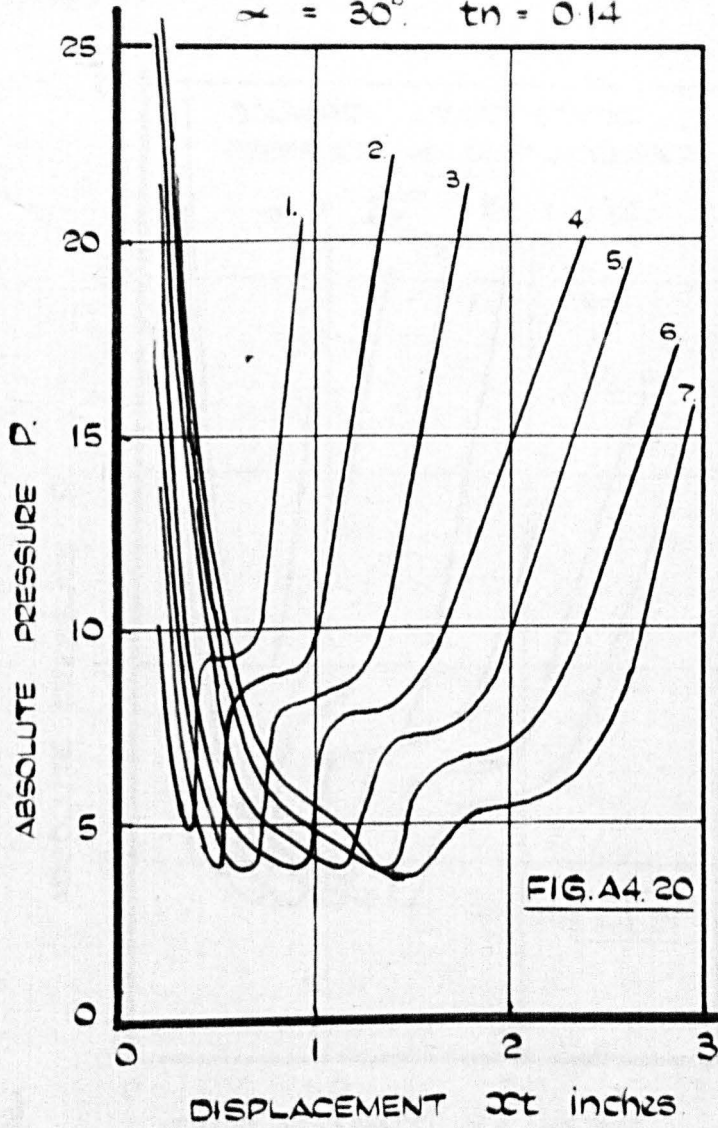


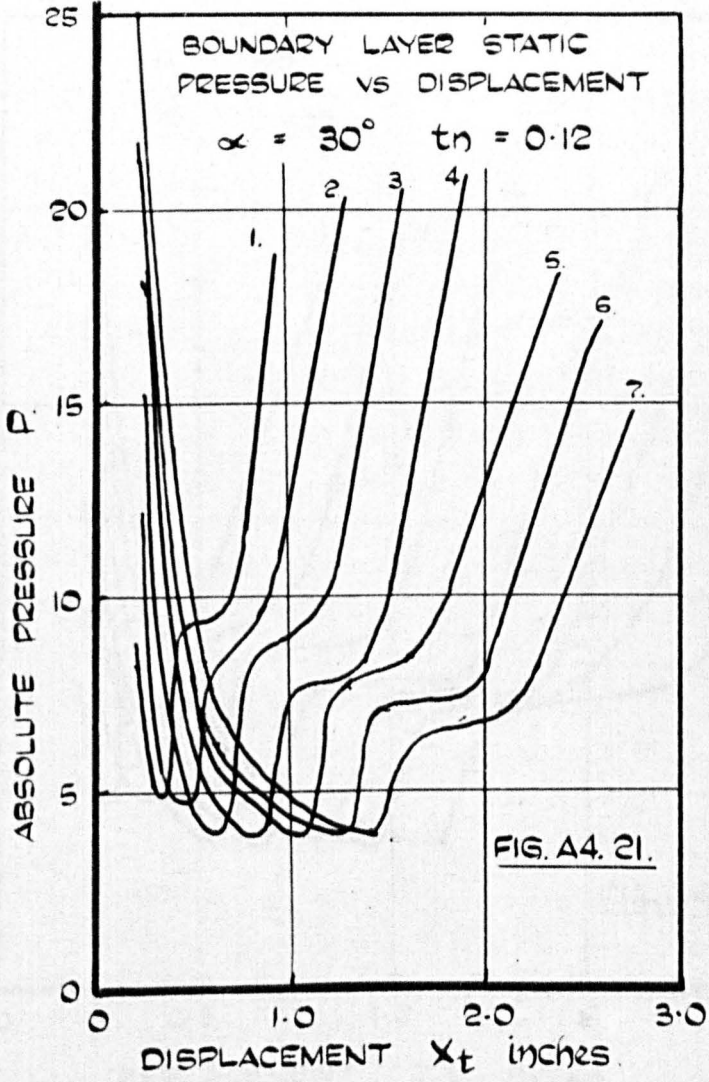




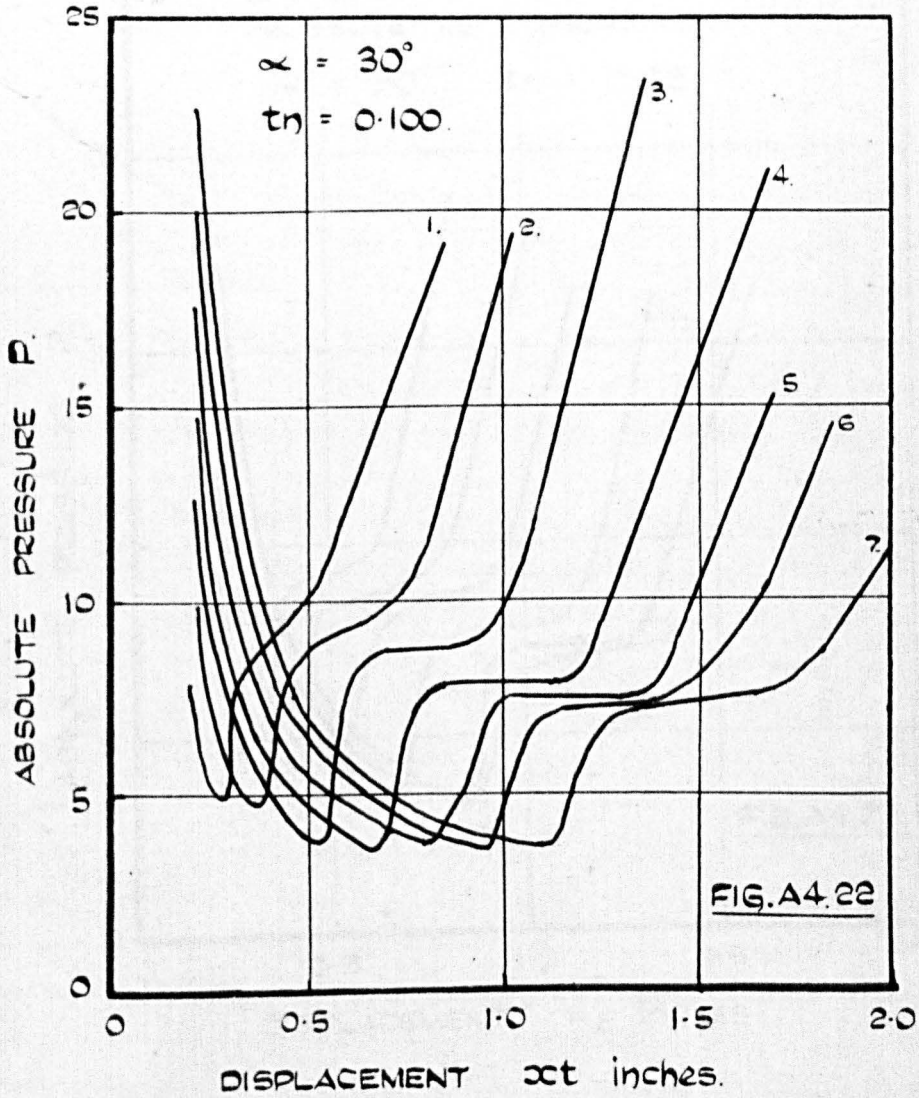
BOUNDARY LAYER STATIC  
PRESSURE VS. DISPLACEMENT.

$$\alpha = 30^\circ \quad t_n = 0.14$$

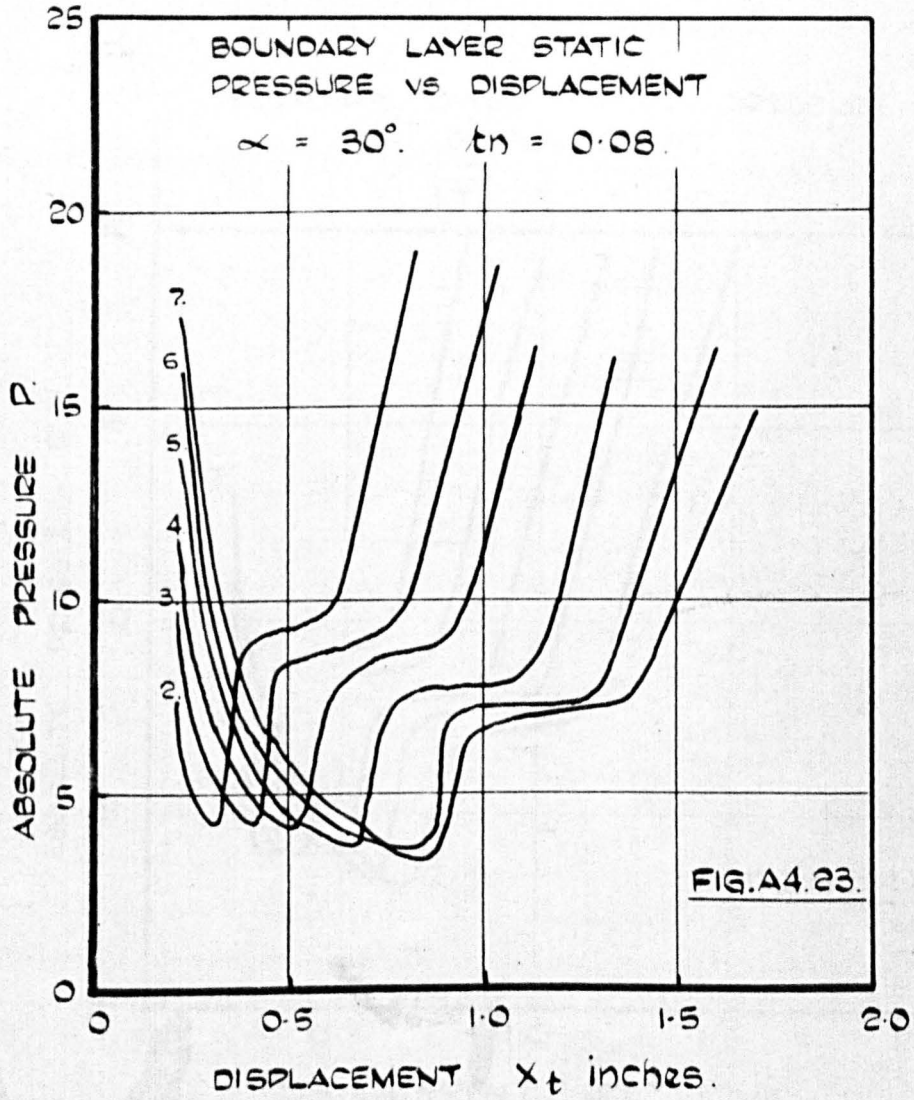


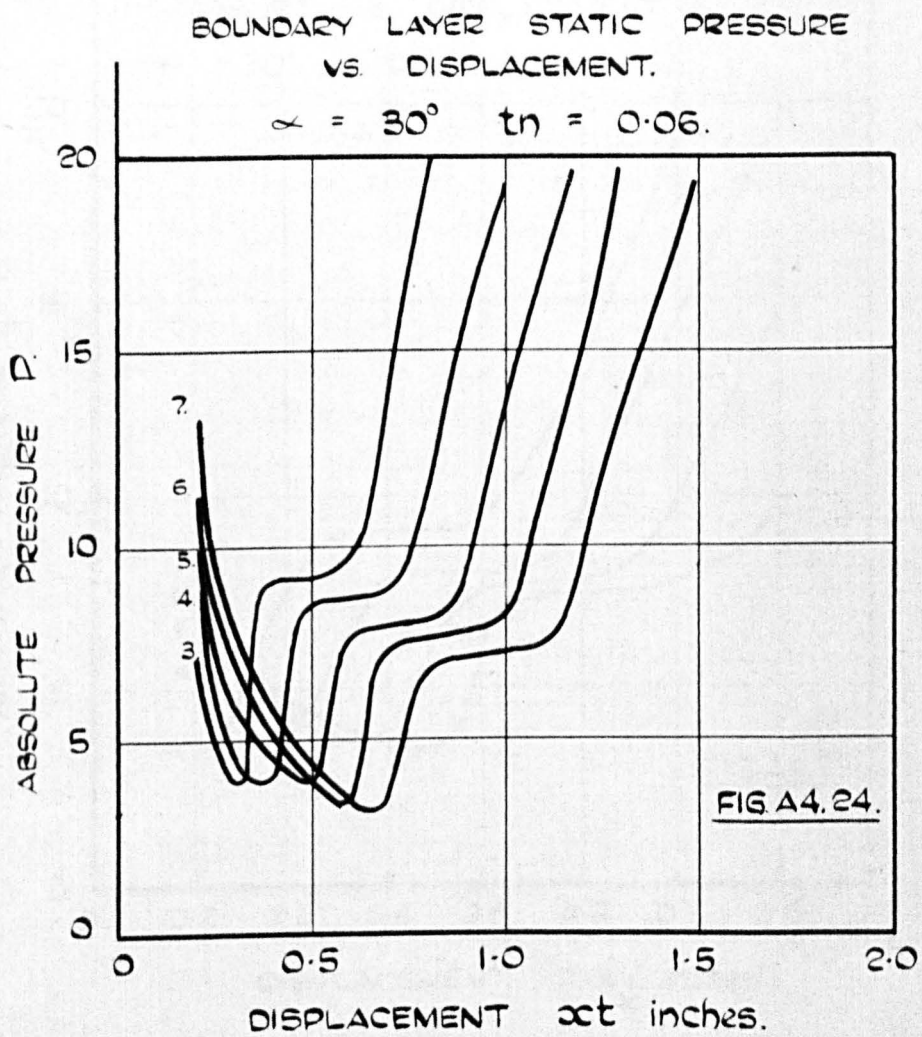


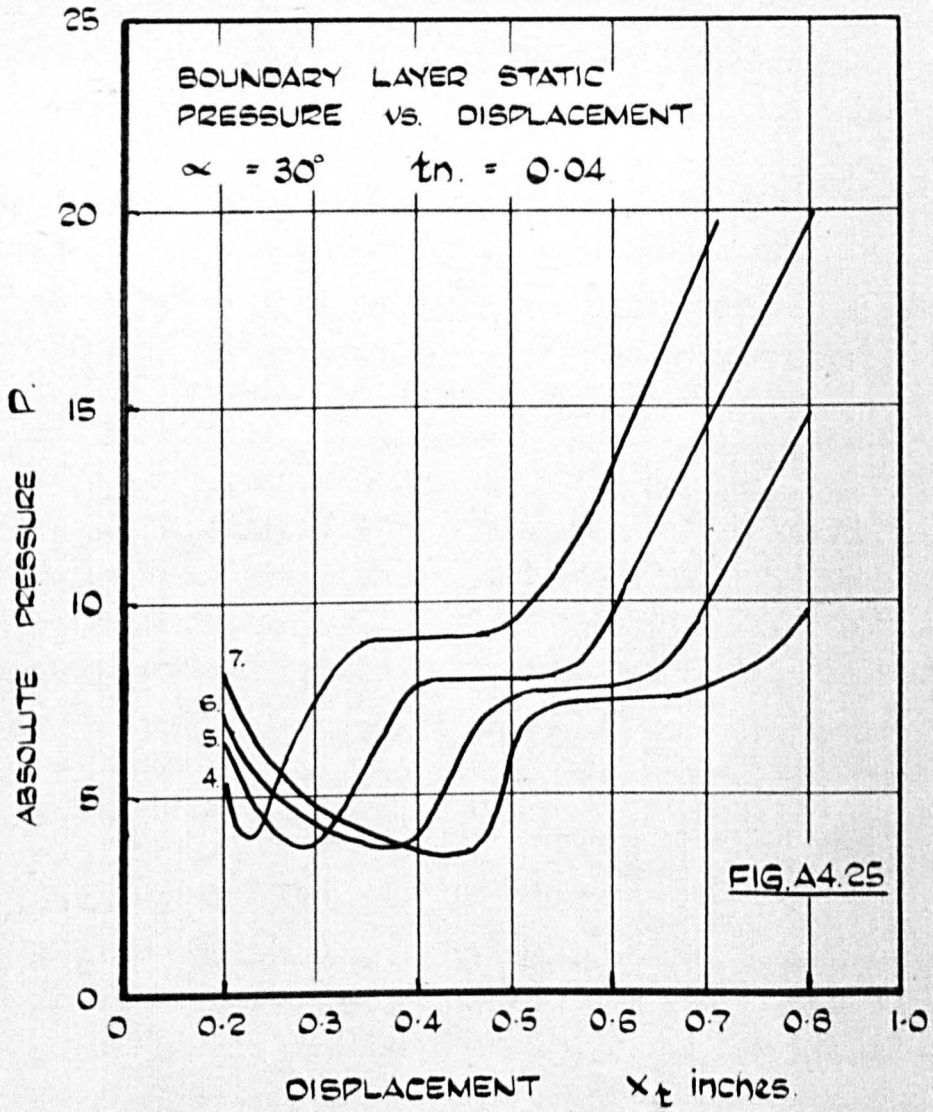
BOUNDARY LAYER STATIC PRESSURE  
VS DISPLACEMENT.



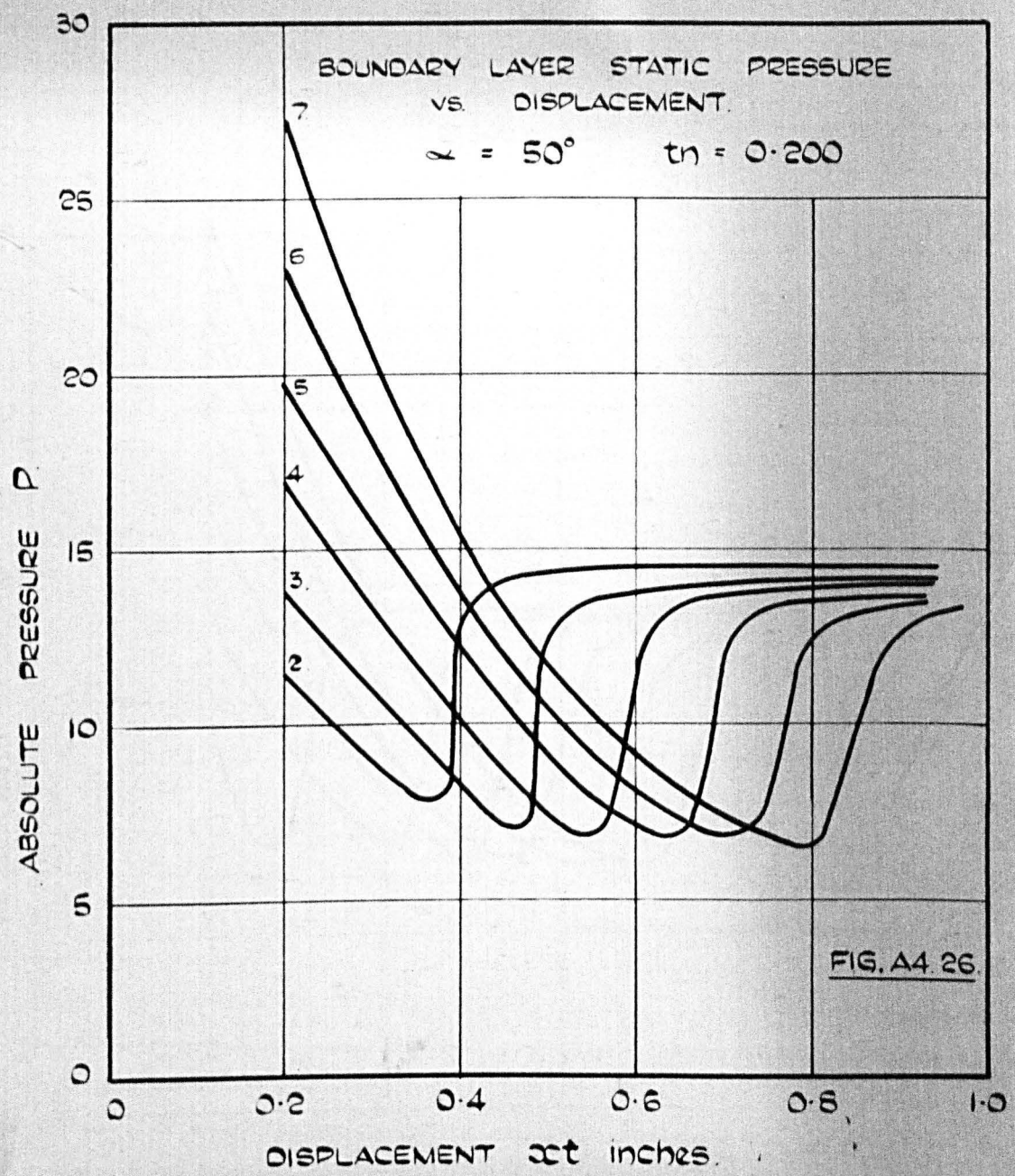


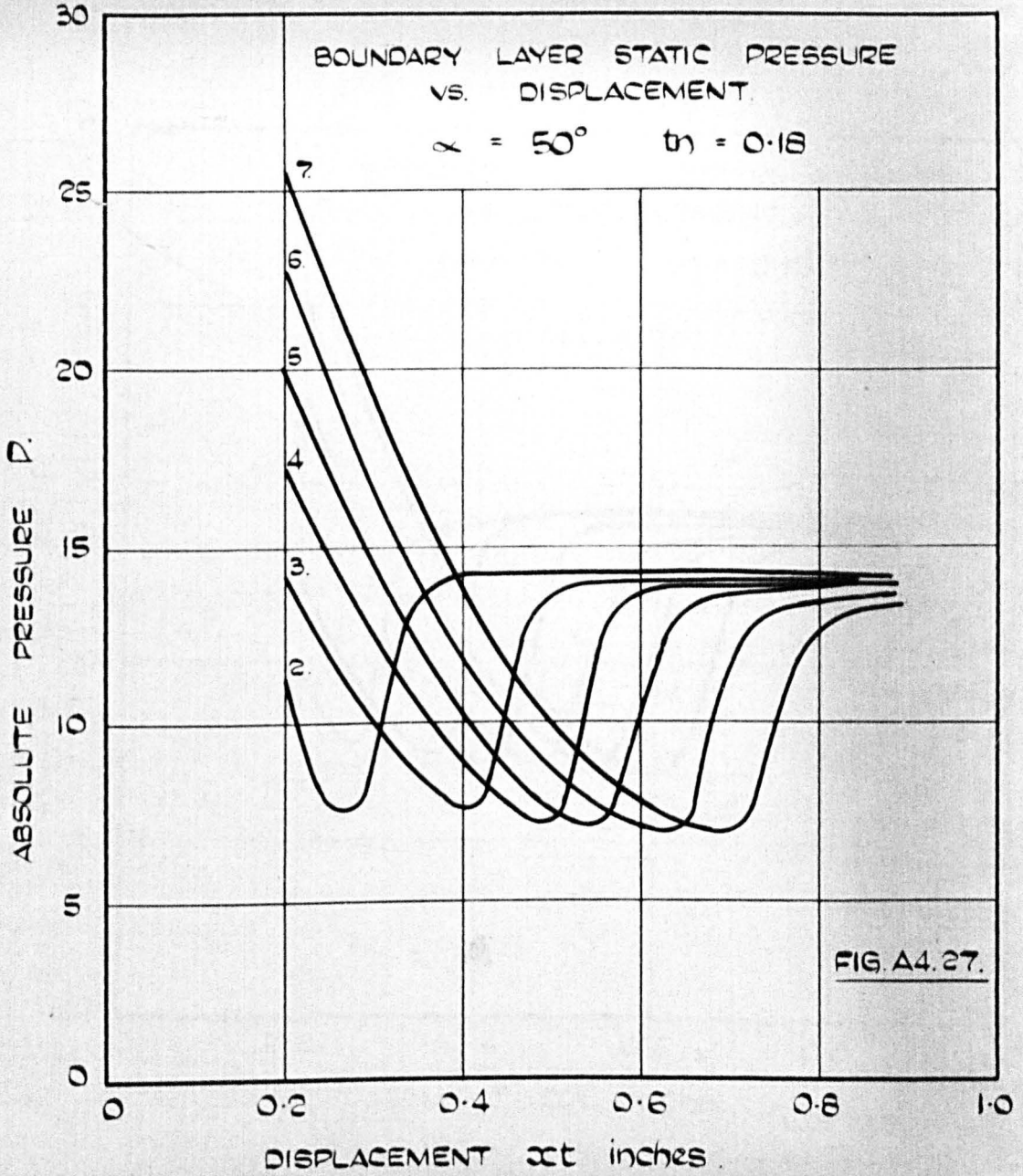


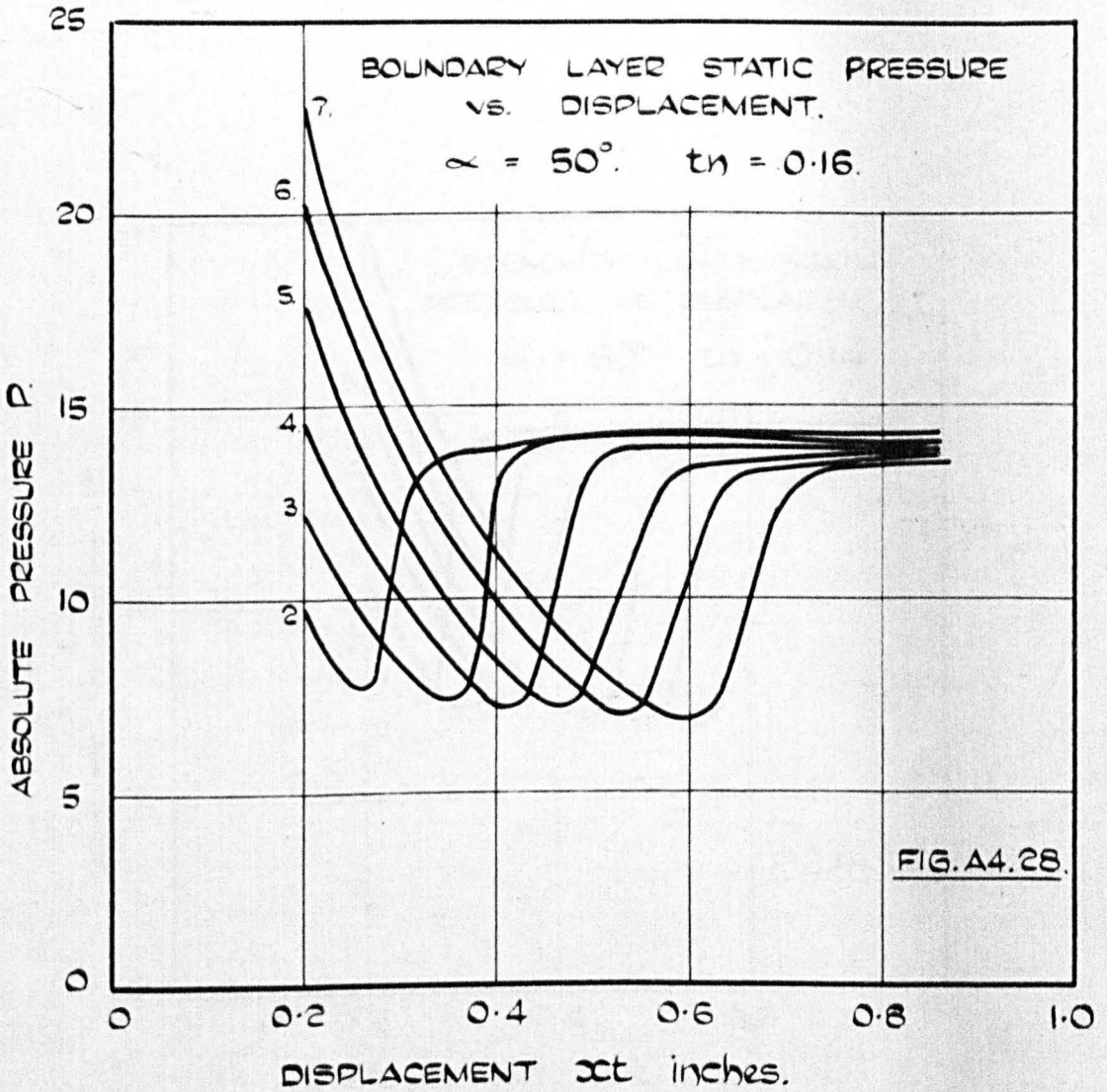


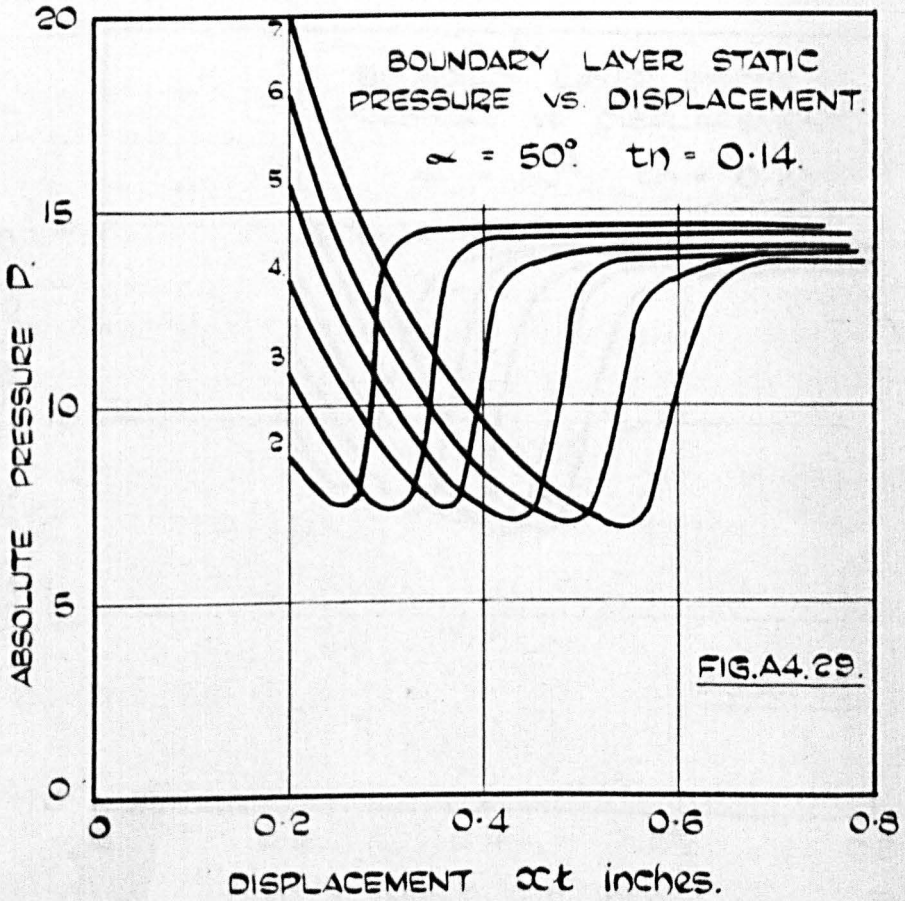


PRESSURE CHARACTERISTICS SHOWING BOUNDARY  
LAYER SEPARATION WITHOUT SUBSEQUENT  
REATTACHMENT



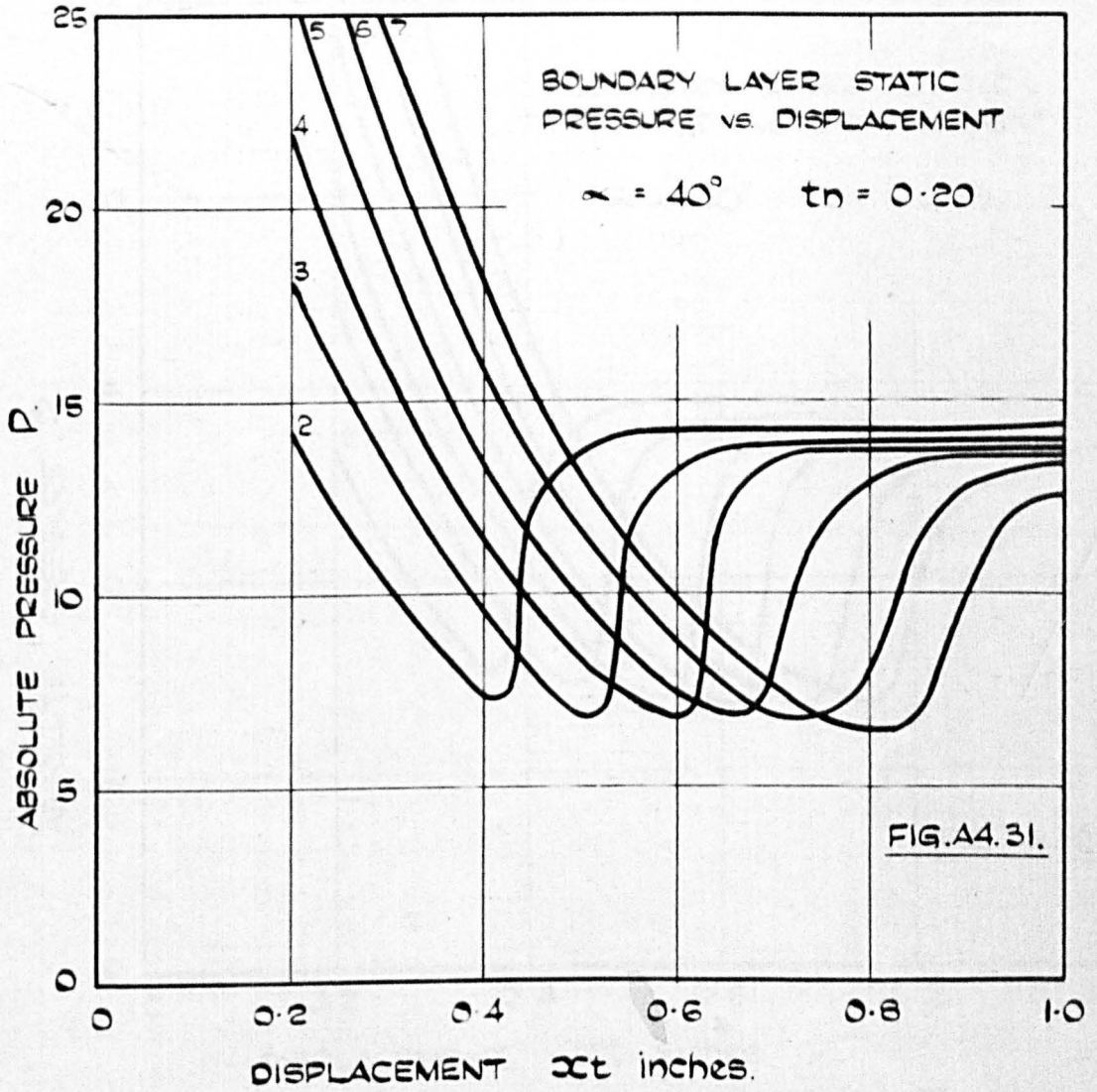




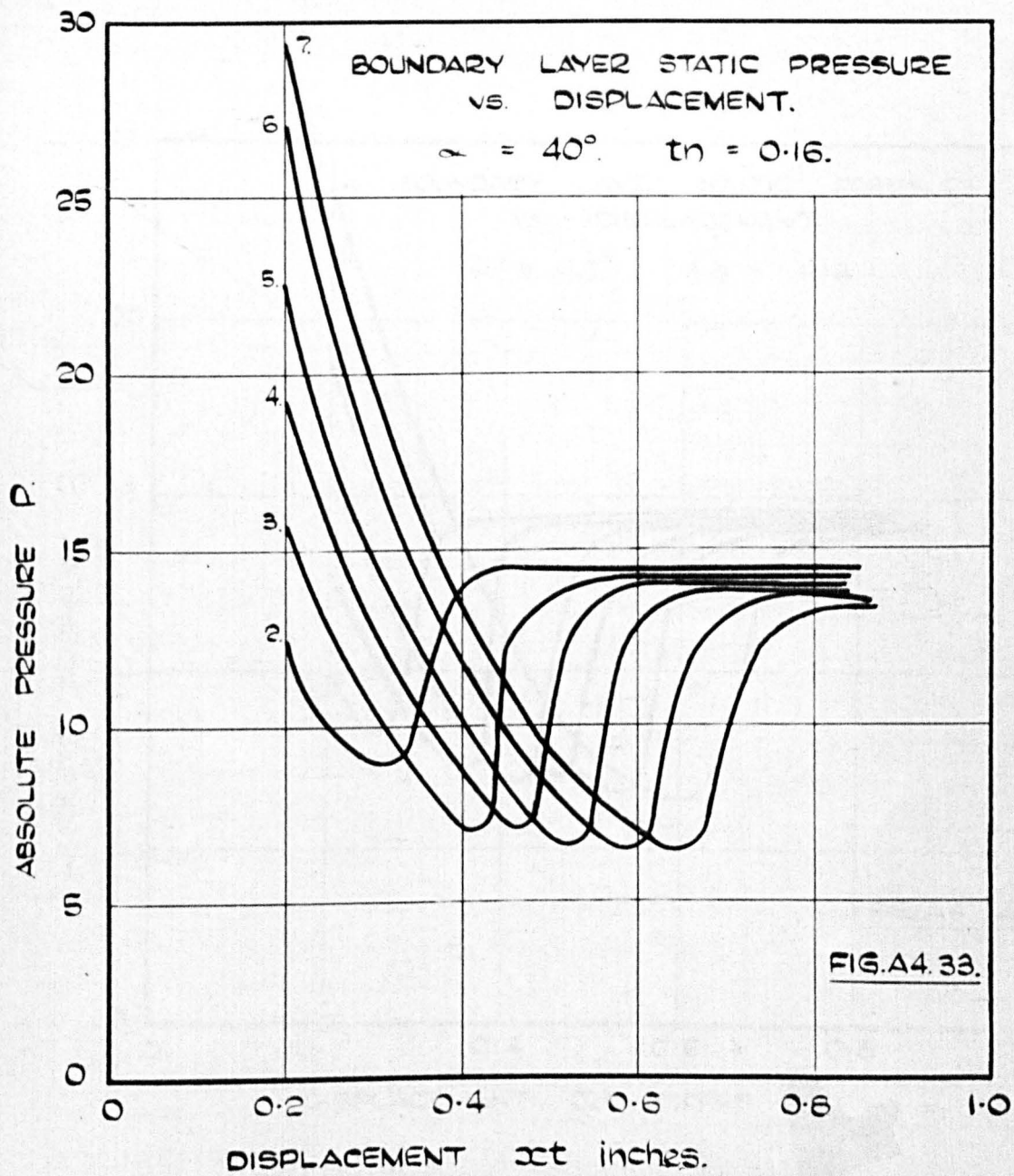


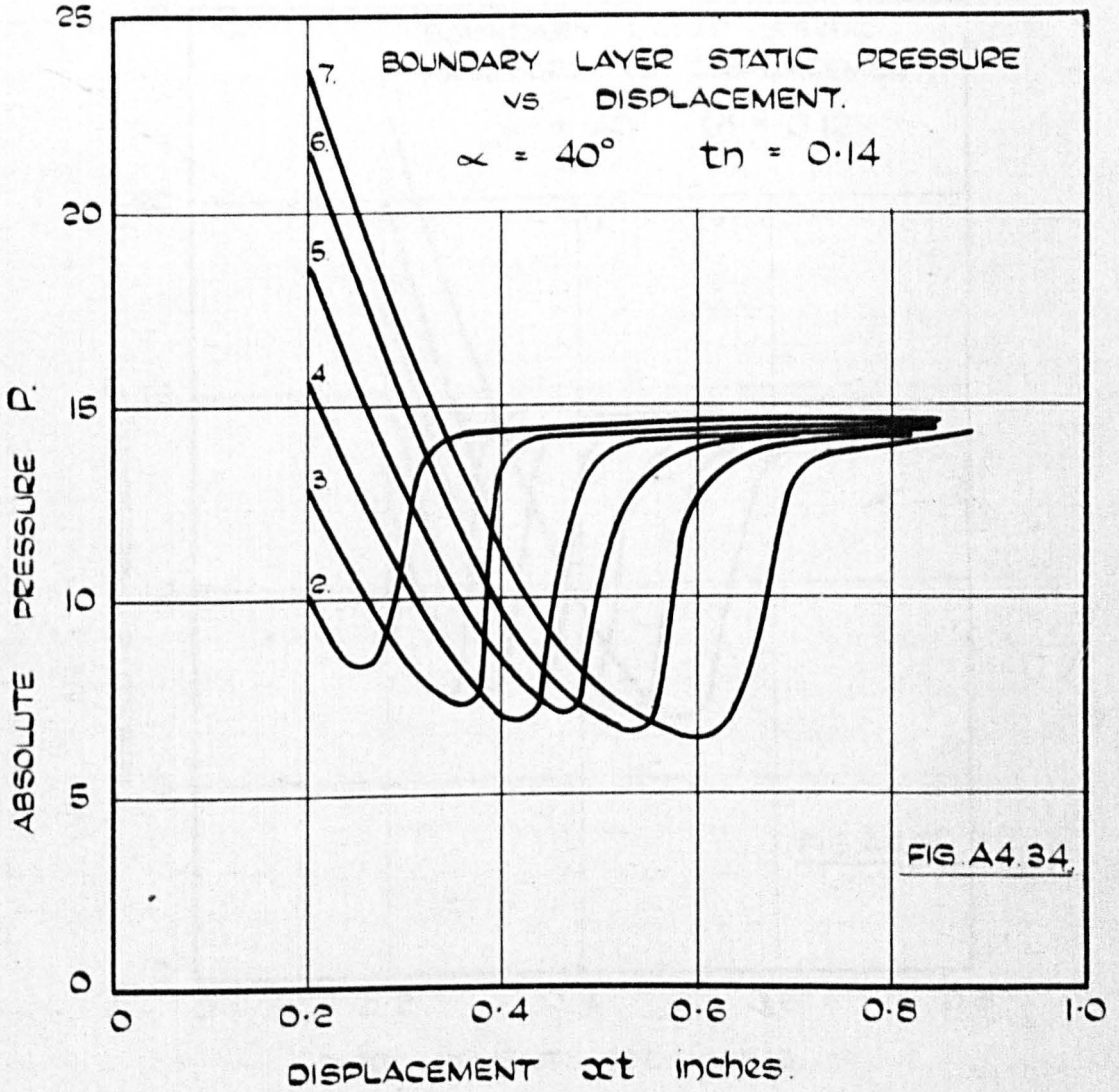


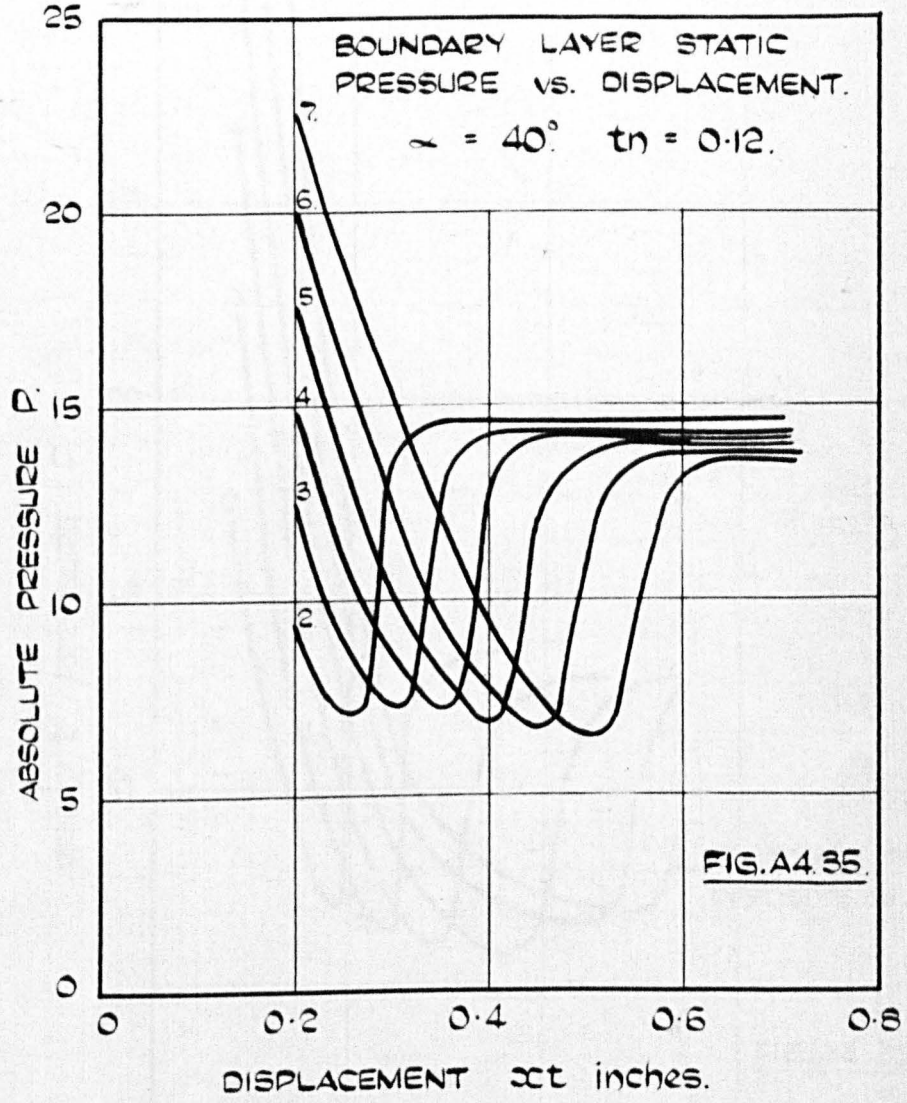


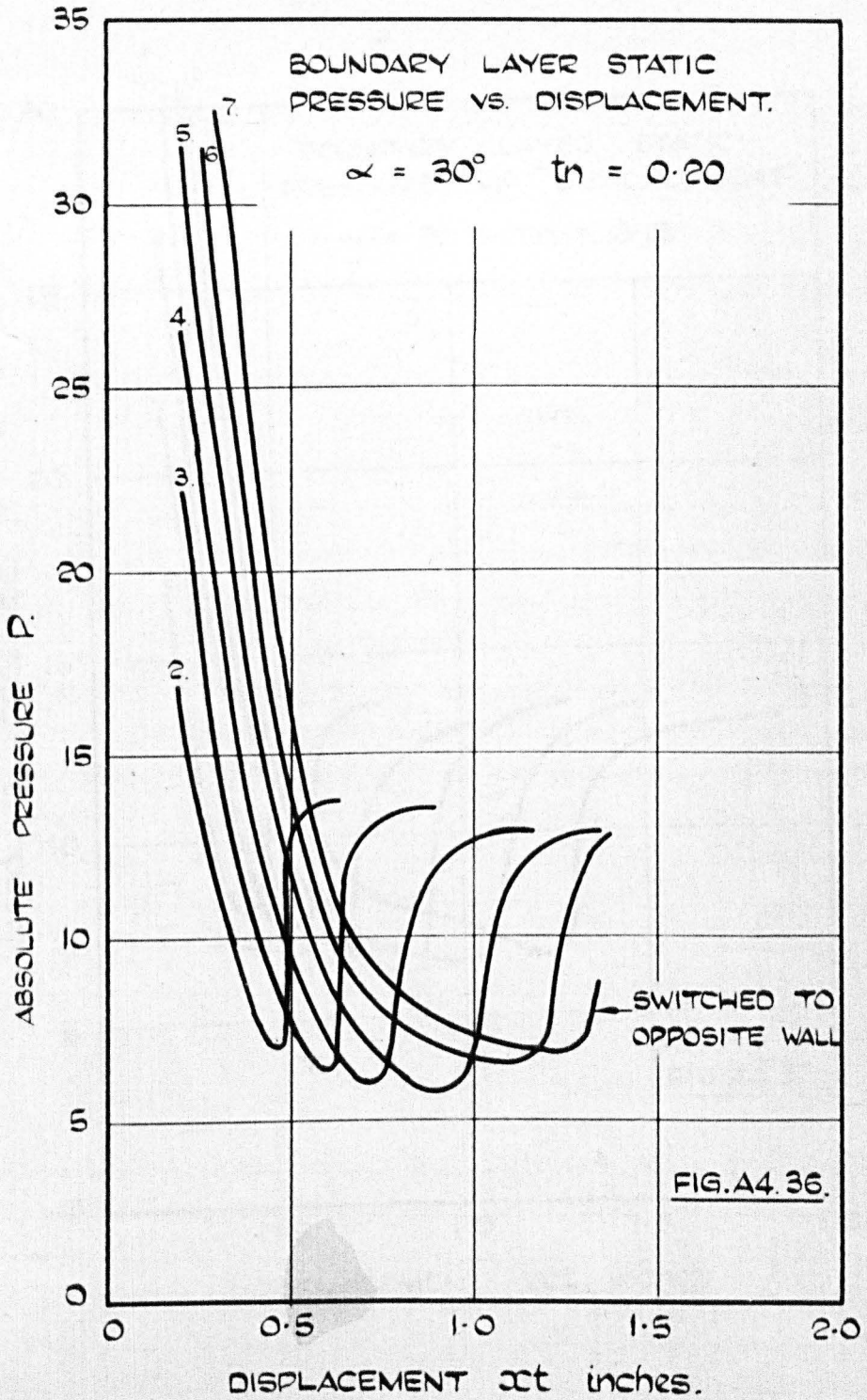


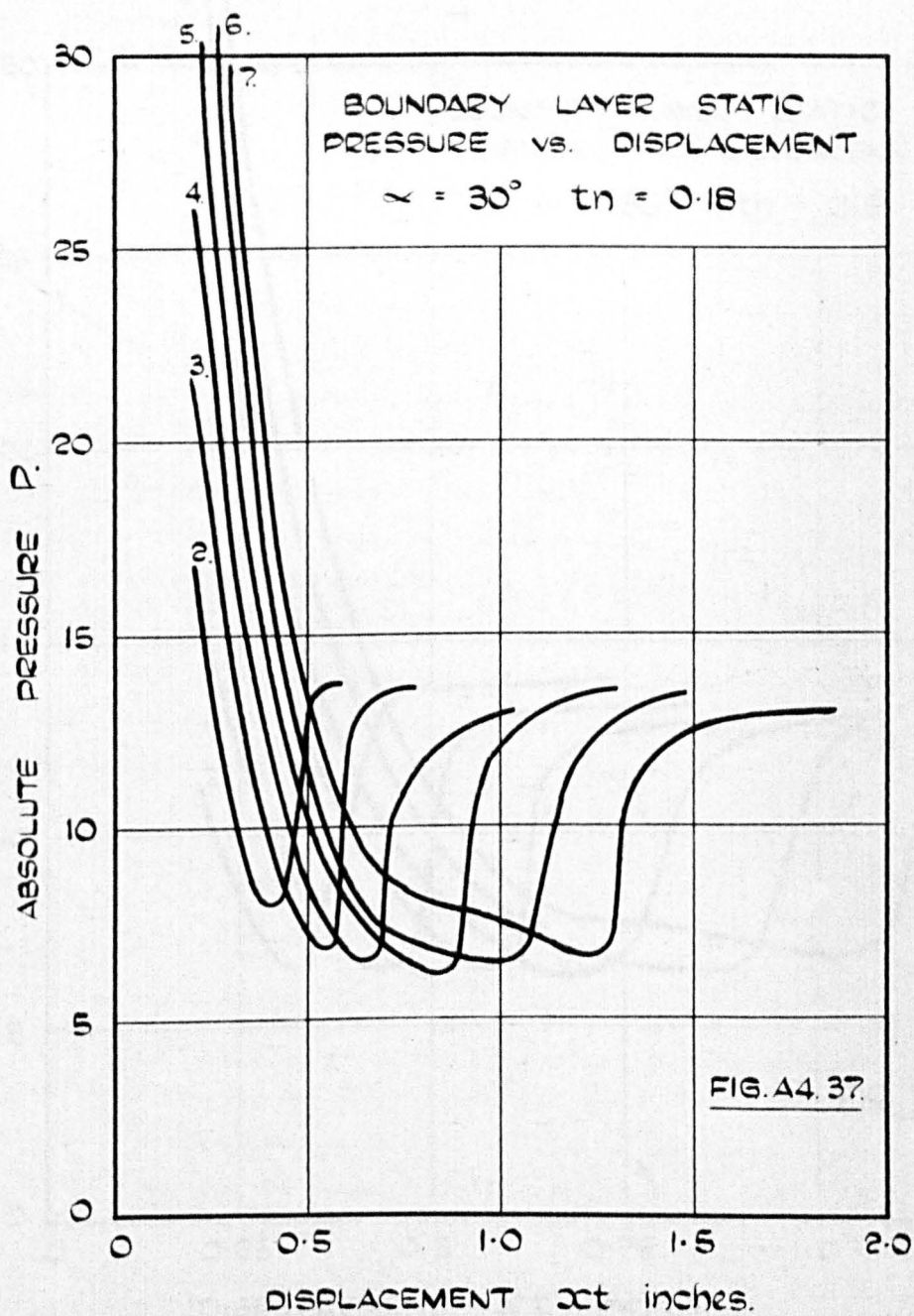




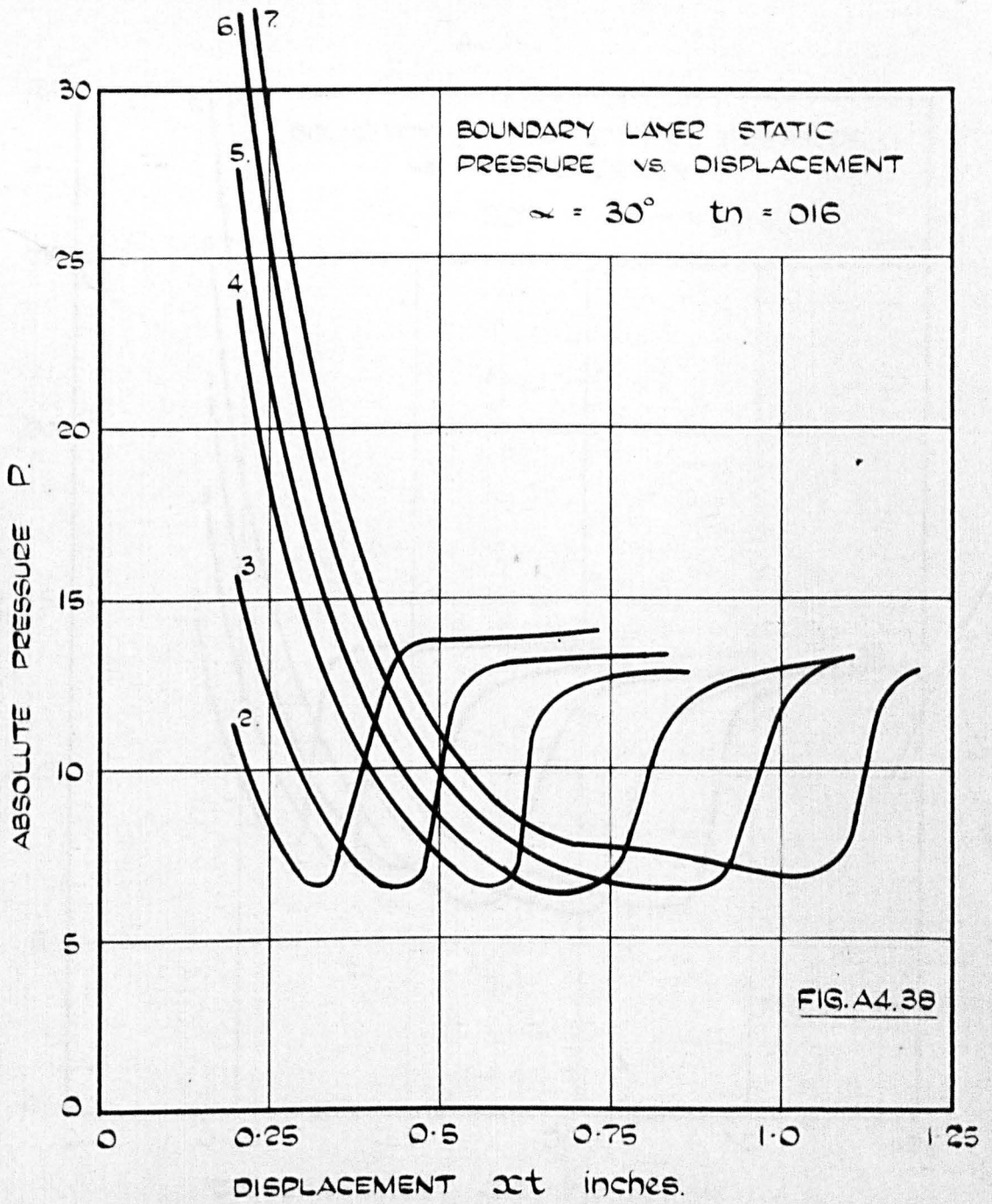


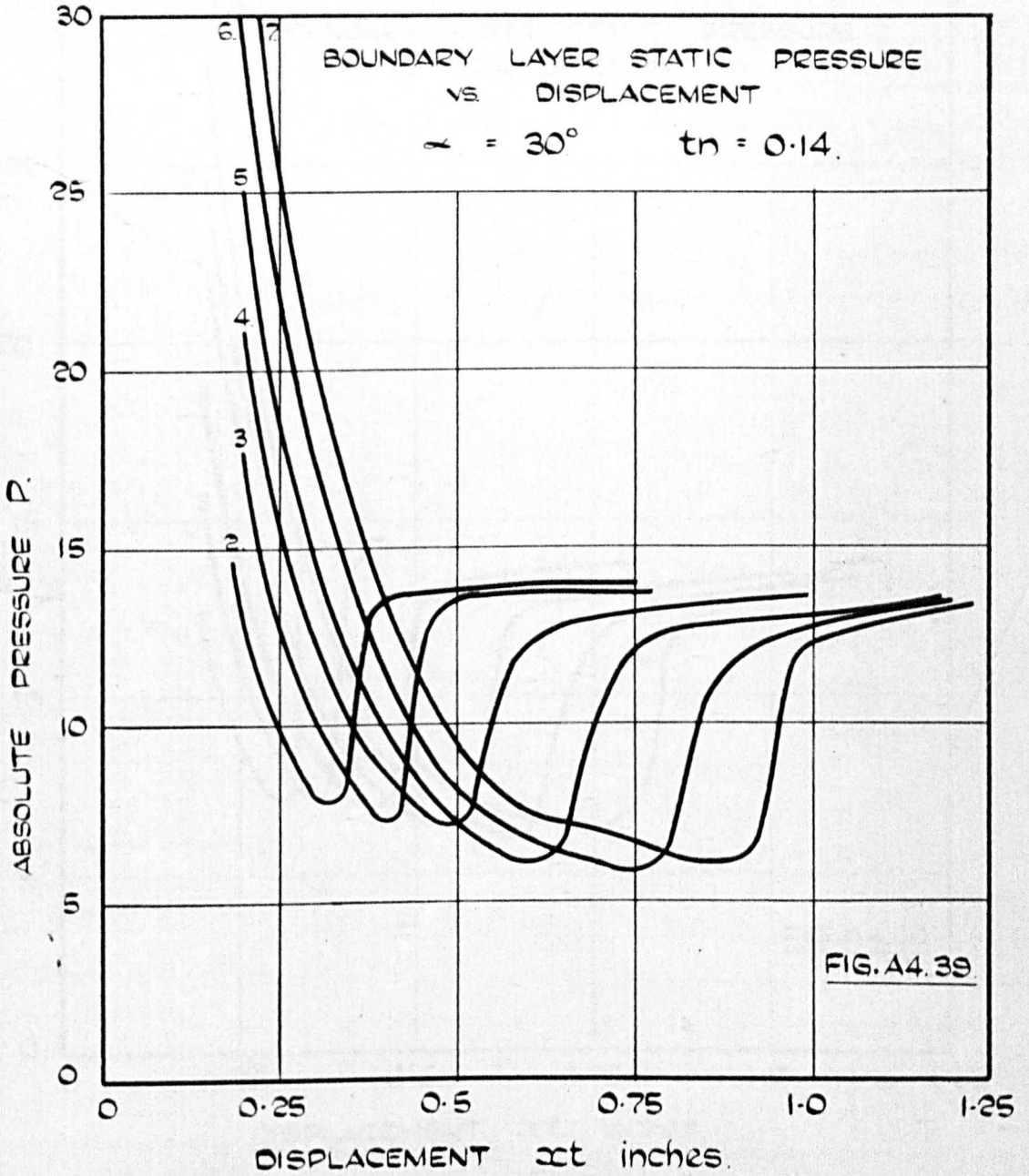


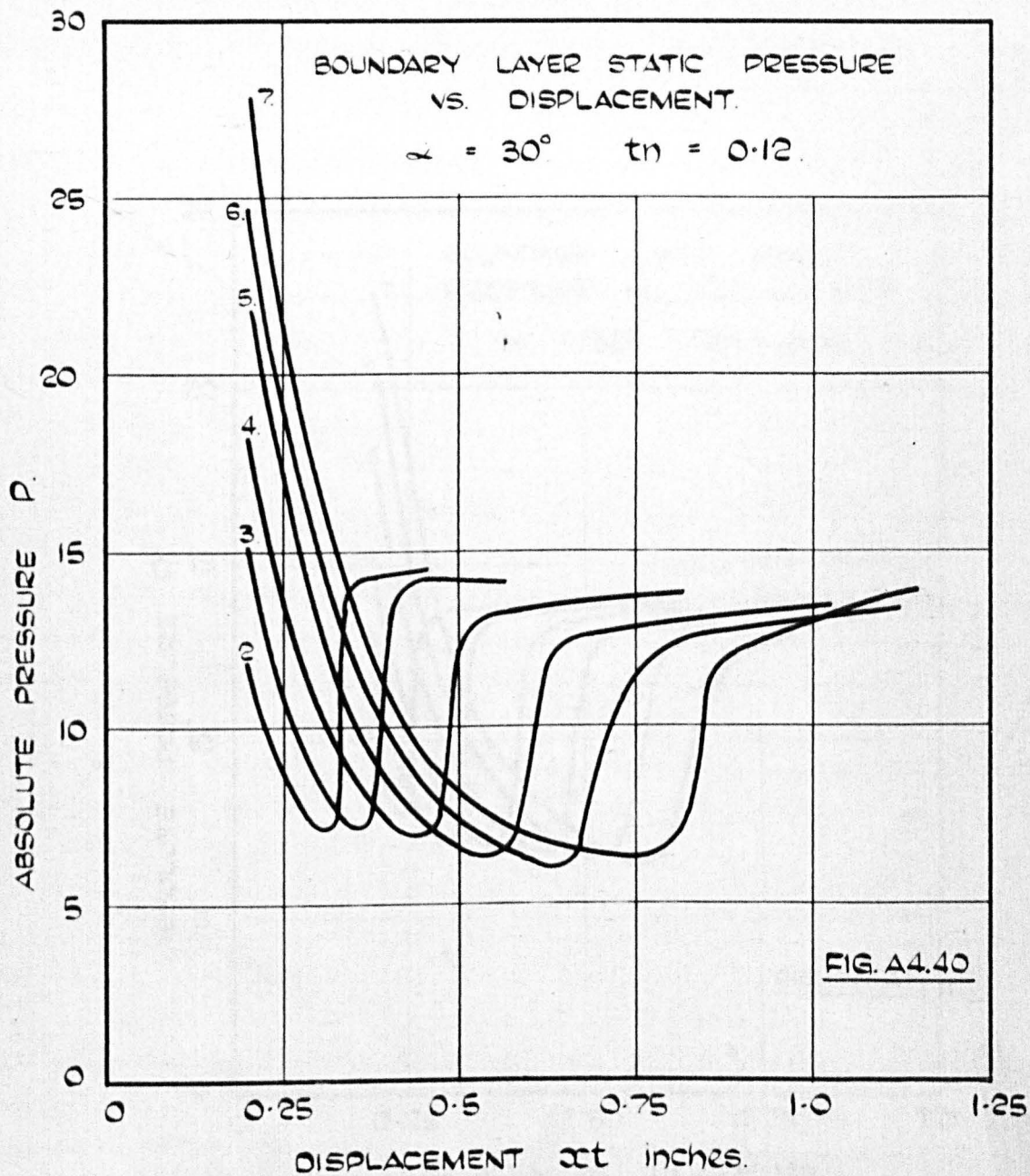


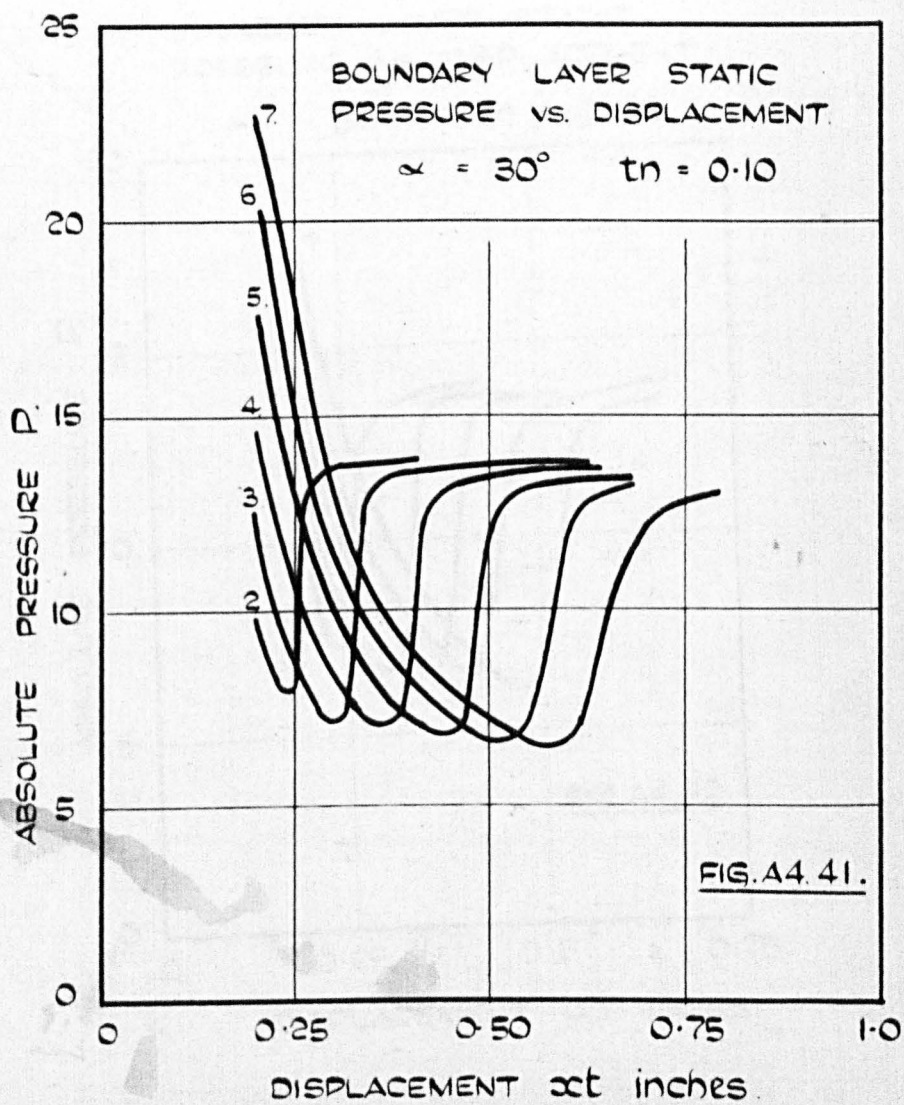






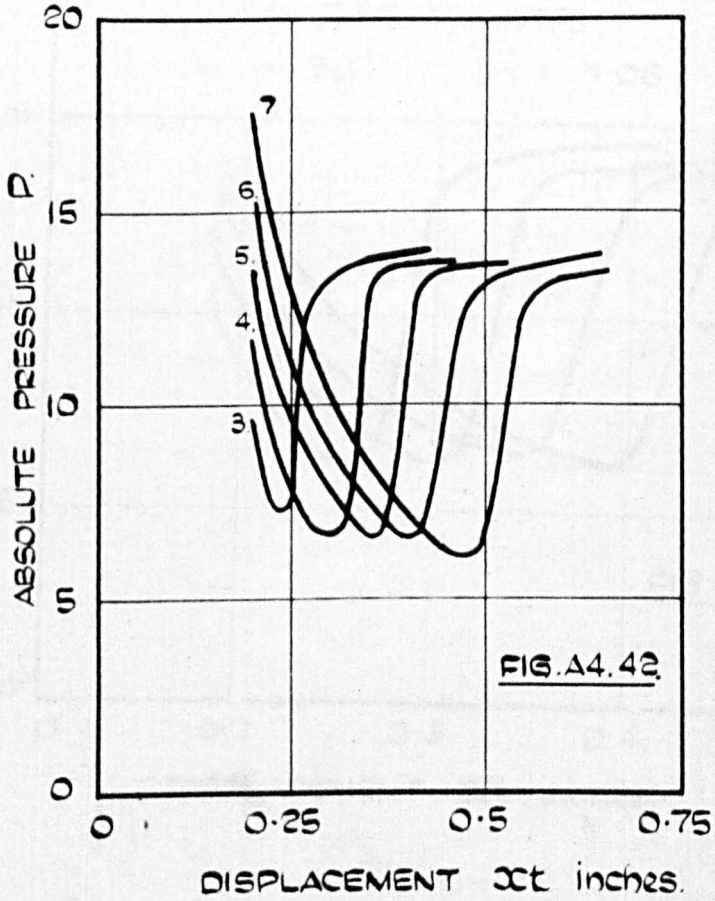


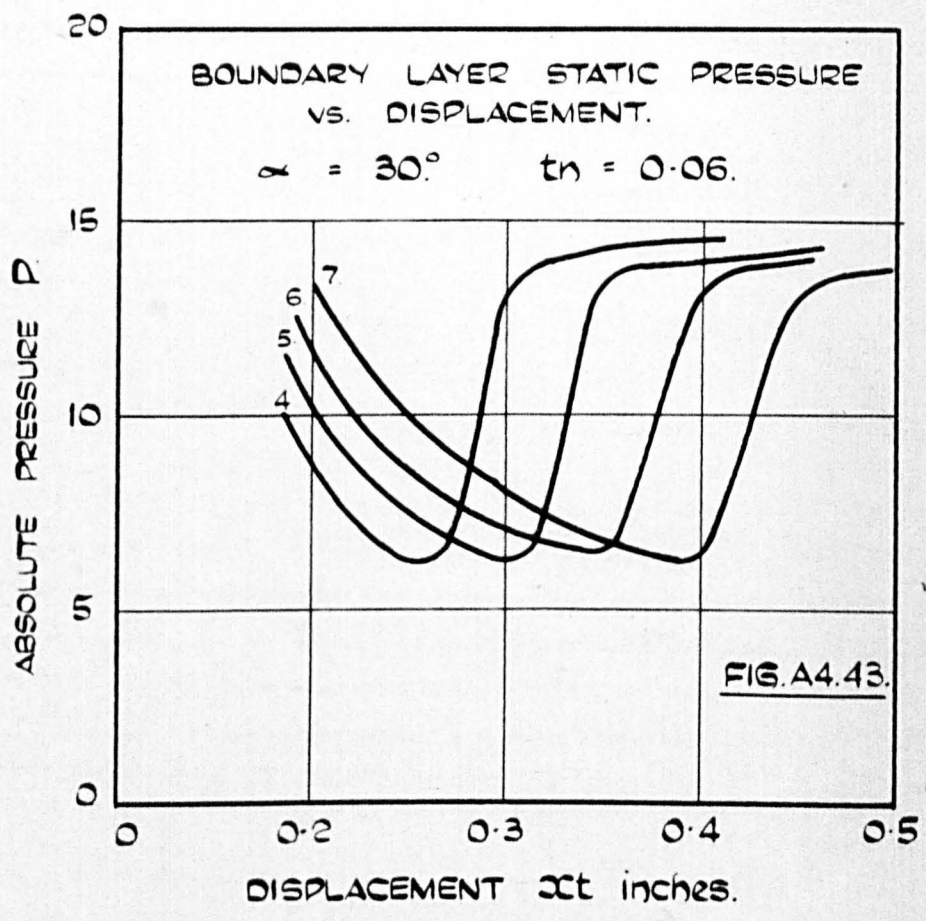




BOUNDARY LAYER STATIC  
PRESSURE VS. DISPLACEMENT.

$$\alpha = 30^\circ \quad t_n = 0.08.$$





APPENDIX 5.

The results of Dunaway and Ayre.

Table 1. - EXPERIMENTAL COLD GAS VALVES

Report- number No.	Test No.	Supply press- sure, psi	Submer- sion press- ure, psi	Manile div by angle, deg	Manile throat aspect E	Manile mic aspect E	Manile mic (1/2") area	Control port-area mic area	Seetch, in.	Offset, in.	Recurve wall by angle, deg	Recurve wall length, in.	Dist to aperture, in.	Remarks
0-1	1	125-375	22-40	15	7	7	.04	1.3	.2		15	3	.375	Sharp splicer switching range 125-375 psi
	2	125-375	22-40	15	7	7	.04	1.3	.2		15	3	None	No splicer switching range 125-375 psi
	3	125-375	22-40	15	7	7	.04	1.3	.25		15	3	None	No splicer switching range 125-375 psi
	4	125-375	22-40	15	7	7	.04	1.9	.25		15	3	None	No splicer switching range 125-400 psi
	5	125-375	22-40	15	7	7	.04	1.7	.25		15	3	None	No splicer switching range 125-375 psi
	6	125-600	22-100	15	7	7	.04	2.9	.30		25	3	None	No splicer switching range 125-600 psi
	7	outlet	22-100	15	7	7	.04	2.9	.32		25	3	1.45	Sharp splicer, no switching
1	1	0-1000	0-120	None	0.1	0.1	.0000							No satisfactory results were obtained
	2	0-1000	0-27	15	0.1	2.1	.0130	2	.004	0	15	.75	None	Switching, stream width unsatisfactory
	3	0-1000	0-27	7 1/2	0.1	2.1	.0130	2	.004	0	15	1.5	1.3	Good to 8-0 psi
6	1	0-1000	0-14.7	7 1/2	0.1	2.1	.0420	1.5	1 1/2"	0	22.5	1.5	None	Switching unsatisfactory
	2	0-1000	0-14.7	7 1/2	0.1	2.1	.0420	1.5	1 1/2"	0	22.5	1.5	None	Switching 500-750 psi
	3	0-1000	0-14.7	7 1/2	0.1	2.1	.0420	1.0	1 1/2"	0	22.5	1.5	None	Switching 500-1000 psi
	4	0-1000	0-14.7	7 1/2	0.1	2.1	.0420	1.5	2 1/2"	0	22.5	1.5	None	Switching 500-1000 psi
	5	0-1000	0-14.7	7 1/2	0.1	2.1	.0420	1.5	2 1/2"	0	15	1.5	None	Switching unsatisfactory
	6	0-1000	0-14.7	7 1/2	0.1	2.1	.0420	1.5	1 1/2"	0	15	1.5	None	Switching unsatisfactory
	7	0-1000	0-14.7	7 1/2	0.1	2.1	.0420	1.5	1 1/2"	0	15	1.5	None	Switching 500-1000 psi
	8	0-1000	0-14.7	7 1/2	0.1	2.1	.0420	1	2 1/2"	0	7 1/2	1.5	None	Switching unsatisfactory
	9	0-1000	0-14.7	7 1/2	0.1	2.1	.0420	1	1 1/2"	0	7 1/2	1.5	None	Switching good except 900-1000 psi
	10	0-1000	0-14.7	7 1/2	0.1	2.1	.0420	1	1 1/2"	0	7 1/2	1.5	None	Switching good except 900-1000 psi
	11	0-1000	0-14.7	7 1/2	0.1	2.1	.0420	1.5	2 1/2"	0	7 1/2	1.5	None	Switching good
	12	0-1000	0-14.7	7 1/2	0.1	2.1	.0420	1.5	2 1/2"	0	7 1/2	1.5	None	Switching good
	13	0-1000	0-14.7	7 1/2	0.1	2.1	.0420	1.5	2 1/2"	0	7 1/2	1.5	None	Unsatisfactory
5	1	0-1000	0-10	7 1/2	0.1	1.74:1	.0555	1.25	.1	.07	15	1.5	1.20	.05 common splicer switching 650-1100 psi
	2	0-1000	0-10	7 1/2	0.1	1.74:1	.0555	1.25	.1	.07	15	1.5	1.33	.07 common splicer switching 750 psi
	3	0-1000	0-10	7 1/2	0.1	1.74:1	.0555	1.25	.1	.07	15	1.5	1.37	.12 common splicer no switching
	4	0-1000	0-10	7 1/2	0.1	1.74:1	.0555	1.25	.1	.07	15	1.5	1.20	.09 common splicer switching 750-1100 psi
	5	0-1000	0-10	7 1/2	0.1	1.74:1	.0555	1.25	.1	.07	15	1.5	1.00	.07 common splicer switching 750-1000
	6	0-1000	0-10	7 1/2	0.1	1.74:1	.0555	1.25	.1	.07	15	1.5	1.20	.06 common splicer switching 700-800 psi
	7	0-1000	0-10	7 1/2	0.1	1.74:1	.0555	1.25	.1	.07	15	1.5	1.33	.12 common splicer switching 650-1050
	8	0-1000	0-10	7 1/2	0.1	1.74:1	.0555	1.25	.1	.07	15	1.5	1.37	.07 common splicer switching 1025-1100
	9	0-1000	0-10	7 1/2	0.1	1.74:1	.0555	1.25	.1	.07	15	1.5	1.20	.09 common splicer no switching
	10	0-1000	0-10	7 1/2	0.1	1.74:1	.0555	1.25	.1	.07	15	1.5	1.00	.07 common splicer switching 650-900

Experimental manile No. 5, tests 6 through 10 were conducted with .51 ID manifold and were used as a model for further work.  
up to width of manile at exit section.





Table II. (Continued)

Valve No.	Seat No.	Thrust opp. lbf.	Stroke comp. cham ratio	Stic exponent ratio	Verti- cal off- set, in.	Com- troi part dia. in.	Com- troi part width, in.	Sec- ond half angle, deg.	Sticness to nozzle or spitter, in.	Stic dust cham. in.	Britch- ing	Gas pres- sure range, psi	Range on air, psi	No. of pieces	Perce. lb.
11	29	.0117	7.9	04	None	.39	.75	15	1.9	.028, .34	Disc	-900		2	10.3-11.30
	31									.3125	Disc	-970			9-10
	34										Disc	-900			11-12.30
67	26	.0100	11.05	04	None	.3	.17	15	1.05	.4325	Disc	630/1005	600/1000	2	10.4-11.30
	40	.0107	11.05	04	None	.35		15		.0825	Poor	900		2	9-10
80-ly 2	39	.0175	11.75	04	None	.437	.350	15	2.1	.0825	Poor	600/975		2	100
	44	.0100	11.05	04	None	.35	.4	15	1.75	.0825	Disc	500/975	500/975	2	110
870	50										Pole				60
	52										Good				20
	61										Good				9.50
	61										Disc		600/1000		
8831-12	43	.0141	0.06	04	None	.5	11/4	0	2.1	.0825	Good		600/1000	2	5.30
	45	.0150				.47	.08	15	2.25		None		600/1000		60
	46					.5					None		500/1000		3-120
	48	.0154									None				120
	48										Poor				140
	51										Poor				150
	53										Poor				13.30
	54										None				12.00
	56										Pole				130
	58										Poor				140
8831-7	68	.014	13.3	04	None	.39	.48	15	2.1	.1425	Good		700/900	2	14.30
	68					.45				.0825	Poor		700/1000		13.30
	68									.1425	Disc		775/1000		13.30
	68									.1425	Disc				11.30

0 Side Piece - Receiver Section on Valve  
 on Total Thrust - No Receiver Section on Valve

## ACKNOWLEDGEMENTS.

The author wishes to express his gratitude to Professor A.S.T. Thomson, D.Sc., Ph.D., A.R.C.S.T., M.I.C.E., M.I.Mech.E., F.R.S.E., Head of the Department of Mechanical Engineering, University of Strathclyde, for permission to use the laboratory facilities in connection with this research programme.

Many thanks are due to Mr. C. Rodgers for his skill in making much of the apparatus and to Mr. C. Richardson, Chief Technician, for obtaining everything from everywhere.

Further thanks are due to Mr. W.B. McHutchison, B.Sc., A.R.C.S.T., Wh.Sch., A.M.I.E.E., M.I.Mech.E., Reader in Dynamics and Control, University of Strathclyde, for help, guidance and advice given by him at all times during the research and preparation of this thesis and to Dr. R. McLean, M.Sc., A.R.C.S.T., A.M.I.Mech.E., for his assistance with the computer programme.

Without the assistance of these people and others the work could not have been completed.